ISSN 1880-6503

Sustainable Humanosphere

BULLETIN OF
RESEARCH INSTITUTE FOR SUSTAINABLE HUMANOSPHERE
KYOTO UNIVERSITY

No. 5 September 2009

PUBLISHED BY
RESEARCH INSTITUTE FOR SUSTAINABLE HUMANOSPHERE
KYOTO UNIVERSITY
UJI, KYOTO 611-0011, JAPAN

'Sustainable Humanosphere' is a serial publication issued annually by the Research Institute for Sustainable Humanosphere (RISH) of Kyoto University, which aims to provide a report on the ongoing research at our Institute along with new research field of sustainable humanosphere. This journal is a continuation of 'Wood Research' published by Wood Research Institute of Kyoto University, which will be distributed free of charge and prefers to exchange similar articles with scientific institutions and libraries throughout the world. All communications concerning 'Sustainable Humanosphere' should be addressed to Research Institute for Sustainable Humanosphere (RISH), Kyoto University, Uji 611-0011, Japan. (Email: oubunshi@rish.kyoto-u.ac.jp)

CONTENTS

Tree rings: do we find record of economic growth?

(Laboratory of Biomass Morphogenesis and Information, RISH, Kyoto University)

Suyako Mizuno and Junji Sugiyama

In order to improve our knowledge of the past climate, it is important to have methods that allow for investigation, providing better correlations of significant climatic events. Hinoki trees having a wide distribution ranging from north to the south of our country are an ideal substrate to develop such records that can potentially be further extended to explore the climate down to Asuka period by analyzing the wood used in Horyu-ji temple. Recently, by taking advantage of properties at Xylarium at RISH, we started tree ring analysis of Hinoki, and here we introduce a preliminary result of an carbon isotopic investigation from the species grown in Kiso area.

The Japanese forest was exposed to high levels of sulfur and nitrogen deposition during the economic growth period in 1960s to 1970s. The change in growth of Hinoki tree caused by such pollution has been studied using the ^{13}C isotopic chemistry of the tree rings. Tree rings were sectioned by years, and whole wood was analyzed for isotopic composition ($\delta^{13}C$) and annual ring width. Only those rings that formed after the juvenile effect in early rings were used and trends from the beginning of 20th century were evaluated. The mean $\delta^{13}C$ of the Hinoki tree rings was ca. -20‰. The $\delta^{13}C$ did not follow climate parameters, such as relative humidity, temperature, precipitation, but showed a rapid change during 1960s-1970s, implying a negative effect of pollution on tree physiology.

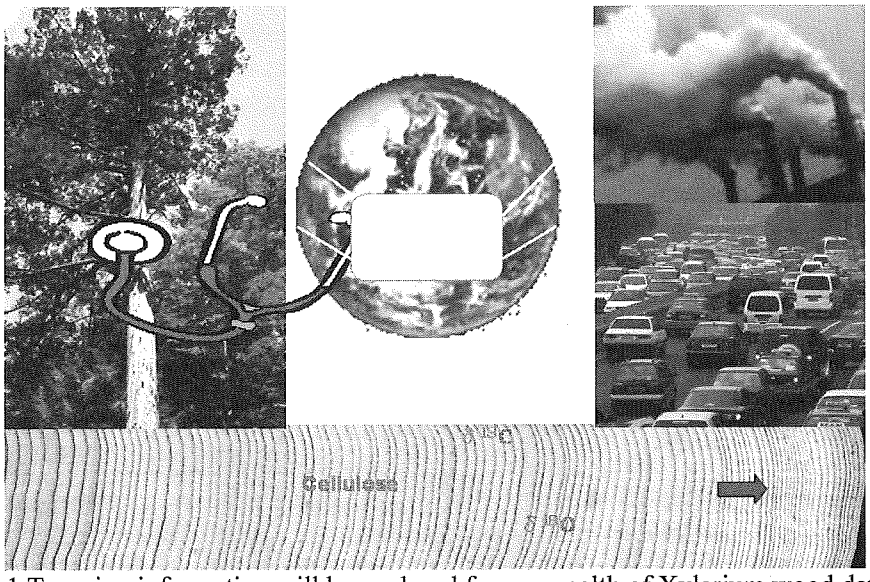

Figure 1 Tree ring information will be explored from a wealth of Xylarium wood database.

Molecular mechanism of direct oxidation of polymeric substrate by a versatile peroxidase from white-rot fungus, *Pleurotus ostreatus*

(Laboratory of Biomass Conversion, RISH, Kyoto University)

Yoichi Honda, Takahito Watanabe and Takashi Watanabe

Conversion of biomass resources to useful materials such as energy compounds or biodegradable plastics are getting received more and more interests in the light of world-wide demands to prevent global warming and to substitute fossil resources. White-rot fungi play a critical role in the carbon cycle in biosphere by degrading plant cell wall substances produced by photosynthesis. Especially, the unique ability to decompose a recalcitrant polymer, lignin, in a mild condition has advantages as a strong tool for pretreatment of wood biomass subjected to saccharification. Toward the elucidation and application of the mechanism for lignin biodegradation, we are operating intensive approaches using biochemical, enzymological and molecular genetical methodologies.

A white-rot basidiomycete,*Pleurotus ostreatus* MnP2 was earlier mentioned as a typical manganese peroxidases (MnP) isozyme, MnP2 oxidizes veratryl alcohol, a typical substrate for lignin peroxidases (LiPs), and even high molecular-weight compounds such as RNase A and a polymeric azo dye Poly R-478. From these results MnP2 is called as a versatile peroxidase (VP) and are considered to be the key enzyme in the lignin biodegradation system by the fungus. The deduced amino acid sequence from the cloned *mnp2* gene demonstrated that this isozyme contains the tryptophane residue (W170) conserved among LiPs and VPs. Chemical modification of purified MnP2 by *N*-bromsuccimide blocked the oxidizing activity for veratryl alcohol, RNase A and Poly R-478, suggesting that W170 plays an essential role in oxidizing these compounds. Using a genetic transformation system, *P. ostreatus* strains with elevated MnP2 productivity were isolated [1]. In these strains, the recombinant *mnp2* was expressed under the control of *P. ostreatus* promoter sequence from *sdi1* which encodes for Iron-sulphur protein subunit of succinate dehydrogenase, one of the components of the mitochondrial respiratory chain. The recombinant strains exhibited enhanced Poly R-478-decolorizing and benzo[*a*]pyrene-removing activities [1], demonstrating their high potential as biocatalysts in biological processes such as pretreatment of wood biomass and bioremediation of polluted soil or water. Under a certain culture condition, one of the transformant showed about 30-fold production of MnP2 compared to wild type strain.

Furthermore, through optimization of the culture conditions, an exclusive expression of the recombinant MnP2 without background expression of endogenous MnP isozymes was achieved [2]. We used this exclusive expression system for recombinant MnP2, to elucidate the unique mechanism of direct polymer oxidation by this enzyme. Four variants with site-directed mutation at W170 and its surrounding amino acid residues were successfully expressed and their catalytic activities for low and high molecular-weight substrates are being analyzed [3]. It was demonstrated that W170 is essential for oxidation of aromatic and polymeric substrates and that relatively open circumstances of its proximal microenvironment make the polymeric substrates accessible to the oxidation site, which is not possible in case of other fungal ligninolytic peroxidases including LiP from *Phanerocheate chrysosporium*.

REFERENCES

[1] Tsukihara, T., Honda, Y., Watanabe T. and Watanabe, T., (2006) *Appl. Microbiol. Biotechnol.*, 71: 114-120.

[2] Tsukihara, T., Honda, Y., Sakai, R., Watanabe T. and Watanabe, T., (2006) *J. Biotechnol.*, 126: 431-439.

[3] Tsukihara, T., Honda, Y., Sakai, R., Watanabe T. and Watanabe, T., (2008) *Appl. Environm. Microbiol.*, 74: 2873-2881.

Gene co-expresson network analysis and tropical tree biotechnology

(Laboratory of Metabolic Science of Forest Plants and Microorganisms, RISH, Kyoto University)

Toshiaki Umezawa and Takefumi Hattori

It is becoming more important to establish a sustainable society, which depends on renewable resources. Because wood biomass is the most abundant renewable resource, studies of wood formation is the key to improve forest biomass production. In this context, we are involved in analyzing metabolic functions of forest plants and microorganisms from a wide variety of aspects, including organic chemistry, biochemistry, molecular biology, and metabolomics, in order to conduct basic investigations contributing cultivation and protection of forest resources. These projects are conducted in collaboration with Assistant Professor Shiro Suzuki, Institute of Sustainability Science, Kyoto University.

1. Gene co-expression network analysis

During the last two decades, significant advances have been made in molecular biology of wood formation. For example, many genes involved in lignin biosynthesis have been cloned and their functions have been unequivocally identified. Having the genes in our hands, the major concern in tree biotechnology is the elucidation of comprehensive gene expression control mechanisms for cell-wall formation. Identification of transcription factors (TFs), as well as microRNAs, controlling expression of genes encoding enzymes involved in cell-wall formation is one of the most important steps. Following the completion of genome sequences of *Arabidopsis thaliana*, a large number of microarray data sets of *A. thaliana* gene expression are open to public, which can be exploited to analyze co-expression of genes. We are conducting gene co-expression network analysis starting with the genes encoding enzymes of the cinnamate/monolignol pathway providing monolignols. This allowed us to find out several genes encoding TFs which possibly control the gene expression of the pathway enzymes. Next, in order to confirm the roles of the TFs, we prepared transgenic *A. thaliana* cells where the individual TF genes were upregulated. Lignin characterization of the transgenic cells thus obtained and *A. thaliana* T-DNA tag line mutants with the target genes being downregulated are under way by the use of Forest Biomass Analytical System, so that we can identify TFs which controls the metabolic flow of the cinnamate/monolignol pathway in *A. thaliana*.

2. Mechanisms for organic acid metabolism of wood-rotting fungi and ectomycorrhizal fungi

Biodegradation of wood components by wood-rotting (WR) fungi including white- and brown-rot basidiomycetes is important as a first process leading to humus production, which in turn contributes greatly to sustainable forest ecosystems. Oxalate excreted from WR fungi plays a wide variety of roles in the degradation owing to its various chemical natures. We have proposed that oxalate metabolism is an important biochemical device to produce energy for fungal growth of WR fungi. Previously, we purified terminal enzyme for oxalate synthesis, cytochrome *c* dependent glyoxylate dehydrogenase (FpGLOXDH), from brown-rot fungus *Fomotpsis palustris*. Recently, cDNA encoding the FpGLOXDH was cloned. The deduced FpGLOXDH possessed the peroxisomal target signal S-K-L at the C-terminus, suggesting that FpGLOXDH is localized in the peroxisome. The peroxisomal localization of FpGLOXDH was shown by electron microscopic and immunocytochemical analysis with an anti-FpGLOXDH antibody. In addition to our previous results on cytosolic oxalate production by oxaloacetase, the present results strongly suggest that oxalate is also formed by FpGLOXDH in the peroxisome of *F. palustris*.

Cytochemical and molecular approaches for enzymes and transporters involved in organic acid metabolism are being investigated for WR fungi. Furthermore, comprehensive study for elucidation of regulatory mechanisms for organic acid metabolism in WR and ectomycorrhizal fungi has just begun.

Discovery of the first vacuolar transporter responsible for the endogenous alkaloid accumulation

(Laboratory of Plant Gene Expression, RISH, Kyoto University)

Kazufumi Yazaki

Among a large number of plant secondary metabolites, alkaloids comprise one of the most important groups due to their strong and divergent biological activities, and some are applied for clinical use [1]. Alkaloids are defined as nitrogen-containing low-molecular-weight organic substances. They are often highly accumulated in particular organs of medicinal plants, which are called the 'medicinal part', whereas it is known that some alkaloids are translocated from source organs to such sink organs. The movement of biosynthetic intermediates from specific cells to other types of cells in tissue, and further detailed movement within the organelles in a cell is also suggested. However, little is known how alkaloids are transported across membranes and finally accumulated in specific organelles such as vacuole of the sink organ. Actually, vacuoles are the main subcellular compartment for the accumulation of alkaloids, and in many model experiments, vacuolar uptake of endogenous alkaloids have been reported [2]. However, no endogenous transporter molecule has been identified for the vacuolar transport of those alkaloids thus far.

As a representative of such alkaloids, we selected nicotine, a pyridine alkaloid, which is biosynthesized in root tissues, then translocated to the leaves, and finally accumulated in the leaf vacuoles in *Nicotiana* species. Recently, we have identified a novel multidrug and toxic compound extrusion (MATE)-type transporter in cDNA AFLP as a strong candidate of nicotine transporter in tobacco plant [3]. This gene, designated as *Nt-JAT1* (*Nicotiana tabacum* jasmonate-inducible alkaloid transporter 1) was co-regulated with nicotine biosynthetic genes following methyl jasmonate treatment of tobacco BY-2 cells. This MATE gene was expressed in the leaves, stems, and roots in tobacco plants. Biochemical analyses using a yeast cellular transport system and proteoliposome system suggested that Nt-JAT1 transported nicotine using the H^+ gradient across the membrane as its driving force [4]. The location of Nt-JAT1 was shown to be the tonoplast. These data suggested that Nt-JAT1 plays an important role in the nicotine translocation by acting as a transporter responsible for the unloading of nicotine in the aerial parts of the plant and its deposition in the vacuoles. To our knowledge, this is the first identification of a vacuolar transporter for alkaloids in plant. A possible application of this alkaloid transporter for the production of valuable alkaloids is also discussed in the reference.

References

[1] Shitan, N., Yazaki, K., Chapter 12. Membrane transport of plant secondary metabolites. In: Plant Membrane and Vacuolar Transporters (Eds. Pawan K. Jaiwal, Rana P. Singh, and OM Parkash Dhankher), CAB International, Oxfordshire, UK, pp. 283-300, 2008.

[2] Shitan, N., Yazaki, K., Accumulation and membrane transport of plant alkaloids. *Curr. Pharm. Biotech.*, vol. 8, no. 4, pp. 244-252, 2007.

[3] Yazaki, K., Sugiyama, A., Morita, M., Shitan, N., Secondary transport as an efficient membrane transport mechanism for plant secondary metabolites. Phytochem. Rev., vol. 7, pp. 513-524, 2008.

[4] Morita, M., Shitan, N., Sawada, K., Van Montagu, M., Inzé, D., Rischer, H., Goossens, A., Oksman-Caldentey, K-M., Moriyama, Y., Yazaki, K., "Vacuolar transport of nicotine is mediated by a novel multidrug and toxic compound extrusion (MATE) transporter in *Nicotiana tabacumi." Proc. Natl. Acad. Sci. USA*, vol. 106, no. 7, pp. 2447-2452, 2009.

Application of Radar Remote-Sensing Technique to Measure Atmospheric Temperature and Humidity to the Tropical and Subtropical Region

(Laboratory of Atmospheric Sensing and Diagnosis, RISH, Kyoto University)

Jun-ichi Furumoto

Behaviors of various meteorological phenomena are determined by wind velocity, atmospheric temperature, and humidity. It is very important to observe them simultaneously to reveal the mechanism of such atmospheric phenomena. Because severe meteorological phenomena such as a typhoon and heavy rainclouds, which sometimes bring severe disasters for us, have short lifetime, it is essential to observe them simultaneously with a good temporal resolutions. Our laboratory has been developing the new radar remote-sensing technique to monitor them with a good temporal resolution regardless weather conditions.

A wind profiling radar detect an echo backscattered by the turbulence in the atmosphere. Three dimensional wind profiles are calculated from the Doppler shift of turbulence, since atmospheric turbulences are advected by the background wind. The Radio Acoustic Sounding System (RASS) can measure virtual temperature profiles by combining the acoustic source with a wind profiling radar. In the RASS measurements, the acoustic wave is transmitted by the ground-based acoustic source. The wind profiling radar detects the RASS echo backscattered by the acoustic wavefront in the atmosphere. Atmospheric temperature can be derived from the Doppler shift of RASS echo since the acoustic velocity is determined by the atmospheric temperature.

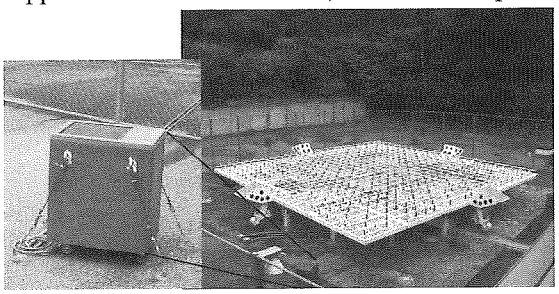

Figure 1. (right) appearance of 443MHz-WPR antenna array. (left) the acoustic horn developed for RASS measurements of 443MHz WPR.

We have also been developing a new remote-sensing technique to estimate humidity profiles from the atmosphere radar. Humidity profiles are calculated from the turbulence echo intensity, since the echo power intensity is mainly determined from the vertical gradients of atmospheric humidity.

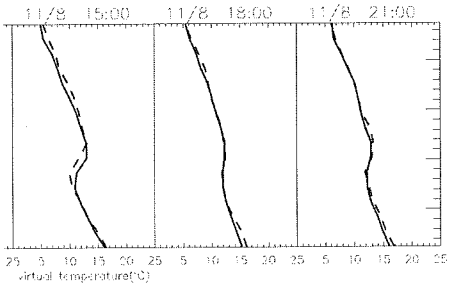

Figure 2. Successive temperature profiles obtained with RASS (solid) and radiosonde (dashed) measurements.

The above techniques have originally been developed with the MU radar of Research Institute for Sustainable Humanosphere. These techniques are recently applied to the other wind profiling radars under the collaboration with domestic or international research laboratories. In the Equatorial region, where the cumulus convections are actively generated, the RASS observations are operated with the Equatorial Atmosphere Radar (EAR) at the Sumatra Island and the MST (Mesosphere, Stratosphere, and Trposphere) radar of National Atmospheric Research Laboratory (NARL) in India.

For applying our techniques to the Okinawa subtropical region, we collaborate with National Institute of Communication and information Technology (NICT) to develop the RASS system for the 443MHz wind profiling radar (443MHz-WPR) (Figure 1) at NICT Ogimi wind profiling observatory (Ogimi observatory). RASS observation in the Okinawa subtropical region has been continuously operating everyday during 0700-2000 LT. The solid lines in Figure 2 show the successive atmospheric temperature profiles obtained by 443MHz-WPR with RASS. The results of radiosondes launched at the Ogimi observatory are also shown by dashed lines. The both results shows good agreements including the structure of temperature inversion layers at 1.5 km.

Range-imaging observation of turbulence in the tropical tropopause layer by the Equatorial Atmosphere Radar

(Laboratory of Radar Atmospheric Science, RISH, Kyoto University)

Mamoru Yamamoto, Hiroyuki Hashiguchi, and Masayuki K. Yamamoto

Observations of temperature, winds, and atmospheric trace gases suggest that the transition from the troposphere to the stratosphere occurs in a layer, rather than at a sharp tropopause. In the tropics, this layer is often called the tropical tropopause layer (TTL). TTL has a bottom at 150 hPa, 355 K, 14 km (pressure, potential temperature, and altitude) and has a top at 70 hPa, 425 K, 18.5 km. TTL acts in many ways as a gate to the stratosphere, and understanding all relevant processes is of great importance for reliable predictions of future climate [1]. The 47-MHz atmospheric radar referred to as the Equatorial Atmosphere Radar (EAR) has been operated at Sumatra island, Indonesia (0.2°S, 100.32°E), and has revealed features of turbulence in TTL, which is expected to contribute airmass mixing there [2, 3]. In December 2009, we carried out the observation campaign named Cloud experiment by Lidar and the Equatorial Atmosphere Radar (CLEAR). During CLEAR campaign, the EAR was operated with a frequency-domain interferometric imaging (FII) mode to observe fine time and altitude variations of turbulence. On pulse-to-pulse basis, the EAR changed transmitted frequencies from 46.5 to 47.5 MHz with 250 kHz spacing. Using phase difference of received signals caused by transmitted frequency difference and location of turbulence, altitudes of enhanced turbulence were determined. Figure shows an example of range-imaging result in TTL. Wavy echoes with a period of about 7 minutes show presence of shear instability, which causes airmass mixing. Previous study has shown that shear instability frequently occurs around the tropopause due to large wind shear [3], and the wavy echoes as shown in the Figure further provide detailed information on observed scales of shear instability in TTL.

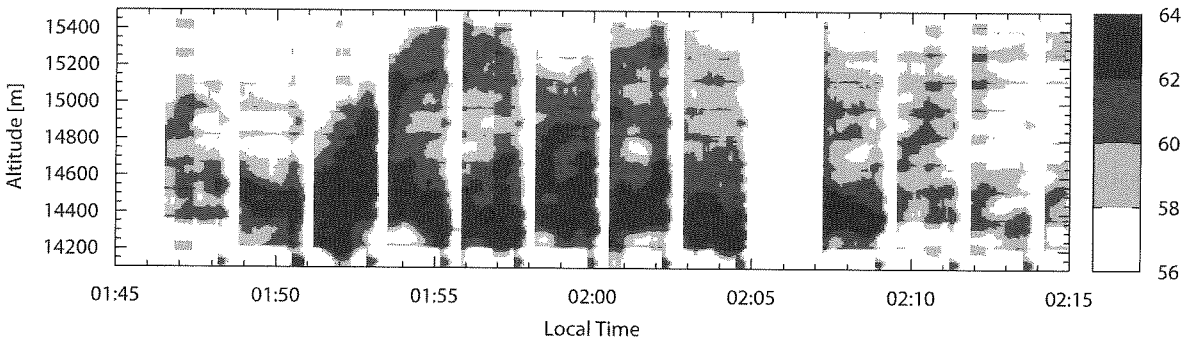

Figure. Time-altitude plot of brightness observed by FII the mode of the EAR.

Acknowledgements

We thank Dr. Tomoaki Mega of RISH for his great contribution in FII data analysis.

References

[1] Fueglistaler, S., A. E. Dessler, T. J. Dunkerton, I. Folkins, Q. Fu, and P. W. Mote, "Tropical tropopause layer", *Rev. Geophys.*, 47, RG1004, doi:10.1029/2008RG000267, 2009.

[2] Fujiwara, M., M. K. Yamamoto, H. Hashiguchi, T. Horinouchi, and S. Fukao, "Turbulence at the tropopause due to breaking Kelvin waves observed by the Equatorial Atmosphere Radar", *Geophys. Res. Lett.*, 30, 1171, doi:10.1029/2002GL016278, 2003.

[3] Yamamoto, M. K., M. Fujiwara, T. Horinouchi, H. Hashiguchi, and S. Fukao, "Kelvin-Helmholtz instability around the tropical tropopause observed with the Equatorial Atmosphere Radar", *Geophys. Res. Lett.*, 30, 1476, doi:10.1029/2002GL016685, 2003.

Transparent Nanofiber Paper - 21st century paper-

(Laboratory of Active Bio-based Materials, RISH, Kyoto University)

Masaya Nogi, Antonio Norio Nakagaito, and Hiroyuki Yano

We cannot see through ordinary paper because it's constituent micrometer sized cellulose fibers and large cavities scatter light, which makes paper opaque (Fig. 1. left). Now, we have developed transparent paper (Fig. 1. right) [1, 2]. Using cellulose—as in normal paper—and downsizing the fibers using a simple processing technique, we produced 'transparent paper' which, unlike many transparent plastics, does not expand significantly on heating. This paper is ideal as an alternative substrate for electronics, which could even be used in roll-to-roll processing.

The transparent paper was made using wood flour, in which cellulose nanofibers are usually bundled together to make larger, 30 μm-wide fibers. We started by swelling the bundled cellulose fibers in water and then mechanically grinding them just once. This broke them down into single nanofibers.

To form optically transparent sheets of paper, the fibers must be squashed together to prevent large gaps forming between them—large spaces would scatter light and render the material opaque. We filtered the suspension to bring the fibers together and then sandwiched the resulting layers between wire mesh and filter paper and dried it for three days. Once the fibers are compacted together in this way, hydrogen bonds hold them in this configuration even after the pressure is removed.

After polishing the surfaces, the sheet became transparent with 71.6% light transmittance at 600nm (Fig.2). The sheets were foldable like normal paper and had high strength and a thermal expansion coefficient comparable to that of glass. This flexibility makes it perfect for roll-to-roll processing, which will be vital for making future bendable electronic devices.

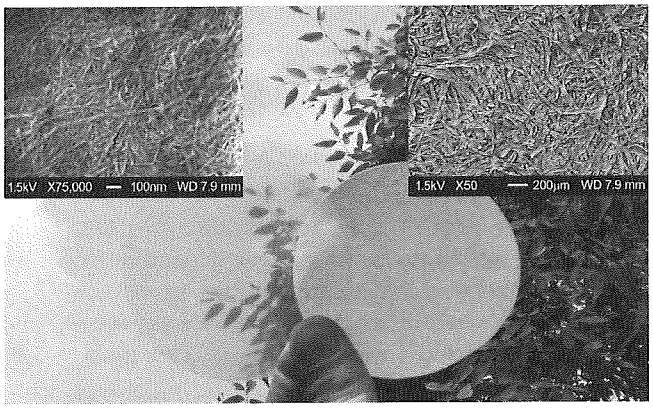

Figure 1. Optically transparent nanofiber paper (left) composed of 15nm cellulose nanofibers (upper left, scale bar in inset: 100 nm) and conventional cellulose paper (right) composed of 30 μm pulp fibers (upper right, scale bar in inset: 200μm).

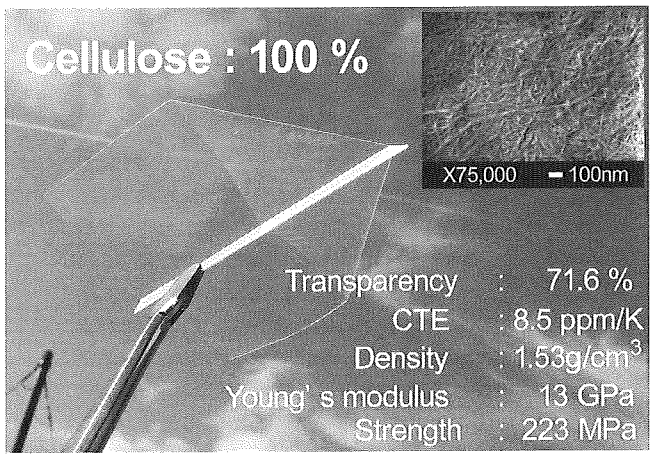

Figure 2. Paper airplane; The transparent nanofiber sheet folds like traditional paper.

References

[1] M. Nogi, S. Iwamoto, A. N. Nakagaito, and H. Yano, "Optically Transparent Nanofiber Paper", *Advanced Materials*, vol. 21, no. 6, pp1595-1598, 2009.

[2] D. Pile, "Materials: Transparent Nanofibre Paper", *Nature Photonics*, vol. 3, no. 6, pp314, 2009.

Development of acacia mangium bark molded products

(Laboratory of Sustainable Materials, RISH, Kyoto University)

Sasa Sofyan Munawar, Kenji Umemura, Shuichi Kawai

Biopolymers are seen as a potentially greener alternative to petroleum based plastics which are non-biodegradable. In order to reduce synthetic polymers for more environmental friendly products, utilization of various renewable resources have been the object of intensive academic and industrial research. Recently, the utilization of acacia mangium bark added with citric acid for the production of molded products was investigated. Utilization of bark has become an important goal because bark disposal has been threat to environmental quality. As byproducts from utilization of trees on the production of pulp paper and boards, bark has very potential as raw material.

Molded product from acacia mangium bark only

Fig. 1 shows the effect of pressing temperatures, times and pressures on the tensile properties of molded products. The higher values of MOR were 22.8 MPa and 22.1 MPa for molded products that made at 260°C, 8 MPa, 10 min and at 280°C, 8 MPa, 20 min, respectively. Moreover, an increase in temperatures, pressures and pressing times, the tensile properties were effectively increased, except for molded products that manufactured at 280°C, 12 MPa and 10-20 min.

Based on TG analysis, the rate of weight loss increased rapidly above 225°C for molded products made at 140-220°C and above 275°C for molded products made at 260-280°C, and attains a maximum at 350°C. After decreased of 40% and 50% for molded products that made at 280°C and 260°C, respectively, and decreased of 65% for others, the reaction rate decreased again above 400°C.

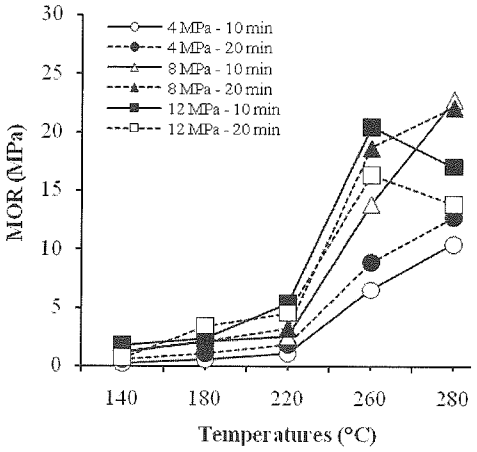

Fig 1. Tensile strength of molded products made from acacia bark only.

Molded product from acacia mangium bark added with citric acid

The effects of citric acid content and pressing temperatures on the tensile properties of the molded products are showed in Fig.2. The molded products that produced at 180°C showed higher in tensile properties than other pressing temperature conditions. By adding citric acid, the tensile strength of acacia molded products increase about 40%. The highest tensile strength obtained on the products that made by adding 25% of citric acid. The pressing temperature of acacia molded products can be reduced from 260-280°C to 180-200°C when citric acid was added. It's because by influence of the melting and boiling temperature of citric acid, that was found around 157°C and 175°C, respectively.

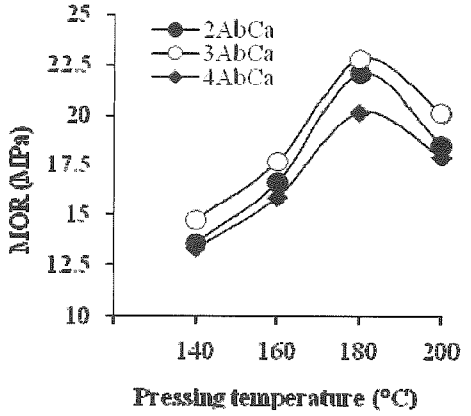

Fig 2. Tensile strength of molded products made from acacia bark (Ab) reinforced with citric acid (Ca) and pressed on 4 MPa for 10 mins. 2AbCa = 33.33% of Ca; 3AbCa = 25% of Ca and 4AbCa = 20% of Ca.

Therefore, it was made clear that the citric acid is a promising substitute for curing accelerator and binder in producing high performance molded products. This may be due to the carboxyl groups in the citric acid moieties that get bound to the hydroxyl groups on the bark via esterification process.

Investigation on "Sumiya", an important National Cultural Treasure in Kyoto

(Laboratory of Structural Function, RISH, Kyoto University)

Kohei Komatsu, Takuro Mori and Akihisa Kitamori

Sumiya is located at the place where about 300m south from Tanbaguch station of JR Sagano line. This building is well known as the place in which the members of Shinsen-gumi or Samurais in Meiji Restoration made a lot of actions and now is an important National Cultural Treasure being considered as the only surviving masterpiece of the architectural style of "Ageya"(a two story building where guests were escorted to the main sitting room on the second floor) in Japan. During the summer in 2008, our project team could have an important chance for investigating this novel cultural building from the wood science and technology point of view by accepting special budget admitted by the Chancellor of Kyoto University. Our team was constituted from the specialists of wood anatomy, degradation and preservation of wooden building, fine architectural techniques including coloring investigation and those who investigate timber structures and their seismic resisting performance.

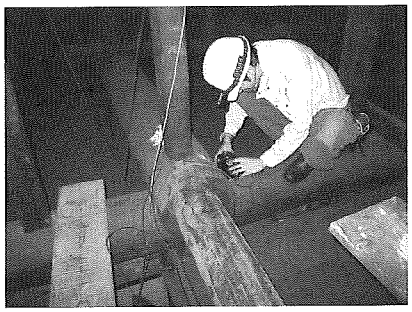

Photo1. Dr. Shimizu setting a precise velocity meter carefully on a roof girder.

One day in hot summer, our team spent busy time for investigating under floor level, inside of roof, or/and taking microscopic photographs of important wood particles. Photo.1 shows a scientist set a precise velocity meter on a roof girder for measuring micro vibration of building. Photo.2 shows a feature of micro vibration measurement of Syu-oku building. Owing to this series of investigations, so far as we know, quite complicated 3-D structures of Sumiya could be first appeared as shown in Figure 1 although this is still not perfect. This building composed of two part, one of which is "Omote-ya"(rectangular building) along street and the other of which is "Syu-oku" (rough square) located at inside. We predicted seismic resisting performance of these two buildings by assuming strength properties of mud shear walls, columns and so on. Consequently we got a conclusion that these two buildings might be collapsed as shown in Figure 2 if quite devastating earthquake attacks on them. At the end of 2008 fiscal year, we had a seminar for presenting our all research activities and concluded our project by publishing an final investigation report.

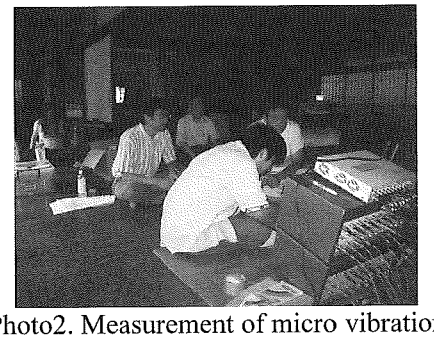

Photo2. Measurement of micro vibration of Syu-oku building.

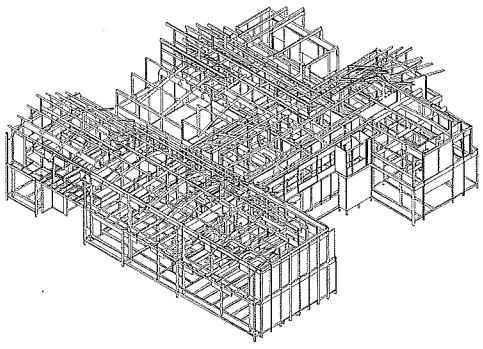

Figure1. Three dimensional image of Sumiya composed of Omote-ya (front side) and Syu-oku (upper side).

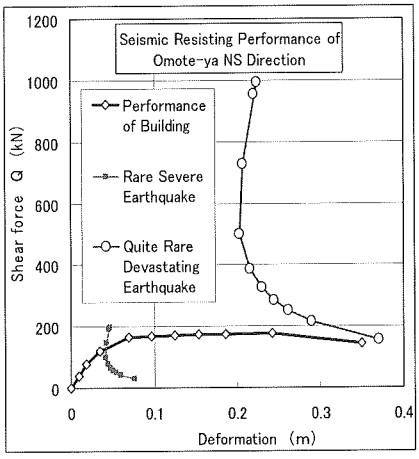

Figure2. Analytical result of the seismic resisting performance of Omote-ya.

Lithium insertion characteristics of carbonized Sugi (Cryptomeria japonica) wood sintered under high pressure

(Laboratory of Innovative Humano-habitability, RISH, Kyoto University)

Toshimitsu Hata

Much attention has focused on the development of negative electrode for lithium-ion batteries using nanostrutured carbons that have high storage capacity [1-3, Figure 1], as intrinsic irreversible capacity and high hysteresis have limited their practical application [4, 5]. The present paper reports on the effects of temperature during carbonization treatment, particle size and sintering conditions on the lithium insertion characteristics of the wood-based material.

Sugi (Cryptomeria japonica) wood was first carbonized in an electric furnace at 500°C and 700°C under argon at a heating rate of 4 °C/min. The carbonized wood was then sintered under vacuum in a pulse current sintering apparatus at up to 1050°C for 15 min. The resulting carbon material was investigated in a two-electrode cell against metallic lithium using 1 M $LiPF_6$ in EC/DEC as the electrolyte. The effects of textural and chemical characteristics of the material on electrochemical performance, including reversible and irreversible capacities, and cycleability, were analysed.

Our data showed a beneficial effect of optimizing the parameters such as the precarbonization treatment, the material particle size and the sintering process on improving the electrochemical performance of lithium cells. The materials sintered under high pressure showed a decrease in their irreversible capacity compared with materials prepared with a binder on a Cu foil. Although wood char is generally considered to consist of hard carbons, the galvanostatic characteristics of sintered carbons are very similar to those of soft carbons. The most effective sample (having the lowest irreversible capacity and highest reversible capacity) was prepared at 700°C with a particle size of 45-63 μm before sintering under pressure. Future studies will examine the porous texture of these materials in performing N_2 adsorption at 77K, in order to understand the effect of pressure during sintering and to further optimize their electrochemical performance.

Acknowledgements

This research was carried out with support from a Grant-in-Aid for Scientific Research (18380107) from the Ministry of Education, Culture, Sports, Science and Technology of Japan.

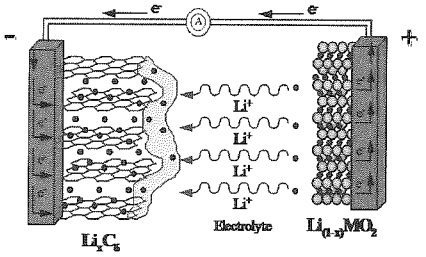

Figure 1. Electrode reactions in lithium ion cells.

References

[1] Dominko, R., M. Gaberŝĉek, J. Drofenik, M. Bele, S. Pejovnik, *Electrochemical and Solid-State Letters* 4(11) (2001) A87-A190.

[2] Letellier, M., F. Chevallier, C. Clinard, E. Frackowiak, J.-N. Rouzaud, F. Béguin, *Journal of Chemical Physics* 118(13) (2003) 6038-6045.

[3] Béguin F., F. Chevallier, C. Vix-Guterl, S. Saadallah, V. Bertagna, J.N. Rouzaud, E. Frackowiak. *Carbon* 43 (2005) 2160-2167.

[4] Frackowiak E., F. Béguin, *Carbon* 40(2002) 1775–1787.

[5] Béguin F., F. Chevallier, C. Vix, S. Saadallah, J.N. Rouzaud, E. Frackowiak, *Journal of Physics and Chemistry of Solids* 65 (2004) 211–217.

Nonlinear mechanisms of lower band and upper band VLF chorus emissions in the magnetosphere

(Laboratory of Computer Simulation for Humanospheric Sciences, RISH, Kyoto University)

Yoshiharu Omura, Mitsuru, Hikishima, Yuto Katoh, and Danny Summers

Coherent electromagnetic waves called chorus emissions have been frequently observed in the inner magnetosphere. Chorus emissions typically consist of a series of rising tones near the magnetic equator, excited by energetic electrons from several keV to tens of keV injected into the inner magnetosphere at the time of a geomagnetic disturbance.

We develop a nonlinear wave growth theory [1,2]of magnetospheric chorus emissions, taking into account the spatial inhomogeneity of the static magnetic field and the plasma density variation along the magnetic field line. We derive theoretical expressions for the nonlinear growth rate and the amplitude threshold for the generation of self-sustaining chorus emissions. We assume that nonlinear growth of a whistler-mode wave is initiated at the magnetic equator where the linear growth rate maximizes. Self-sustaining emissions become possible when the wave propagates away from the equator during which process the increasing gradients of the static magnetic field and electron density provide the conditions for nonlinear growth. The amplitude threshold is tested against both observational data and self-consistent particle simulations of the chorus emissions. The self-sustaining mechanism can result in a rising tone emission covering the frequency range of 0.1 - 0.7 of the equatorial electron gyrofrequency. During propagation higher frequencies are subject to stronger dispersion effects that can destroy the self-sustaining mechanism. We obtain a pair of coupled differential equations for the wave amplitude and frequency.

Solving the equations numerically, we reproduce a rising tone of VLF whistler-mode emissions that is continuous in frequency. Chorus emissions, however, characteristically occur in two distinct frequency ranges, a lower band and an upper band, separated at half the electron gyrofrequency as shown in Figure 1.. We explain the gap by means of the nonlinear damping of the longitudinal component of a slightly oblique whistler-mode wave packet propagating along the inhomogeneous static magnetic field.

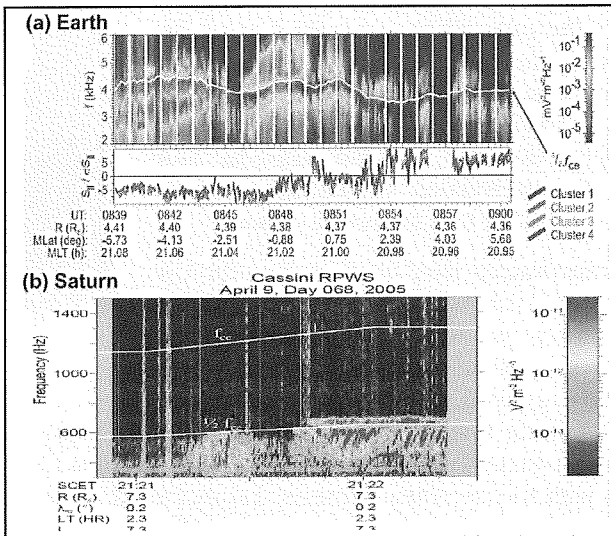

Figure 1 (a) Chorus emissions observed by the Cluster spacecraft in the Earth's magnetosphere (L = 4:4) [after Santolik et al., 2003].
(b) Chorus emissions observedby the Cassini spacecraft in Saturn's magnetosphere (L = 7:0) [after Hospodarsky et al.,2008].

References

[1] Y. Omura, , M. Hikishima, Y. Katoh, D. Summers, and S. Yagitani, "Nonlinear mechanisms of lower band and upper band VLF chorus emissions in the magnetosphere", *Journal Geophysical Research*, doi:10.1029/2009JA014206, in press, 2009.

[2] Y. Omura,Y. Katoh, and D. Summers, "Theory and simulation of the generation of whistler-mode chorus", *Journal Geophysical Research*, 113, A04223, doi:10.1029/2007JA012622, 2009.

Experiments of Microwave Power Transmission from an Airship

(Laboratory of Applied Radio Engineering for Sustainable Humanosphere, RISH, Kyoto University)

Tomohiko Mitani, Kozo Hashimoto, Naoki Shinohara

Our research group successfully conducted the world's first experiments of microwave power transmission from an airship to the ground. The objectives of the experiments are simultaneous transmission of electricity and information, technical verification of miniaturizing a microwave transmitting system, remote control of the system, and demonstrations of wireless power supply to electronic devices. This microwave power transmission system will be available for emergency power supply to a disaster area, helping search and rescue operations by the simultaneous transmission of electricity and information, etc.

The experiment system consists of a microwave transmitting system, a microwave receiving system, a retro-directive system and a telemetry system. In the microwave transmitting system, a 2.46GHz microwave power of 220W is radiated from two elements of radial line slot antennas (RLSA) fed by phase-controlled magnetrons at a frequency of 2.46GHz and each output power of 110W. The microwave power is received by the microwave receiving system, which consists of a set of 7cm-square rectennas (rectenna = antenna + rectifier) to convert from the microwave power to dc power, a dc-dc converter, and electronic devices (electronic buzzers, LEDs and cell phones) which work by the dc power. The retro-directive system makes a microwave beam transmit to the direction of arrival of a 5.8GHz pilot signal sent from the ground. The telemetry system controls and monitors the microwave transmitting system which is commanded by a PC on the ground.

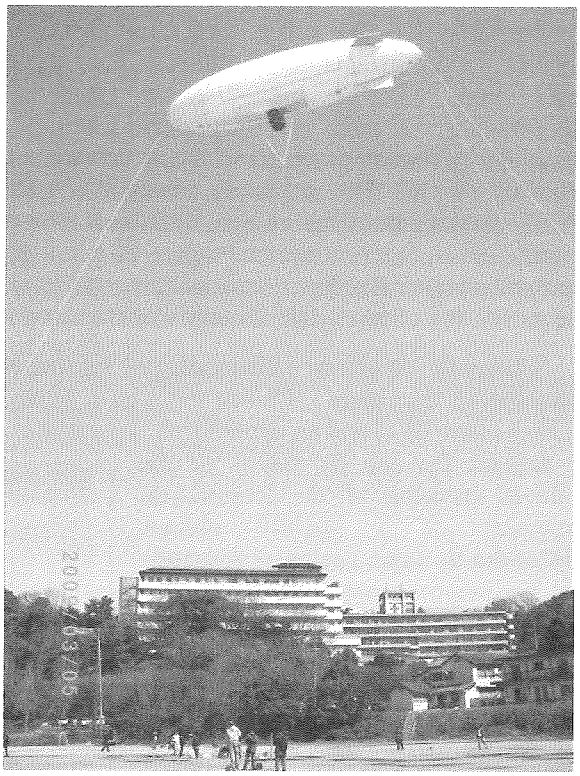

Figure 1. A photo of the experiment.

The experiments were conducted on the Uji ground, Kyoto University on March 5 and 10, 2009, as shown in Figure 1. An airship was launched at 33m altitude. The transmitting system was remotely operated from the ground. As soon as the transmitting system was turned on, electronic buzzers loudly sounded and LEDs brightly lit. We successfully demonstrated that an electronic buzzer and a LED worked by the wireless power supply from the airship with four rectenna elements, and that a cell phone charging system worked with twelve rectenna elements, the size of which is as large as A4 paper.

Acknowledgements

The experiments have been conducted under the leadership of Prof. Hiroshi Yamakawa (RISH). We would like to express our sincere appreciation to Mr. Teruo Fujiwara (Sho Engineering), Mr. Kenji Nagano (Space Technology), Prof. Shigeo Kawasaki (ISAS/JAXA), Mr. Takahiro Hirano, Mr. Fumito Takahashi and Mr. Hideaki Yonekura (our ex-students) for accomplishing the experiments. We are deeply grateful to Mr. Hideki Ueda and Prof. Makoto Ando (Tokyo Institute of Technology) for designing RLSAs, and we are greatly thankful to Mr. Takeshi Ikeyama and his crew in Makes Inc., for launching the airship.

Novel Space Environment Monitor, Instrument, and Space Mission Concepts

(Laboratory of Space Systems and Astronautics, RISH, Kyoto University)

Hiroshi Yamakawa, Hirotsugu Kojima, and Yoshikatsu Ueda

Near-Earth Asteroid Flyby Survey Mission Using Solar Sail

A novel near Earth (NEA) asteroid flyby survey scheme is proposed using solar sailing technology by reducing the orbital angular velocity of the solar sail and keeping the heliocentric distance constant. This realizes the potential for a very fast NEA survey mission of about one year from the time of launch, and could enhance the asteroid discovery rate. This scheme also has the potential for indirectly reducing the potential Earth impact risk by accumulating information about asteroids, as well as directly reducing this risk by utilizing the spacecraft as a kinetic impactor.

Lorentz Force Spacecraft Formation Dynamics

We proposed a spacecraft formation scheme augmented by Lorentz force using the interaction between an electro-statically charged satellite and the Earth's magnetic field to provide a thrust. The orbital dynamics is investigated and the existence of periodic orbits is shown which can be applied for near-future formation flight missions.

Magneto-Plasma Sail (MPS) Space Propulsion System

An MPS (Magneto-Plasma Sail) is a unique propulsion system, which travels through interplanetary space by capturing the energy of the solar wind, which inflates a weak original magnetic field made by a super-conducting coil of about 2-10 m in diameter with an assistance of a high-density plasma jet. From our theoretical estimations, momentum transfer from the solar wind to a spacecraft with a coil is large enough if the plasma source is operated to inflate only the magnetic field away from the spacecraft. Our activities in 2006 are as follows: (a) Sizing (mass, dimension, current, etc.) of the super-conducting coil to produce magnetic field around the spacecraft, (b) Preparation of the experiment facility to measure magnetic field, temperature, current etc. around super-conducting coil.

Monitor system for Space Electromagnetic Environments (MSEE)

The main objective of the MSEE (Monitor system for Space Electromagnetic Environments) is to monitor the electromagnetic disturbances caused by human activities in space. It consists of the small sensor units distributed around the target space. Our main activities on the development of the MSEE in 2006 are as follows: (a) Development of the analogue ASIC containing the differential amplifiers and A/D converters, (b) Simulation study on the location estimation method for each sensor unit.

Wave-Particle Correlator (WPC) Instrument for Spacecraft Observation.

For a practical application of a plasma wave instrument, a direct measurement system of wave-particle interactions is one of the important systems to the space science mission. WPC instrument can observe wave-particle interactions by calculation of the cross correlation functions between obtained waveforms and detected particles onboard. Our designed system is assembled in one FPGA (Field Programmable Gate Array) IC and data calibration and correlation method is programmed in FPGA.

Airship Experiment for Microwave Power Transmission Technology

A flight experiment aiming at exploring the applications of microwave transmission of power and information was conducted. The experiment configuration is composed of a flight system onboard an airship and ground system. Power on the order of several hundreds Watt is transmitted from the flight system, using a flat dish type antenna, onboard an airship at the altitude of approximately 30 m, to the ground system, downward and vertically. The receiving antenna on the ground collects the transmitted power, which is used for charging cell phones, lighting small bulbs, etc. The flight system is remotely controlled through the commands sent from the ground system to the onboard computer.

Professor emeritus Shoichiro Fukao was awarded the Medal with Purple Ribbon by the Japanese government

On 18 November 2008, Professor Emeritus Shoichiro Fukao was awarded the Medal with Purple Ribbon ("Shiju-hosho" in Japanese) for his outstanding contribution to the atmospheric science through atmospheric-radar development and studies. The Medal with Purple Ribbon is the medal for individuals who have contributed to academic and/or artistic developments, improvements and accomplishments.

Associate Professor Hiroyuki Hashiguchi was awarded the Horiuchi Prize by the Meteorological Society of Japan

On 20 November 2008, Associate Professor Hiroyuki Hashiguchi was awarded the Horiuchi Prize for his outstanding contribution to the development of Lower Troposphere Radar (LTR) and its application to observational studies of the atmosphere. The Horiuchi Prize is a prize for individuals who have contributed to development of meteorology or improvement of meteorological techniques through their investigations, studies or writing on boundary, adjoining, or unexplored fields of meteorology.

Mr. Hajime Fukuhara was awarded the British Interplanetary Society Award at the 59th International Astronautical Congress

Mr. Hajime Fukuhara (Graduate School of Engineering) was awarded the British Interplanetary Society Award (Best Student Paper Award) for his paper titled "System Design of One-Chip Wave Particle Interaction Analyzer for Future Space Plasma Observations" at the 59th International Astronautical Congress held in Glasgow, UK, October 2008.

Professor Kozo Hashimoto received IEICE fellow award for his contribution to the study on natural waves emitted from Earth and promotion of research on Solar Power Satellites

Professor Hashimoto contributed to establish IEICE (Institute of Electronics, Information and Communication Engineers of Japan) Technical Committee on Solar Power Satellite/Station (SPS) and served as its secretary and chairperson. He made a big contribution on the SPS whitepaper of the International Union of Radio Science (URSI) as an editor and author.
He obtained the results which solve international disputes on the propagation modes of natural electromagnetic waves of 100-kHz band which comes out of the auroral plasma of the earth by conducting ray tracings of the electric wave. He and his colleagues discovered electromagnetic waves which come out of equatorial plasma in a similar frequency band and the waves are later observed by various satellites. He contributed to the research on the electric wave which comes out from terrestrial plasma through these studies. Moreover, he had been involved with many wave observation instruments from their hardware design phase.

Professor emeritus Hiroshi Matsumoto was awarded the Booker Gold Medal at the XXIXth URSI General Assembly

On 10 August 2008, Professor emeritus Hiroshi Matsumoto (Former Director of RISH and Current President of Kyoto University) was awarded the Booker Gold Medal for his outstanding contributions to the understanding of nonlinear plasma wave processes, promotion of computer simulations in space plasma physics, and international leadership in plasma wave research at the XXIXth URSI (International Union of

Radio Science) General Assembly. The Booker Gold Medal, which honors the memory of Professor Henry G. Booker who served as URSI Vice President from 1969 to 1975 and Honorary President until his death in 1988, is awarded for outstanding contributions to telecommunications or a related discipline of direct interest to URSI.

Assistant Professor Tomohiko Mitani was awarded the 2008 URSI Young Scientists at the XXIXth URSI General Assembly

On 10 August 2008, Assistant Professor Tomohiko Mitani was awarded the 2008 URSI (International Union of Radio Science) Young Scientists for his paper titled "A Fundamental Study on Spectral Purity of a CW Magnetron for Microwave Power Transmission" at the XXIXth URSI General Assembly.

Characterization of *O*-methyltransferases and pinoresinol reductases involved in lignin and lignan biosynthesis

**(Graduate School of Agriculture,
Laboratory of Metabolic Science of Forest Plants and Microorganisms,
RISH, Kyoto University)**

Tomoyuki Nakatsubo

Fossil resource-based industrial society has provided us prosperity, especially in the developed countries. However, it has also brought serious negative impacts on the global environment due to the increase in the atmospheric concentration of carbon dioxide. Therefore, it is becoming more and more important to establish a sustainable and recycling-based society, which depends on renewable resources.

Wood biomass is the most abundant and potentially renewable resource and is composed mostly of secondary xylem which is formed through two metabolic events, cell-wall formation and heartwood formation. Hence, biochemical and molecular biological studies of cell-wall and heartwood formation provide the basic knowledge for establishing systems for sustainable production of wood biomass.

For the studies of cell-wall and heartwood formation, it is important to elucidate the biosynthetic mechanisms of phenylpropanoid, because the biosynthesis of phenylpropanoid is the principal metabolism of both cell-wall and heartwood formation. For example, lignin which is a phenylpropanoid polymer is one of the major cell wall components and lignans which are phenylpropanoid dimers are deposited in significant amounts in heartwood regions of trees.

Lignins and lignans are biosynthesized through the cinnamate/monolignol pathway and are closely related in terms of their chemical structures. Lignins are formed via non-enantioselective polymerization of monolignols, whereas typical lignans are formed by enantioselective coupling of two coniferyl alcohol units where central carbon (C8) atoms of the allyl moieties are linked to each other.

During plant development, lignins encase the cellulose microfibrils and confer mechanical strength to cell walls. Regardless of its importance during plant growth, lignins become problematic to post harvest, cellulose-based wood processing such as pulping and saccharification which leads eventually to bioethanol production. As a result, there has been long-standing incentive to develop healthy trees that accumulate less lignin and/or more removable lignin to facilitate pulping and saccharification, which depends largely on the knowledge of lignin biosynthetic mechanisms. On the other hand, lignans have a wide range of biological effects on various organisms, including humans, at molecular, enzymatic, physiological, pharmacological, and even clinical levels. Hence, lignans are considered to be involved in plant defense systems in living tissues, though less information is available on their function and role in the plants producing them. In addition, antimicrobial lignans which are biosynthesized in transition wood regions, i.e. the inner parts of sapwood, are deposited in significant amounts in heartwood and serve as preservatives to prevent heartwood rot. Because heartwood formation is specific to trees and does not occur in herbaceous plants, biosynthesis of lignans can be a clue to elucidating heartwood formation mechanisms.

The cinnamate/monolignol pathway supplies precursors for various phenylpropanoid compounds including lignins and lignans. Many studies of the cinnamate/monolignol pathway have been conducted in relation to lignin biosynthesis, except that a biosynthetic route for lignan biosynthesis via ferulic acid has been proposed recently. Maturing seeds of *Carthamus tinctorius* (safflower) accumulate both lignins and lignans, and their biosynthesis is initiated at particular points of maturation. This species therefore a good plant material for comparative studies of lignin and lignan biosyntheses.

In the present study, the author aimed to elucidate the difference of lignin and lignan biosynthetic mechanisms. The author cloned caffeoyl CoA *O*-methyltransferase (CtCoAOMT) and 5-hydroxyconiferaldehyde *O*-methyltransferase (CtCAldOMT) that are key enzymes of the cinnamate/monolignol pathway from maturing seeds of *C. tinctorius* and examined the participation of each OMT clone to lignin or lignan biosynthesis. In addition, the author cloned novel *O*-methyltransferase from maturing seeds of *C. tinctorius* and showed that the OMT, named 5-hydroxyconiferaldehyde/5-hydroxyconiferyl alcohol OMT (CtAAOMT), is involved in lignin

biosynthesis.

Umezawa in the author's laboratory cloned the novel gene encoding lignan *O*-methyltransferase (matairesinol *O*-methyltransferase, CtMROMT) from maturing seeds of *C. tinctorius*. In addition, another cDNA which shows a high sequence similarity to *CtMROMT*, named tentatively *CtMROMTlike*, was cloned. In the present study, the author examined its function and found that the *bona fide* function of CtMROMTlike is flavonoid OMT and referred to the OMT as *C. tinctorius* flavonoid OMT1 (CtFOMT1).

At present, a number of genes encoding enzymes involved in lignan biosynthesis have cloned from several plant species. For analyzing the functions of those genes in detail, it is necessary to produce the transformants where the expression of target genes is up- or down-regulated. However, it was very difficult because gene transformation and regeneration systems for plants which are known as lignan producers including *C. tinctorius* were very limited. On the other hand, *Arabidopsis thaliana* is the most widely used model plant in plant bioscience sectors. Thus, the genome sequence is available, and its transformation and regeneration are very easy. So far, there has been no report of isolation of lignans from *A. thaliana*. However, in the *A. thaliana* genome database, there are two genes that are annotated as pinoresinol/lariciresinol reductase (PLR) that is key enzyme of lignan biosynthesis. In this context, the author analyzed the methanol extracts of *A. thaliana*, and found the presence of lignan lariciresinol in the roots. This means *A. thaliana* can be exploited for lignan biosynthetic studies. Therefore, as a first step to elucidate the difference between lignin and lignan biosynthetic mechanisms in *A. thaliana*, the functions of two *A. thaliana* genes that are annotated as PLR were characterized. The author demonstrated that *Arabidopsis thaliana* PLRs showed strict substrate preference towards pinoresinol, but only weak or no activity towards lariciresinol, unlike conventional PLRs, indicating their *bona fide* function is *A. thaliana* pinoresinol reductase (AtPrR). It was also demonstrated that the enantiomeric composition of lariciresinol in *A. thaliana* can be controlled by the differential expression of two *AtPrR*s by using biochemical characterization of their recombinant enzymes and spaciotemporal expression analysis of the genes. Next, the function of *A. thaliana* gene, At5g54160 annotated as caffeic acid *O*-methyltransferase that is a key enzyme of cinnamate/monolignol pathway was characterized and revealed the participation of At5g54160 gene in lignin biosynthesis.

Studies on extracellular metabolites of white rot basidiomycete involved in selective lignin degradation

**(Graduate School of Agriculture,
Laboratory of Biomass Conversion, RISH, Kyoto University)**

Hiroshi Nishimura

Photosynthetic plants are the principal solar energy converter sustaining life on Earth. In particular, woody plant is the most abundant carbon fixed in terrestrial and an important renewable organic resource. In recent years, the global warming and environmental pollution caused by excessive use of fossil fuels became serious problem for our environment. Hence, it is an urgent task to utilize wood biomass as energy and chemical resources, in harmony with environmental safeguard.

In biological conversion of woody biomass, selective lignin degradation is a key process because cell wall polysaccharides in wood are surrounded by lignin. In nature, the degradation of lignin in wood occurs primarily through the action of lignin-degrading basidiomycetes called white rot fungi; consequently, this ecological group has received a considerable amount of research attention. Most of white rot fungi simultaneously decompose lignin and cellulose, accompanied by erosion of wood cell walls, while some fungi called selective white rot fungi, such as *Ceriporiopsis subvermispora* are able to degrade lignin without intensive damage of cellulose [1, 2].

Previous studies revealed that selective lignin degradation by *C. subvermispora* is catalyzed by low molecular weight metabolites at a site far from extracellular enzymes and fungal hyphae. For the possible wood decay system, an *in situ* radical generating system by lipid peroxidation initiated with manganese peroxidase (MnP) or its oxidation products, diffusible manganic chelates has been proposed. In selective white rot, control of cellulolytic active oxygen species, hydroxyl radicals by ceriporic acids has also been proposed as a central system to suppress cellulose depolymerization. However, mechanisms behind the selective ligninolysis after incipient stage of wood decay are not well understood. The present doctoral thesis aimed at elucidating the unique wood decay mechanism by analyzing structure and functions of key extracellular metabolites in sheath, a glucan matrix interfacing fungal hyphae and wood cell wall regions.

Regarding the extracellular metabolites of *C. subvermispora*, three novel alkylitaconic acids—tetradecylitaconic (ceriporic acid A), hexadecylitaconic (ceriporic acid B) and (*Z*)-7-hexadecenylitaconic acid (ceriporic acid C) have been isolated and identified [3–5]. Production of a trace amount of the other alkenylitaconic acids with different chain lengths has been suggested by GC–MS of crude extracts from eucalyptus wood cultures of *C. subvermisopra* [6] but only the three metabolites, ceriporic acids A, B and C were so far isolated. The molecular functions of ceriporic acids have been analyzed in relation to the control of production of active oxygen species. An important function of ceriporic acid is inhibition of cellulose degradation by hydroxyl radicals ($HO^{\bullet}$) produced in the Fenton reaction system [7–9]. In brown rot and non-selective white rot fungi, a cellulolytic active oxygen species, $HO^{\bullet}$ is a principal low-molecular mass oxidant that erodes wood cell walls to enhance the accessibility of the extracellular enzymes. This is because phenols are good reductants of Fe^{3+}, and reductive radicals such as formate anion and semiquinone radicals from oxalate and benzoquinones reduce molecular oxygen to yield superoxide, which in turn disproportionates into H_2O_2 or reduces Fe^{3+} to Fe^{2+}. Reduction of Fe^{3+} and formation of H_2O_2 leads to the production of $HO^{\bullet}$. In selective ligninolysis in an environment where free radicals and lignin-derived phenols are produced in the presence of O_2 and Fe ions, suppression of the Fenton reaction system by ceriporic acid is essential.

In this thesis, the author profiled metabolites pooled in the extracellular sheath, and found that *C. subvermispora* secretes a series of ceriporic acids and other metabolites. It was found that *C. subvermispora* produce a new ceriporic acid derivative bearing (*E*)-7-hexadecenyl chain from the culture of *C. subvermispora*. To identify the natural metabolite, (*E*)- and (*Z*)-7-hexadecenylitaconic acids were chemically synthesized. The new metabolite isolated was identical to the synthetic (*E*)-hexadecenylitaconic acid, and designated as ceriporic acid D. *De novo* synthesis of the *cis*- (ceriporic acid C) and *trans*-7-hexadecenylitaconic acids (ceriporic acid D) was demonstrated by feeding experiments

with [^{13}C-U]-glucose. The biosynthesis of ceriporic acid D was discussed with a focus on the formation of *trans*-desaturated bond, in comparison with structurally-related lichen acids [10]. Ceriporic acids have an asymmetric centre at carbon-3, but absolute configuration has not been determined. The author determined absolute configuration of ceriporic acid as *R* by measuring NMR spectra of the natural and synthetic compound with a chiral shift reagent. Considering an asymmetry of the chiral center and a possible biosynthetic pathway of ceriporic acids involving in the condensation of acyl-CoA and oxaloacetate, it was proposed that ceriporic acids are biosynthesized through attack of acyl-CoA to the *re* face of a keto carbonyl group of oxaloacetate. The stereospecificity is opposite to most of citrate synthase. Absolute configuration of ceriporic acids and structurally related lichen acids was reviewed [11].

In conclusion, the author analyzed metabolites pooled in the extracellular sheath, and found that *C. subvermispora* secretes a series of ceriporic acids and other metabolites. Structural analyses and function analyses of these metabolites involved in selective lignolysis were demonstrated and described the unique wood decay mechanism.

References

[1] Messner, K., Srebotnik, E. (1994) FEMS Microbiol. Reviews 13, 351–364.
[2] Blanchette, R.A., Krueger, E.W., Haight, J.E., Akhtar, M., Akin, D.E. (1997) J. Biotechnol. 53, 203–213.
[3] Enoki, M., Watanabe, T., Nakagame, S., Koller, K., Messner, K., Honda, Y., Kuwahara, M. (1999) FEMS Microbiol. Lett. 180, 205–211.
[4] Enoki, M., Watanabe, T., Honda, Y., Kuwahara, M. (2000) Chem. Lett., 54–55.
[5] Amirta, R., Fujimori, K., Shirai, N., Honda, Y., Watanabe, T. (2003) Chem. Phys. Lipids 126, 121–131.
[6] del Rio, J.C., Gutierrez, A., Martinez, M.J., Martinez, A.T. (2002) Rapid. Commun. Mass. Spectrom. 16, 62–68.
[7] Watanabe, T., Teranishi, H., Honda, Y., Kuwahara, M. (2002) Biochem. Biophys. Res. Commun. 297, 918–923.
[8] Rahmawati, N., Ohashi, Y., Watanabe, T., Honda, Y., Watanabe, T. (2005) Biomacromolecules 6, 2851–2856.
[9] Ohashi, Y., Kan, Y., Watanabe, T., Honda, Y., Watanabe, T. (2007) Org. Biomol. Chem. 5, 840–847.
[10] Nishimura, H., Tsuda, S., Shimizu, H., Ohashi, Y., Watanabe, T., Honda, Y., Watanabe, T. (2008) Phytochemistry 69, 2593–2602.
[11] Nishimura, H., Murayama, K., Watanabe, T., Honda, Y., Watanabe, T. (2009) Chem. Phys. Lipids, 159, 77-80.

Regulation and physiological function of C5 isoprenoid metabolites in plastids.

(Graduate School of Agriculture, Laboratory of Plant Gene Expression, RISH, Kyoto University)

Kanako Sasaki

Isoprenoids, a diverse group of compounds derived from the five-carbon building units, isopentenyl diphosphate (IPP) and its isomer dimethylallyl diphosphate (DMAPP), are essential for survival in all organisms. In higher plants, IPP and DMAPP are biosynthesized via two pathways, mevalonate pathway localized in cytosol and MEP pathway in plastid. Various plant secondary metabolites such as isoprene, monoterpene, carotenoid, prenylated compounds, are derived from MEP pathway. I have first demonstrated why many plant species emit isoprene, and then performed the molecular cloning and characterization of prenyltransferases involved in biosynthesis of prenylated flavonoids.

Isoprene emission – its physiological role in plants

Isoprene is a volatile C5 isoprenoid emitted from leaves of many plants [1]. Despite its massive amount, the physiological function of isoprene emission from plants is not well understood. In this study, I have cloned isoprene synthase cDNA from *Populus alba* (*PaIspS*) to analyze the gene expression to environmental changes. *PaIspS* was strongly induced by heat treatment, and was substantially decreased in the dark, suggesting that isoprene emission was regulated by light at the transcriptional level [2]. Then, I prepared transgenic *Arabidopsis thaliana* overexpressing *PaIspS* gene, which is thought to be a non-isoprene emitter. A striking difference was observed when both transgenic and wild type plants were treated with heat at 60˚C for 2.5 hr, i.e. transformants revealed clear heat tolerance compared to the wild type (Figure 1). High isoprene emission and a decrease in the leaf surface temperature were observed in transgenic plants during the heat stress treatment [3]. Contrary, neither strong light nor drought treatments gave an apparent difference. These data suggest that the isoprene emission plays a crucial role as a heat protection mechanism in plants.

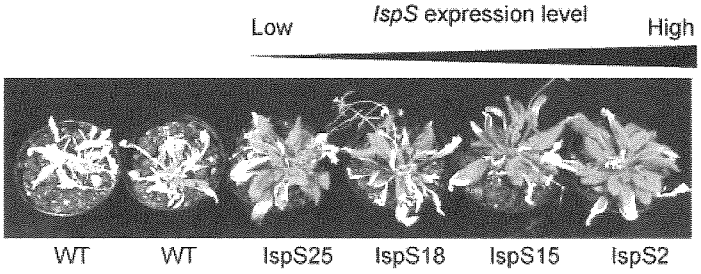

Figure 1. Heat treatment (60˚C for 2.5 hr) of transgenic and wild-type plants (4-week-old).

Discovery of the first gene for flavonoid-specific prenyltransferase

The prenylation of aromatic compounds is a major contributor to the diversification of plant secondary metabolites due to differences in prenylation position on the aromatic ring, various length of prenyl side chain, and further modifications of the prenyl moiety, e.g. cyclization and hydroxylation, resulting in the occurrence of more than 1,000 prenylated compounds in plants. In particular, prenylated flavonoids in higher plants protect them by exhibiting strong antibacterial and antifungal activities [4]. Also, many prenylated flavonoids have been identified as active components in medicinal plants with biological activities, such as anti-tumor, anti-androgen, anti-leishmania, and anti-NO production. Due to the beneficial effects for human health, prenylated flavonoids are of particular interest as lead compounds for producing new drugs and functional foods. The prenylation of the flavonoid core increases the

lipophilicity and the membrane permeability, which is one of the proposed reasons for the enhanced biological activities of prenylated flavonoids [5]. However, none of genes responsible for the prenylation reactions have been identified for more than 30 years in this research field.

I have isolated a prenyltransferase gene from *Sophora flavescens*, *SfN8DT-1*, responsible for the prenylation of the flavonoid naringenin at the 8-position, which is specific for flavanones and dimethylallyl diphosphate as substrates (Figure 2) [6]. Phylogenetic analysis shows that SfN8DT-1 has the same evolutionary origin as prenyltransferases for vitamin E and plastoquinone. The gene expression of *SfN8DT-1* is strictly limited to the root bark where prenylated flavonoids are solely accumulated *in planta*. The ectopic expression of *SfN8DT-1* in *Arabidopsis thaliana* resulted in the formation of prenylated apigenin, quercetin, and kaempferol, as well as 8-dimethylallylnaringenin. SfN8DT-1 represents the first flavonoid-specific prenyltransferase identified in plants and paves the way for the identification and characterization of further genes responsible for the production of this large and important class of secondary metabolites.

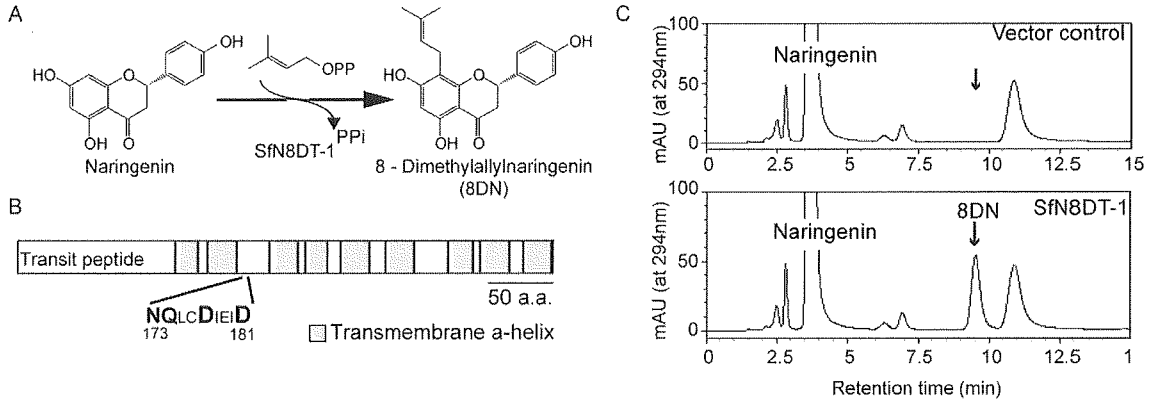

Figure 2. Enzymatic characterization of recombinant SfN8DT-1 expressed in yeast.

(A) Prenylation reaction of naringenin by SfN8DT-1.

(B) Structural features of the SfN8DT-1 polypeptide.

(C) HPLC chromatograms of ethyl acetate extract of incubation mixture of naringenin and DMAPP with recombinant protein.

References

[1] Guenther A, Hewitt CN, Erickson D, Fall R, Geron C, Graedel T, Harley P, Klinger L, Lerdau M, Mckay WA, Pierce T, Scholes B, Steinbrecher R, Tallamraju R, Taylor J, Zimmerman P. "A global model of natural volatile organic compound emissions.", *J Geophys Res,* vol. 100, pp. 8873-8892, 1995.

[2] Sasaki K, Ohara K, Yazaki K. "Gene expression and characterization of isoprene synthase from *Populus alba.*", *FEBS lett*, vol. 579, pp. 2514-2518, 2005.

[3] Sasaki K, Saito T, Lämsä M, Oksman-Caldentey KM, Suzuki M, Ohyama K, Muranaka T, Ohara K, Yazaki K. "Plants utilize isoprene emission as a thermotolerance mechanism.", *Plant Cell Physiol*, vol. 48, pp. 1254-1262, 2007.

[4] Botta B, Vitali A, Menendez P, Misiti D, Delle Monache G. "Prenylated flavonoids: Pharmacology and biotechnology. ", *Curr Med Chem*, vol. 12, pp. 713-739, 2005.

[5] Wang BH, Ternai B, Polya G. "Specific inhibition of cyclic AMP-dependent protein kinase by warangalone and robustic acid.", *Phytochemistry,* vol. 44, pp. 787-796, 1997.

[6] Sasaki K, Mito K, Ohara K, Yamamoto H, Yazaki K. "Cloning and characterization of naringenin 8-prenyltransferases, a flavonoid-specific prenyltransferase of *Sophora flavescens.*", *Plant Physiol,* vol. 146, pp. 1075-1084, 2008.

Evaluation of Mechanical Behavior on Traditional Timber Interlock Joint and Its Structural Applications

**(Graduate School of Agriculture,
Laboratory of Structural Function, RISH, Kyoto University)**

Akihisa Kitamori

Japanese traditional timber structures mainly consist of interlock joints and therefore have lasted against earthquakes. This is because resistance of the interlock joint depends on compression perpendicular to the wood grain and friction between wood members, which are able to show large ductile deformation different from other wooden characteristics. However detailed study has not been performed about mechanical behavior of the joint. In this study, Nuki joint as a representative of traditional joints was investigated especially being focused on the initial stiffness. The re-evaluation on the mechanical behavior of the joint and structural elements was carried out depending on the latest knowledge and technology, and its practical application to the modern building was considered by giving improvement on the joint. There have been a lot of remained uncertain factors on the evaluation of interlock joints. Therefore, quantitative approach was performed step by step in each level of structural components, which are material, joint and structural element, fundamentally by depending on mechanical models and experiment, aiming to contribute to the improvement of accuracy of design method.

Firstly, in terms of material properties, embedment and friction characteristics were studied. Especially the influence of supporting condition on the apparent elastic modulus of partial compression was focused. A finite element method was used in order to investigate the difference of surface deformation between the models with different additional length and boundary conditions. Those tendency obtained by the model was verified by the accurate experimental result in which the influence of friction was removed. Finally factors of surface deformation were proposed on the equations for structural designing [1]. Moreover, basic material properties such as elastic modulus and strength on compression perpendicular to the grain, and coefficient of friction were analyzed depending on the experiment, and their influence on the embedment property was quantitatively verified. As a result, the problem of double standard in terms of usage of material properties was solved on current design formulas.

Then structural behavior in the joint level was studied focusing on Nuki joint in which embedment and friction are the fundamental resisting factors. In particular, the influence on the stiffness by wedge insertion and generation of gap were studied, which have been neglected in practical design though high improvement with wedges or reduction by gaps on the stiffness are observed in actual experiments. Those influences were analyzed in detail depending on mechanical model and mechanical properties proposed in previous investigation. Consequently simple equations were introduced which are able to estimate the rotational behavior of Nuki joint to the extent of plastic range, and those estimated curves showed satisfactory agreement with experimental results [2].

As a next step, the aforementioned results were applied on the analysis of structural element, i.e. the lattice shear wall. The lattice shear wall is consist of many number of half-lap joints, which mechanism of resistance is almost as same as Nuki joint, and is

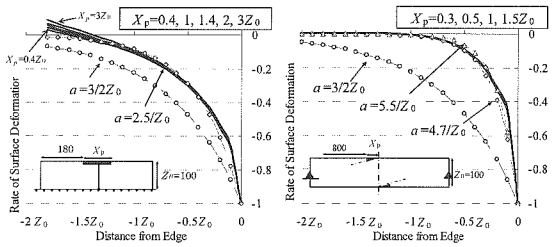

Figure 1. FE result of surface deformation at additional part in different support condition.

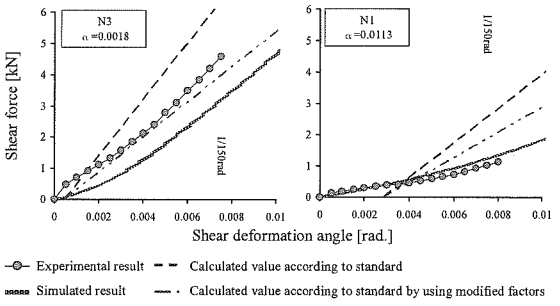

Figure 2. Example of simulated and experimental results on shearing of lattice shear wall.

regarded as one of the important structural element to reinforce traditional buildings such as Machiya residential house by virtue of its ductile load carrying capacity. The simulating analysis on the initial stiffness was performed by taking the variation of gap generation between each individual joint into account. At the same time, the long term evaluation on the behavior of shear wall was carried out by periodically applying load on the same specimen over one year. As a consequence, the result of simulated agreed very well with that of experimental, and the influence of clearance of the joint on shear-resistance-factor was quantitatively clarified [3].

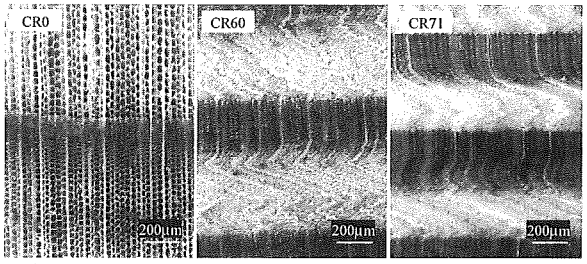

Figure 3. Difference in the section of compressed wood in accordance with compression ratio.

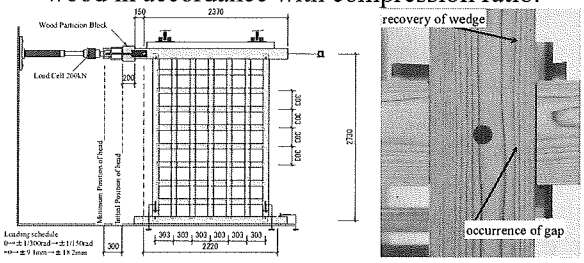

Figure 4. Test setup and detail of joint on lattice shear wall with compressed wooden wedges.

By taking above results into consideration, an application of compressed wooden fasteners into the traditional joint was investigated. Compressed wood is manufactured by compressing softwood in radial direction with moderate heat and high pressure, which is thought to be suitable for the use in traditional construction. Moreover since compressed wood spring back gradually when being subjected cyclic humidity change, it is expected to work to compensate for the gap generation so that the initial stiffness of the joint is sustainable. In order to verify those characteristics more clearly, stress relaxation test was carried out. Consequently it was found out that compressed wood can work in terms of not only recovering its dimension but also maintaining compressive stress between timber bodies when compression ratio is high. Besides, fundamental mechanical properties of compressed wood were investigated with focusing its use as structural elements. In result, calculation formulas which include only compression ratio and original mechanical properties were introduced [4] which is expected to contribute to the optimal design of compressed wood as fasteners.

Based on the results in previous section, the effect of compressed wooden fasters was studied in the case they were used in traditional structural elements such as Nuki joint or lattice shear wall. As a result of long term experiment on structural behavior, the sustainable capacity on stiffness was verified [5]. This means that mechanical behavior of traditional joint became more independent from duration of time and accumulation of damages.

Through the above-mentioned findings, the reliability on the design of traditional structures which consist of interlock joints became more improved, which is expected to lead to the better recognition on traditional techniques and the promotion of timber structure in long-life buildings.

References

[1] A. Kitamori, T. Mori, Y. Kataoka, K. Komatsu, "Effect of Additional Length on Partial Compression Perpendicular to the Grain of Wood -Difference among the supporting conditions", *Journal of Structural and Construction Engineering, Transactions of AIJ*, in press.

[2] A. Kitamori, Y. Kato, Y. Kataoka, K. Komatsu, "Proposal of Mechanical Model for Beam- Column 'Nuki' Joint in Traditional Timber Structures" *Mokuzai Gakkaishi*, vol. 49, no. 3, pp. 179-186, 2003.

[3] A. Kitamori, K. Jung, M. Minami, K. Komatsu, "Evaluation on Stiffness of Lattice Sehar Wall -Influence of gap and its verification by long term test-" *Journal of Structural Engineering*, vol. 55B, pp. 109-116, 2009.

[4] A. Kitamori, K. Jung, T. Mori, K. Komatsu, "The Evaluation on Mechanical Properties of Compressed Wood in accordance with the Compression Rate", *Proceedings of the IAWPS2008*, Vol.1(CD), 2008.

[5] A. Kitamori, K. Jung, M. Minami, K. Komatsu, "Improvement of Shear Resistance on Traditional Lattice Shear Wall", *Proceedings of the 10th world conference on timber engineering*, Vol.1(CD), 2008.

Anatomical study of the degradation of canker wood in tropical trees and identification of the causal fungi

(Laboratory of Innovative Humano-habitability, RISH, Kyoto University)

Erwin

Many studies have reported fungal stem canker diseases associated with wood decay in various species of tropical forest trees, either in plantation forest, e.g. *Acacia mangium* [1] and *Gmelina arborea* [2], or in natural forest and rubber plantations, e.g. *Shorea smithiana* [3] and *Hevea brasiliensis* [4]. Generally, the trees exhibit localized dead areas in the bark, cracks and ruptures on the surfaces of the bark near the canker zone, and apparently decayed exposed sapwood.

Microscopic observations have been conducted to reveal the anatomical features of the xylem of meranti trees [light red meranti (*Shorea smithiana*) and yellow meranti (*Shorea gibbosa*)] and rubberwood (*Hevea brasiliensis*) infected with stem canker [5,6]. Although microscopic observation techniques are not directly applicable to field use, they can provide valuable information for understanding the altered properties of infected xylem. By microscopic observation, the decay pattern of the infected xylem also can be categorized easily and a preliminary identification made of the causal microorganism.

In *S. smithiana* and *S. gibbosa* canker, intensive degradation of xylem cells in the canker margin was conspicuous (Fig. 1). In the degraded xylem, patterns of simultaneous white-rot fungi, such as thinning of cell walls, bore hole formation, rounded pit erosion and eroded channel opening, as well as large voids resulting from the coalition of completely removed xylem cells, could be well recognized. However, the extent of cell damage in *S. smithiana* xylem was higher than that in *S. gibbosa*. In degraded xylem of *S. smithiana*, erosion troughs and numerous conspicuous holes in cell walls were more obvious, and the large voids resulting from the coalition of completely removed cells were also severely enlarged and extended.

The isolation of decay fungi and their identification in affected xylem of cankerous trees is a useful method of detecting their presence in decayed xylem. By phylogenetic analysis based on the sequences of the internal transcribed spacer region of rDNA, Basidiomycete fungi isolated from the decayed xylem of *S. smithiana* and *S. gibbosa* canker were identified as *Schizophyllum commune* and *Phlebia breviospora*, respectively. This is the first report of successful isolation of decay fungi from *S. smithiana* and *S. gibbosa* canker. Therefore, the results of this study could be a useful reference for further pathological studies of tropical trees.

The anatomical changes caused by the isolated decay fungi in the laboratory could provide the basis for diagnosing and evaluating decay by *S. commune* and *P. breviospora* on *S. smithiana* and *S. gibbosa* wood, respectively. In laboratory conditions, simultaneous white rot of *S. smithiana* and *S. gibbosa* wood caused by *S. commune* and *P. brevispora*, respectively, was well characterized. Their decay patterns were similar to those of the decayed xylem of *S. smithiana* and *S. gibbosa* cankerous trees in field conditions. In *S. smithiana* wood, slight erosion of wood cell walls over 12 weeks' incubation with *S. commune* resulted in a small weight loss and could be classified as the early stage of simultaneous decay. These results showed that *S. commune* was a serious destroyer of wood under natural conditions, especially in tropical regions, but caused little wood decay *in vitro*. Meanwhile, in *S. gibbosa* infected with *P. brevispora*, the intermediate decay features of numerous, conspicuous holes as well as erosion troughs in cell walls were found after 8 weeks' incubation. Furthermore, complete degradation of wood cell components, defined as the advanced stage of decay, was found in some areas of wood after 12 weeks' incubation *in vitro*.

In *H. brasiliensis* canker, typical characteristics of infected xylem were confirmed by the presence of abnormal xylem formation in the vicinity of enclosed bark in the stem as well as xylem decay in the canker margin. The abnormal xylem contained fewer shorter vessels of smaller diameter, and significantly wider rays compared with normal xylem, and around the wide growth zones of the canker, axial cells were disoriented and warped towards the canker zones. The decayed xylem exhibited separation among cells and rounded pit erosion, similar to that seen in decay caused by white-rot fungi. I considered that even though the bark was tapped repeatedly, while the trees were still actively producing latex canker did not occur on *H. brasiliensis* stems. Apparently, the latex acts as an antifungal compound and plays an important role in restricting fungal infection of the wounded tissues, so that the fully developed surface callus could

completely close the bark wound when wound cambium had formed. Canker disease on *H. brasiliensis* was assumed to be initiated by unhampered pathogen infection of the open wound of the tapping bark, when the trees were not producing latex or when their latex yield was extremely low.

To increase our understanding of canker wood in tropical trees, the progress of infection by pathogenic fungi should be studied in different types of plantation forest using various kinds of trees and under different physiological conditions.

Plantation forests are increasing in tropical countries. In East Kalimantan, Borneo, plantations of rubberwood and meranti species are increasing. Because high quality timber from these plantation forests is in strong demand, cankerous wood should be reduced by introducing cultural methods to prevent infection by pathogenic fungi.

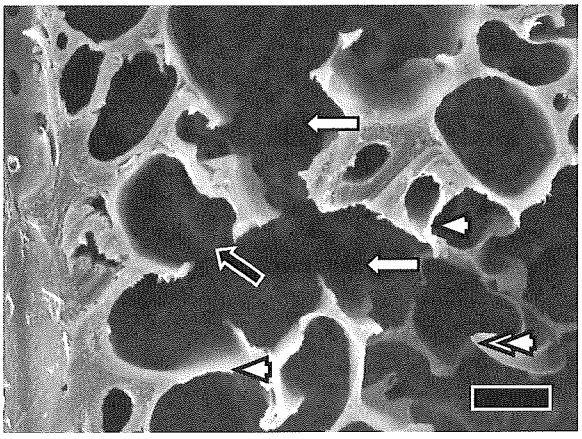

Fig. 1. Decay features of xylem in the canker margin of *S. smithiana*. Note thinning (single head arrows) and collapse (double head arrow) of the cell walls, erosion channel (black arrow), and complete removal of cells (white arrows), which simultaneously occurred in one region of decay. *Bar* 10 μ

REFERENCES

[1] Old KM, See LS, Sharma JK, Yuan ZQ (2000) Center for International Forestry Research, Jakarta, pp 7–8
[2] Erwin (2001) Rimba Kalimantan 5:67–77
[3] Mardji D (1999) Workshop proceedings: Rehabilitation of degraded tropical forest ecosystems. Bogor, pp 45–56
[4] Bao E (2003) Food and Agriculture Organization of the United Nations. Rome
[5] Erwin, Takemoto S, Hwang WJ, Takeuchi M, Itoh T and Imamura Y (2008) J Wood Sci 54:233–241
[6] Erwin, Hwang WJ and Imamura Y (2008) J Wood Sci (DOI 10.1007/s10086-008-0959-3)

Designing and Development of Novel Chelating Method for Extraction of Heavy Metals from Chromated Copper Arsenate (CCA)-treated Wood

(Laboratory of Innovative Humano-habitability, RISH, Kyoto University, Present: Tsukuba Research Institute, Sumitomo Forestry Co., Ltd.)

Tomo Kakitani

Most wood material used for houses, utility poles, ground sills and other structural materials in damp conditions are generally treated with preservatives to enhance the durability. Some wood preservatives include chromated copper arsenate (CCA), ammoniacal copper quaternary compound-based wood preservative (ACQ), and copper azole compound-based wood preservative (CuAz) and other water-borne wood preservatives.

Among wood treated with preservatives, CCA-treated wood has been widely used because of its high performance against attack from fungi with a very wide antimicrobial spectrum and from termites, as well as against weathering over long periods of time. Although treatment with CCA has held the majority of the market share for pressure-treated wood preservation for a long period, increasing environmental regulations and disposal problems, particularly during wood combustion, have resulted in manufacturers limiting production of CCA-treated wood.

The present study focuses on designing and development of a novel solvent, in particular chelate, extraction process, which can easily and efficiently remove toxic metals of chromium, copper and arsenic from CCA-treated wood, and copper from ACQ-treated wood and CuAz-treated wood.

The extractability of CCA metals with various types of solvents, inorganic and organic acids, was studied [1] at first. The solvents of sulfuric, phosphoric, citric and oxalic acid, were relatively effective to remove CCA metals but these were too severe for wood. Thus more moderate solvent extraction condition should be needed.

The behavior of arsenic during pyrolysis of CCA-treated wood and the effect of pyrolysis on the extractability of CCA metals were studied [2, 3]. It was found that there are two possible ways of release of arsenic during pyrolysis. The first possible pathway is caused by reacted arsenic compound, $CrAsO_4$, which appears to be released at around 400-500°C. The second possible pathway is caused by unreacted arsenic compound, As_2O_5, in CCA-treated wood, which appears to be released at a much lower temperature than chromium arsenate, possibly 200°C.

Based on this result, pyrolysis of CCA-treated wood was conducted carefully without loss of arsenic. The results showed that the resistance of CCA metals to extraction increased drastically after pyrolysis. The toxic metals in CCA-treated wood were highly stabilized by heating at 300°C for 60 min. Immobilization of toxic metals in the residue was promoted by pyrolysis, resulting in the transformation of toxic metals to various types of stable compounds.

Various types of two-step extraction were designed and tested on CCA-treated wood instead of simple solvent extraction [4]. Among them, we found the best combination was oxalic acid as the 1st step and bioxalate (BO) solution, pH adjusted oxalic acid with sodium hydroxide, at pH=3.2 as the 2nd step. The latter conditions efficiently removed almost all CCA metals, approximately 90%, from treated wood powder in 3 hours extraction following the 1 hour pre-extraction by oxalic acid. However, the bioxalate solution under alkaline conditions (pH=11.2) proved ineffective.

Application of one-step metal extraction, that would effectively remove CCA metals from treated wood powder or chips with BO, was conducted [5]. A BO solution consisting of 0.125 M oxalic acid adjusted to pH 3.2 with sodium hydroxide was tested for its ability to extract chromium, copper and arsenic, from CCA-treated wood in single step (at 75°C). The extraction proceeded efficiently with 6 hours of treatment, and was insensitive to the differences in chemical characteristics, including solubility of individual metals. The preferential extractability for copper from CCA-treated wood was observed, although acid extraction, in general, tends to extract arsenic preferentially. After 6 hours of treatment, approximately 90% of chromium, copper and arsenic were effectively removed from CCA-treated wood.

The characteristics of the BO chelating extraction process for CCA metals were studied as a function of solvent pH, BO concentration, extraction temperature and liquid to solid ratio, and with various alkaline metal hydroxides as pH-adjusting reagents. The experimental results showed that the extraction efficiency

was highly affected by BO solvent characteristics.

The solubility of chromium, copper and arsenic depends on pH of the BO solvent. Decreased pH clearly increases the solubility of chromium and arsenic, while copper had high solubility at higher pH. The solubility of chromium and arsenic was also highly affected by BO concentration in the solvent, while copper is dissolved at a wide range of concentrations (0.0125-0.125M). Higher temperatures increased the solubility of chromium and arsenic, while copper was easily dissolved at a wide range of temperatures from 25 to 75°C. Higher liquid to solid ratios were preferable for obtaining good stirring efficiency and preventing re-absorption of CCA metals into wood. Various alkaline metal hydroxides (lithium, sodium and potassium) and sodium carbonate, as pH-adjusting reagents for BO solvent were found to be almost equally effective. Based on the present data, the recommended extraction conditions are pH=2.2 to 3.2, oxalic acid concentration of 0.125M adjusted with sodium hydroxide, and 75°C (Table 1).

Table1 Recommended condition for extraction of CCA metals by using BO chelating process

	Metals			***Total***
	Cr	Cu	As	***Cr, Cu, As***
pH	1.0-3.2	2.2-5.2	1.0-3.2	***2.2-3.2***
Concentration (M)	$1.25x10^{-1}$	$1.25x10^{-2}$-$1.25x10^{-1}$	$1.25x10^{-1}$-$6.50x10^{-2}$	***$1.25x10^{-1}$***
Temperature (°C)	75	25-75	75	***75***
Liquid/solid ratio (ml/g)	10-20	15-20	15-20	***15-20***
Duration of extraction (hr)	3-6	4-6	4-6	***4-6***

The characteristics of the extraction processes of CCA-treated wood with two-stage BO, adding sodium hydroxide during simple oxalic acid extraction and adjusting pH to 3.2, were investigated [6]. BO was reconfirmed to be an effective agent for removal of chromium, copper and arsenic. Simple oxalic acid was effective for chromium and arsenic, but ineffective for copper, while sodium hydroxide was ineffective for chromium and copper, but relatively effective for arsenic. It is important to note that the addition of sodium hydroxide to a simple oxalic acid solution during the extraction process resulted in a dramatic increase in the extraction efficiency of copper (up to 90%), compared to simple oxalic acid extraction. Thus, extraction with BO, with addition of sodium hydroxide to the oxalic acid solution not only before but also during extraction process, was concluded to be a highly effective method for removal of CCA metals.

We additionally tested BO extraction process for wood treated with other copper based preservatives such as ACQ and CuAz or a mixture of CCA, ACQ and CuAz-treated wood in single step. The extraction proceeded efficiently with 6 hours of treatment, and was insensitive to the differences in chemical characteristics, including solubility of individual metals. After 6 hours of treatment, approximately 90% of chromium, copper and arsenic were effectively removed from a mixture of CCA, ACQ and CuAz and 90% of copper from ACQ- and CuAz-treated wood chip. These results demonstrate that the solvent extraction technique using pH adjusted BO solution with sodium hydroxide is a suitable method for pollution minimization by various types of wastes contaminated with heavy metals and arsenic.

Cheating extracrtion of CCA-, ACQ-, and CuAz-treated wood was successfully conducted by novel chelating reagent of BO. Oxalic acid has long been known as one of the most popular and important organic acids in the field of wood preservation. Now we would like to add a new knowledge in this field. Thus oxalic acid found new role for purification of CCA-treated wood waste as a BO chelating reagent.

[1] Kakitani T., Hata T., Kajimoto T., Imamura Y., *Journal of Hazardous Materials*.**B109** (2004).
[2] Kakitani T, Hata T., Kajimoto T., Imamura Y., *Journal of Hazardous Materials*.**B113** (2004).
[3] Kakitani T., Hata T., Kajimoto T., Imamura Y., *Waste Management.* **26** (5) (2006).
[4] Kakitani T., Hata T., Katsumata K., Kajimoto T., Imamura Y., *Journal of Environmental Quality.* **35** May-June (2006).
[5] Kakitani T., Hata T., Katsumata N., Kajimoto T., Koyanaka H., Imamura Y., *Environmental Engineering Science.* **24** (8) (2007).
[6] Kakitani T., Hata T., Kajimoto T., Koyanaka H., Imamura Y., *Journal of Environmental Management*, **90** (2009).

Computer Experiments on Electric Antenna Characteristics in Space Plasma Environment

**(Graduate School of Engineering,
Laboratory of Computer Simulation for Humanospheric Sciences,
RISH, Kyoto University)**

Yohei Miyake

An electric antenna commonly occupies an essential part in plasma wave instruments onboard scientific spacecraft. Though principles of electric antenna measurements are fundamental, antenna behavior, modified under the influence of surrounding plasmas, is often problematic, because it could disturb reliable measurements of an electric field component of plasma waves. Then, strong demands arise regarding a better understanding of antenna characteristics in space plasma environment. However, the antenna behavior in plasmas is often too formidable to evaluate quantitatively by means of theoretical approaches because of complex antenna--plasma interactions. Therefore, we must establish a numerical approach for the self-consistent analysis of antenna characteristics in space plasmas.

For the self-consistent numerical analysis of antenna--plasma interactions, we construct a numerical simulation code based on an electromagnetic Particle-In-Cell description of the plasmas [4]. The code can include inner boundaries corresponding to perfect conducing surfaces of an antenna and a spacecraft. At the boundaries, as well as perfect conducting conditions required for electromagnetic fields, we also introduce numerical treatments for the charge and current densities computed from plasma particles interacting with the boundaries. These treatments are necessary for accurate descriptions of the charge accumulation exactly on conducing surfaces and its redistribution to realize a floating equi-potential over the surfaces. By using the constructed code, we perform two basic tests regarding plasma environment around a conducting body. One is the plasma sheath formation as a result of the spacecraft charging. The other is the dispersion relation of a sheath wave, which is a peculiar electromagnetic-wave mode propagating only in an electron-sparse sheath. For both tests, the reproduced environments show a good agreement with results obtained by previous well-proven theories.

Using the code, we begin the antenna analysis in plasmas with a simple situation. First, we apply the code to the impedance calculation in a homogeneous plasma environment and compare the result with the conventional kinetic theory. We correctly confirmed characteristic impedance changes such as an impedance resonance and a finite resistance below the plasma frequency by the computer experiment. Next, we examined the impedance of an antenna surrounded by an ion sheath that is created simultaneously with the antenna charging. We found that the sheath mainly influences reactance values below the electron plasma frequency, which is consistent with empirical knowledge that the ion sheath functions as a capacitance in the low-frequency range. Meanwhile, when we expand the sheath thickness artificially by biasing the antenna potential negatively, it is found that the sheath capacitance less contributes to the total antenna impedance. The trend indicates that the antenna reactance recovers its free-space value in the limit of large sheath dimensions, which corresponds to dilute and hot plasma environment as in the outer magnetosphere of the Earth [1].

As more realistic situations in space plasmas, we focus on effects of the photoelectron emission from sunlit surfaces of an antenna and a spacecraft. To illustrate the photoelectron effects, we perform computer experiments of the electron emission from inner boundaries corresponding to sunlit conducting surfaces. The emitted electrons have higher density but lower temperature than the plasma electrons. We confirmed the positive charging of the antenna and spacecraft bodies, and the formation of an electron-rich region in the vicinity of the sunlit surfaces. It is revealed from impedance calculation that the dense photoelectrons enhance the real part, and decrease the absolute value of the imaginary part, of antenna impedance at low frequencies. The antenna impedance in the photoelectron environment is represented by a parallel equivalent circuit consisting of a capacitance and a resistance. We also show that the above resistance can be well estimated semi-analytically using the numerical results of the electron currents flowing into and out

of the antenna. This suggests that the impedance change is caused by the conduction current induced by the actual motion of photoelectrons contacting with the antenna surfaces [2]. The results also imply that the impedance varies with the spin of the spacecraft, which causes the variation of the photoelectron density around the antenna.

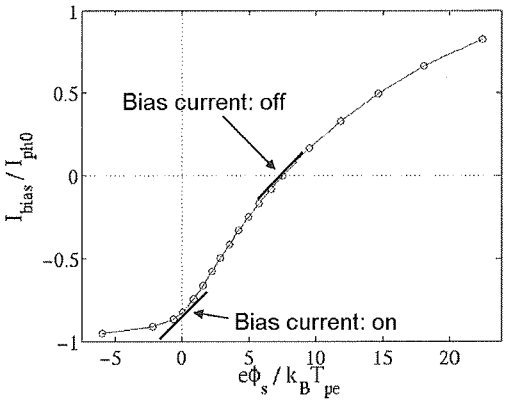

Figure 1. The voltage-current characteristic curve obtained by changing the magnitude of the bias current. The zero potential corresponds to the background space potential.

Finally, we introduce a numerical technique for the direct analysis of receiving antenna behavior and also develop a new model of modern electric antennas toward future satellite missions. In the new analysis technique, we set up wave fields propagating in a computational space and simulate the process of wave reception by the antenna. By using the technique, we examined the effective length of a probe-like antenna, which has a configuration such that sensing wire elements are attached at both ends of a center boom conductor. For this type of the antenna, the effective length becomes shorter than the physical separation between the centers of two sensing elements. It is found that this effect is caused by the distortion of equi-potential surfaces due to the presence of the center boom conductor [3]. We next introduce numerical models of guard electrode and current biasing, which are planned to be installed on future electric field instruments. We performed computer experiments by using the standard setting of electrode potentials, the values of which are not optimized but determined empirically. We found that the guard electrode decreases the photoelectron-current coupling of the sensor conductor with the boom and spacecraft bodies. The effect suggests that the electrode can reduce the influence of large amount of photoelectrons emitted by the spacecraft body on electric field measurements. On the other hand, the bias current draws the sensor potential close to the background plasma potential. The electrode and the current biasing have a small effect on antenna behavior for oscillating fields created by external plasma waves, compared with their significant impacts on the static plasma environment. This result is understood from the voltage--current characteristic curve of the sensor shown in Figure 1, the gradient of which indicates the inverse of the dynamic resistance of the sensor for the oscillating fields. The observed voltage--current curve is considerably deformed by the effect of the photoelectron current coupling even though it is decreased by the operation of the guard electrode. The result emphasizes the significance of more optimal electrode potentials in order to effectively mitigate the influence of the photoelectron coupling.

References

[1] Miyake, Y., H. Usui, H. Kojima, Y. Omura, and H. Matsumoto, "Electromagnetic Particle-In-Cell Simulation on the Impedance of a Dipole Antenna Surrounded by an Ion Sheath," *Radio Science*, vol. 43, pp. RS3004: 1-14, 2008.

[2] Miyake, Y., and H. Usui, "Analysis of Photoelectron Effect on the Antenna Impedance via Particle-In-Cell Simulation," *Radio Science*, vol. 43, pp. RS4006: 1-13, 2008.

[3] Miyake, Y., H. Usui, H. Kojima, and Y. Omura, "Particle-In-Cell Simulation on the Characteristics of a Receiving Antenna in Space Plasma Environment," *Procs. of 26th International Symposium on Rarefied Gas Dynamics*, vol. 1084, pp. 895-900, 2008.

[4] Miyake, Y., and H. Usui, "New Electromagnetic Particle Simulation Code for the Analysis of Spacecraft-Plasma Interactions," *Physics of Plasmas*, vol. 16, no. 6, pp. 062904: 1-11, 2009.

Studies on lignin degradation by free radicals

**(Graduate School of Agriculture,
Laboratory of Biomass Conversion, RISH, Kyoto University)**

Daisuke Ando

Continued usage of fossil fuels caused serious problems such as global warming and depletion of fossil fuels. Development of conversion systems from lignocellulosics into biofuels and chemicals has received much attention due to immense potentials for the utilization of renewable bioresources. Biological systems decomposing lignin by white rot fungi are attractive to develop the lignicellulosic biorefinery system. The lignin biodegradation by white rot fungi is an extracellular free radical event that proceeds in concert with the activation of molecular oxygen and redox cycling of transition metals. In contrast to brown rot and non-selective white rot fungi, selective lignin-degrading fungi like *Ceriporiopsis subvermispora* are able to decompose lignin in wood cell walls at a site far from enzymes without the intensive damage of cellulose. As for the lignin degradation system at a site far from enzymes, lipid peroxidation has been proposed. We analyzed reactivity of free radical species from hydroperoxides or peroxidizable compounds, and developed lignin-degrading free radical reactions. In this thesis, the author synthesized lignin model compounds and analyzed reactions with free radicals, with special emphasis on enantioselectivity of the reactions.

Threo and *erythro* forms of non-phenolic β-*O*-4 lignin dimmer model compounds and a dehydrogenation polymer (DHP) from coniferyl alcohol were chemically synthesized. Radical species were generated by one-electron redox reactions using metal-ligand complexes, enzymes, or thermolysis of azo compounds, and allowed to react with the lignin model compounds in various solvents. Degradation products from the lignin model compounds were analyzed by GC-MS, NMR, and MALDI-TOF-MS. The author found radical reaction systems with different enantioselectivity to the recalcitrant non-phenolic lignin dimmer models. The synthetic lignin, DHP was intensively depolymerized by the radical reactions.

Characterization of lipid-biosynthetic genes from a lignin-degrading fungus, *Ceriporiopsis subvermispora*

**(Graduate School of Agriculture,
Laboratory of Biomass Conversion, RISH, Kyoto University)**

Chihiro Izumi

A selective white rot fungus, *Ceriporiopsis subvermispora* selectively degrades lignin in wood with minimum damage of cellulose. So far, we have analyzed functions and biosynthesis of lipid-related metabolites, which may play a key role in the lignin degradation of *C. subvermispora*. In this study, in order to clarify the lipid metabolism involved in the selective lignin degradation, we have cloned two genes encoding long acyl-CoA synthetases (*Cs*-ACSLs), which esterify long-chain fatty acid to long acyl-CoA in the key step of fatty acid utilization. These *Cs*-ACSLs have two functional domains characteristic of other already-known ACSLs, but no transmembrane domains. Although the *Cs*-ACSLs are phylogenetically similar to some ACSLs derived from basidiomycetes, there is an evolutionary distance between *Cs*-ACSLs and ACSLs derived from a lignin-degrader, *Phanerochaete chrysosporium*. Furthermore, we heterogeneously overexpressed *Cs*-ACSLs in *Escherichia coli* and purified them as His-tagged fusion proteins. On the other hand, a *Cs*-ACSL-gene was inducibly transcribed when *C. subvermispora* was grown on medium supplemented with a lignin fragment and at low temperatures. This induction pattern was partially similar to that of other genes involved in the fatty acid synthesis.

Analytical approach for lipid oxidative mechanism of white rot fungi

**(Graduate School of Agriculture,
Laboratory of Biomass Conversion, RISH, Kyoto University)**

Miki Kashiwakura

Recently wood biomass conversion systems drew attention as one of solutions for environmental problems becuase cyclic utilization of wood is essentially carbon-neutral. White rot fungi are the most efficient lignin degraders in nature and play an important role in carbon recycling.

The fungi secrete extracellular ligninolytic enzymes including manganese peroxidase (MnP). It was reported that MnP is capable of decomposing recalcitrant aromatic compounds such as nonphenolic lignin models in the presence of Mn(II) and unsaturated lipids. This indicates that the MnP/lipid system generates active oxidants leading to radical production involved lignin degradation.

In this study, analytical approaches for lipid oxidation were investigated by genetic engineering and biochemical procedure to elucidate the oxidation mechanism.

i) Suppression of *ku70* gene in *Pleurotus ostreatus*

To establish gene targeting system of white rot fungi, *Poku70*, which encodes protein that functions in nonhomologous end-joining of double-stranded breaks, was targeted for RNAi mechanism.

In basidiomycetes, two pathways have identified, as repairing mechanism of double-strand break (DSB). One is homologous recombination (HR), involves interaction between homologous sequences. The other is non-homologous end-joining (NHEJ), involves direct ligation of the strand ends independent of DNA homology. Homologous recombination is the most efficient method of gene targeting system. However, many organisms, without *Saccharomyces cerevisiae*, seem to use NHEJ preferentially in DSB repair. As a result, exogenous DNA can be integrated randomly in the genome. Under hypothesis that the rate of homologous recombination can be increased by blocking NHEJ, RNAi vector aimed at repression of *Poku70* expression was introduced into protoplasts of *P. ostreatus* with drug-resistant plasmids by co-transformaton.

PCR analyses of DNA of the drug-resistant isolates obtained from co-transformation experiments demonstrated specific amplification of the marker fragment in dikaryon and monokaryon transformants each. The resulting mutants showed slower growth than wild types. By comparison with other transformants which RNAi vector couldn't insert, it seemed not to be influence on growth whether it inserted or not.

ii) Analysis of products formed by lipid peroxidation by lignin-degrading enzyme

At an incipient stage of wood decay, a selective white rot fungus *Ceriporiopsis subvermispora* produced MnP and large amounts of unsaturated fatty acids. MnP oxidized the lipids to produce hydroperoxides and aldehydes. Although, reactions of lipids with MnP have been studied, reaction intermediates produced by the oxidation of lipids with MnP are not fully elucidated. In this study, products formed by the reactions of linoleic acid with MnP were profiled by GC/MS.

Analysis of exposed cellulose surfaces in pretreated wood biomass by carbohydrate binding module (CBM)–cyan fluorescent protein (CFP) complexes

**(Graduate School of Agriculture,
Laboratory of Biomass Conversion, RISH, Kyoto University)**

Takeshi Kawakubo

In enzymatic saccharification of lignocellulosics, access of the enzymes to exposed cellulose surfaces is an initial key step to trigger the hydrolysis. However, knowledge of the structure-hydrolyzability relationship of the pretreated biomass is still limited. Carbohydrate binding modules (CBMs) are noncatalytic substrate binding domains of cellulolytic enzymes[1]. Here we used fluorescent labeled recombinant CBMs specific for crystalline cellulose (CBM3) and non-crystalline cellulose (CBM28) to analyze the complex surfaces of wood fibers pretreated by chemical, hydrothermal and physical methods.

Linear correlation between enzymatic saccharification ratio and the adsorption of CBM3-CFP and CBM28-CFP was observed for the chemically pretreated wood. Adsorption of CBM3-CFP and CBM28-CFP to the physically disrupted wood was much lower than that of the chemically delignified wood. Fluorescent microscopy revealed that CBM3-CFP and CBM28-CFP adsorbed preferentially on fibrillated wood tissues. This phenomenon was remarkable for CBM28-CFP. Thus the quantitative fluorometric method clarified the linear dependency of saccharification ratio on exposure of cellulose surfaces in the chemically delignified wood.

Reference

1) Shoseyov, O., Shani, Z., and Levy, I. (2006) Microbiology and Molecular Biology Reviews, **70**, 283–295.

Studies on extracellular polysaccharide matrix and metabolites produced by selective white rot fungus

**(Graduate School of Agriculture,
Laboratory of Biomass Conversion, RISH, Kyoto University)**

Daisuke Suzuki

Wood biomass conversion has been receiving a great deal of attention as one of measures to solve the environmental problems caused by excessive use of fossil fuels. To convert wood biomass by enzymatic saccharification and fermentation, degradation of lignin network is necessary because cell wall polysaccharides are covered with lignin in lignified plant cell walls. One potential approach to degrade lignin prior to the saccharification and fermentation is to use ligninoltic systems of white rot fungi. Among the numerous fungi so far isolated, a white rot fungus, *Ceriporiopsis subvermispora* is characterized as one of the best biopulping fungi that degrade lignin without intensive damage of cellulose. Previous studies revealed that the selective ligninolysis by this fungus is catalyzed by low molecular mass compounds at a site far from extracellular enzymes and fungal hyphae. To elucidate the molecular mechanism of the selective ligninolysis by this fungus, the author focused on functions of fungal sheath (extracellular polysaccharide matrix) interfacing the wood and haypae, and analyzed structures of the sheath and metabolites trapped in the polysaccharide matrix.

C. subvermispora was cultivated on beech wood specimens placed on PDA. The decayed specimens were fixed by rapid freezing, followed by the treatment with 2 % osmium tetroxide. The wood specimens were stained with uranium acetate/lead citrate, and then subjected to observation by transmission electron microscopy (TEM). For the chemical analysis of sheath, *C. subvermispora* was cultured in a SDW medium at 28°C for 4 weeks. Then, the culture was separated into sheath and fungal body by filtration. The filtrate was dialyzed and then lyophilized. Chemical structure and molecular weight distribution of the sheath were analyzed by MALDI-TOF-MS, GPC, NMR, methylation by Hakomori's method and determination of neutral sugar composition. Metabolites involved in the sheath were analyzed by ESI-LCMS. These microscopic and chemical analyses revealed unique structural features of the sheath and sheath-inherent metabolites produced by *C. subvermispora*.

Studies on secondary metabolites produced by *Ceriporiopsis subvermispora*

**(Graduate School of Agriculture,
Laboratory of Biomass Conversion, RISH, Kyoto University)**

Kyoko Murayama

Exposure of cell wall polysaccharides by removal lignin is an initial key step for enzymatic and microbial conversion of woody biomass. A white rot fungus, *Ceriporiopsis subvermispora* is able to degrade lignin without intensive damage of cellulose at a site far from enzymes. Extracellular metabolites play a central role to control the selective ligninolysis. The unique wood decay system has been receiving a great deal of attention because the biological or biomimetic ligninolytic systems can be applied to the conversion of woody biomass into fuels, chemicals and pulps. We are interested in the key extracellular metabolites of *C. subvermispora,* and found that the fungus produced a series of novel itaconic acid derivatives with a long alk(en)yl side chain at position C-3 of their core (ceriporic acids). So far, ceriporic acid A, B, C and D were isolated and identified in comparison with authentic compounds[1-5]. Ceriporic acid B (1-nonadecene-2,3-dicarboxylic acid) inhibited generation of cellulolytic hydroxyl radicals by the Fenton reaction system[6], leading to suppression of cellulose degradation. At an incipient stage of wood decay, this fungus produced manganese peroxidase (MnP) and fatty acids to initiate extracellular lipid peroxidation[1]. During wood decay, a glucan matrix called sheath is produced by the fungus[7], and the matrix controls transport of metabolites and uptake of lignin and polysaccharide fragments.

In the present thesis, the author profiled metabolites involved in the fungal sheath under ligninolytic conditions. To analyze the metabolites in the sheath under ligninolytic conditions, a new cultivation system was developed. By the analysis of secondary metabolites in the sheath, new analogues of ceriporic acids have been found.

REFERENCES

1) Enoki, M., Watanabe, T., Nakagame, S., Koller, K., Messner, K., Honda, Y. and Kuwahara, M. (1999) *FEMS Microbiol. Lett.*, **180**: 205–211.

2) Enoki, M., Watanabe, T., Honda, Y., Kuwahara, M. (2000) *Chem. Lett.*, 54–55.

3) Amirta, R., Fujimori, K., Shirai, N., Honda, Y., Watanabe, T. (2003) *Chem. Phys. Lipids.*, **126**: 121–131.

4) Nishimura, H., Tsuda, S., Shimizu, H., Ohashi, Y., Watanabe, T., Honda, Y., Watanabe, T. (2008) *Phytochemistry*, **69**: 1253–2602.

5) Nishimura, H., Murayama, K., Watanabe, T., Honda, Y., Watanabe, T. (2009) *Chem. Phys. Lipids*, **159**, 77-80.

6) Watanabe, T., Teranishi, H., Honda, Y. and Kuwahara, M. (2002) *Biochem. Biophys. Res. Commun.*, **297**: 918–923.

7) Blanchette, R.A., Krueger, E.W., Haight, J.E., Akhtar, M., Akin, D.E. (1997) *J. Biotechnol.*, **53**: 203–213.

Gene discovery in lignification by gene expression and metabolic analyses

Graduate School of Agriculture,
Laboratory of Metabolic Science of Forest Plants and Microorganisms,
RISH, Kyoto University

Yuta Tsurumaki

As an alternative energy and carbon source to fossil resources, recently wood biomass has been attracted much attention. Wood biomass, mainly composed of cellulose, hemicellulose, and lignin, are synthesized actively in developing xylem of trees. The understanding of the synthetic mechanism of wood components would be greatly useful to modify wood biomass amenable to the future biorefinary.

Lignin is a phenolic polymer and the synthesis is called "lignification". 4-Hydroxycinnamic alcohols (monolignols) formed via the cinnamate/monolignol pathway are the immediate precursors in the lignin biosynthesis. Several enzymes are responsible for the metabolism, and thus far, the genes encoding the enzymes were identified by biochemical characterization in various plant species. However, the transcriptional regulation of the genes is largely unknown.

In the present study, the author aimed to identify transcription factors involved in lignification. First, the author focused on MYB transcription factors of *Populus trichocarpa*. MYB gene family is the largest transcription factor family in plant. Previous studies revealed that several MYB transcription factors were involved in lignification as well as cellulose and hemicelluloses biosynthesis in pine, eucalypt, and *Arabidopsis thaliana*, but nothing was known about poplar MYB transcription factors. To narrow down the putative MYB genes involved in lignification, we searched MYB transcription factor genes in *P. trichocarpa* genomic database, and the gene expression among organs were evaluated by quantitative reverse-transcriptase polymerase chain reaction (qRT-PCR). Three MYB genes are specifically expressed in developing xylem where lignification was actively occurred, suggesting that the genes were involved in lignification. To narrow down the target genes regulated by the MYB transcription factors, the expression of the genes which encode cinnamyl alcohol dehydrogenase (CAD), an enzyme that catalyzes the formation of monolignols, was evaluated using qRT-PCR. This analysis enabled us to predict a CAD gene putatively targeted by the xylem-specific MYB transcription factors. How these xylem-specific MYB transcription factor in *P. trichocarpa* regulate lignification remains to be elucidated.

Second, the author attempted to narrow down novel transcription factor genes involved in lignification in *A.thaliana*. Using co-expressed genes network analysis, we narrowed down several candidate transcription factor genes which had not been reported. Next, we selected knock-out and over-expression mutant lines of *A. thaliana*. The selected lines were cultivated and harvested to determine the quantities of lignin, intermediates, and related metabolites using GC-MS and LCMS-IT-TOF. As a result, several knock-out and over-expression lines revealed that decrease of the quantity of lignin and the intermediates of the cinnamate/monolignol pathway. These results suggest that the candidate transcription factor may be involved in lignification. Further studies are required to illustrate the relationship between lignin biosynthesis and the novel transcription factors, but the present study may be the first step to identify the novel transcription factor involved in lignification.

Characterization of the flavonoid-specific prenyltransferase *SfN8DT-3* from *Sophora flavesecens*.

(Graduate School of Agriculture, Laboratory of Plant Gene Expression, RISH, Kyoto University)

Yusuke Tsurumaru

Prenylated flavonoids are natural products composed of a flavonoid core and a variety of decorations with prenyl residues of mainly dimethylallyl or geranyl groups, which are derived from isoprenoid metabolism. Many of them show diverse biological activities such as anti-bacterial, anti-tumor, anti-androgen, anti-leishmania, and anti-nitric oxide production, etc, in which prenyl residues play crucial roles for their biological activities. The prenylation reaction of flavonoid couples two major metabolic pathways, the shikimate and isoprenoid pathways, and this reaction step is often known to be a rate-limiting in their biosynthesis. We have recently previously reported the first plant gene for flavonoid-specific prenyltransferase from *Sophora flavescens*, *SfN8DT-1*. This enzyme is responsible for the prenylation of the flavanone, naringenin, at the 8-position, and is specific for dimethylallyl diphosphate (DMAPP) as its prenyl substrate [1]. This enzyme has multiple transmembrane α-helices and shares high similalry with homogentisate prenyltransferases involved in vitamin E or plastoquinone biosynthesis in their amino acid sequence (21%–55%) [2-3].

In this study, we have isolated two homologous cDNAs *SfN8DT-2* and *SfN8DT-3* from *S. flavescens* by reverse transcriptase-PCR (RT-PCR) using specifc primers designed for *SfN8DT-1* and characterized them in detail. Southern blot analysis suggested that at least four copies of *SfN8DT-1* gene were present in *S. flavescens*. *SfN8DT-3* is a paralog of *SfN8DT-1* showing 98% amino acid sequence identity with *SfN8DT-1*. *SfN8DT-3* expressed in yeast revealed clear prenyltransferase activity for naringenin in the presence of DMAPP. The Recombinant SfN8DT-3 has slightly lower affinity for substrates (naringenin, DMAPP) than that of Recombinant SfN8DT-1. Using amplified fragment length analysis, we found that *SfN8DT-3* gene expression was lower compared with *SfN8DT-1* gene. These results suggest that *SfN8DT-3* represents a paralogue gene of *SfN8DT-1* in *S. flavescens*.

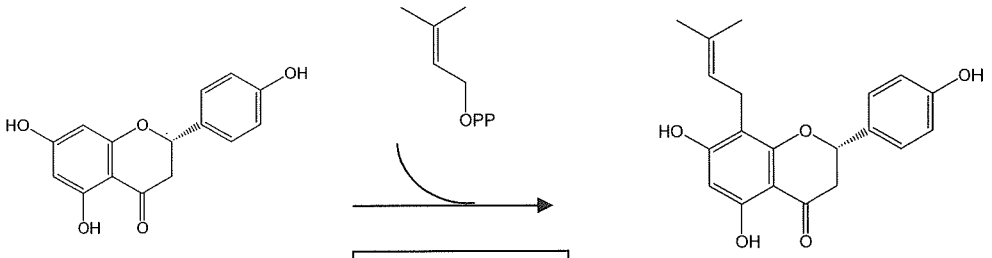

(2S)- Naringenin

8-Dimethylallyl naringenin

[1] Sasaki K, et al., *Plant Physiol.*, 146, 1075-1084 (2008)

[2] Cahoon EB, et al., *Nat Biotechnol.*, 21, 1082–1087 (2003)

[3] Sadre R, et al., *FEBS Lett.*, 580, 5357–5362 (2005)

Continuous observations of temperature profiles by the 443 MHz wind profiling radar with RASS in Okinawa

**(Graduate School of Informatics,
Laboratory of Atmospheric Sensing and Diagnosis, RISH, Kyoto University)**

Tomonori Shinoda

This study is devoted to the continuous monitoring of virtual temperature profiles by the 443 MHz wind profiling radar (443 MHz-WPR) with Radio Acoustic Sounding System (RASS) (443 MHz-WPR/RASS) at the Ogimi Wind profiler Facility of National Institute of Information and Communications Technology (NICT), Okinawa, where the severe weather phenomena with a short lifetime frequently strike. We have been collaborating with NICT on application of the RASS technique to the 443 MHz-WPR since 2006. The previous study designed a horn speaker system for RASS, and conducted a preliminary observation in November 2006, which successfully demonstrated capability of the 443 MHz-WPR with RASS (hereafter, called as 443 MHz-WPR/RASS) in obtaining temperature profiles with the temporal and height resolutions of four minutes and 300 m, respectively.

In the previous study, the 443 MHz-WPR/RASS observation was carried out only for a short period, only when someone attended and monitored manually the RASS observation at the Ogimi observatory. However, it is very important to continuously operate the RASS observation to monitor sporadic severe weather phenomena with a short lifetime which is often occurred in Okinawa subtropical region. In this study, we developed a remote control and monitoring system for 443 MHz-WPR/RASS observation to achieve the unpeopled continuous observation. The real-time processing system is also made to download the power spectral data and derive virtual temperature profiles within a latency of 2.5 hours.

A test observation started on May 23, 2007, and the continuous observation with the new system is operated at 0700-2000LT since February 4, 2008. The virtual temperature profiles agree very well with data from radiosonde launched at the Okinawa meteorological station of Japan Meteorological Agency (JMA). Considerable improvement of accuracy by a numerical weather prediction model of JMA is expected by assimilating the RASS results on a real-time basis.

Application of Frequency domain Interferometric Imaging (FII) technique to RASS (RASS-FII) was also studied to improve the vertical resolution of RASS observation. In the FII analysis for RASS echo, a model temperature profile is required to compensate for the Doppler shift bias due to the shape of range gate weighting. In order to remove this bias, an iteration algorithm was developed so that the temperature profile of the previous FII result can be used for the bias correction of the next FII step. The optimum parameters to minimize the vertical resolution are derived via the simulation study of RASS-FII. The simulation results predicts the vertical resolution of the MU radar/RASS-FII can be improved with the increase in the frequency swept ratio of an FM chirped acoustic wave. We carry out MU radar/RASS-FII observation on November 11-14, 2008 and verified the improvement of vertical resolution with the optimized observation parameters. Then, optimum observation parameters for RASS-FII with 443 MHz-WPR/RASS were proposed to improve the vertical resolution to 36 m.

Synergetic implementation of knowledge and numerical data in geophysical fluid data server

**(Graduate School of Informatics,
Laboratory of Atmospheric Sensing and Diagnosis, RISH, Kyoto University)**

Akinori Tomobayashi

The amount of information on the Earth's atmosphere and ocean has increased greatly by recent dense observations with high sampling. The scale of a numerical simulation is also growing rapidly. So, digital data on "geophysical fluids" are explosively increasing. As such data are mostly recorded in a binary format, the raw digital data are not easily readable by a user. Therefore, the users commonly download them, analyze and visualize them on their own computers. However, the greatness of data size sometimes hinders the effective use of data. Another obstacle is that a user has to prepare software infrastructure to handle the data in variety of different formats.

To solve the problems, our group develops a software tool called "Gfdnavi", with which we have constructed a data server having search, analysis and visualization capability. Then, any user can analyze and visualize data on this server side, and download the results only. Thus, the problem about data transfer size is solved. In this study, we newly add a function to write a document based on knowledge obtained with a Gfdnavi server. The documents are stored on the server for synergetic use with numerical data. This feature enhances capability of the data-server in effective and intelligent use of both digital data and knowledge, and this is superior to other existing data-server tools.

For example, one can find the numerical data and analysis procedures used to create a knowledge document, so one can reproduce, verify, or even extend the analysis. Users can also search a knowledge document from numerical data, and find the knowledge obtained from the data or to understand through an example on how to handle the data. This system also allows the user to add a comment to the knowledge document, which is useful in publishing them to a wide community. In order to make the knowledge documents widely available on Gfdnavi servers, we introduce a new login system, called OpenID, as an external authentication system. We hope the feature and method proposed in this study will be applicable to other fields of science.

Meso-γ-scale convective systems observed by a 443 MHz wind-profiling radar with RASS in the Okinawa subtropical region

**(Graduate School of Science,
Laboratory of Atmospheric Sensing and Diagnosis, RISH, Kyoto University)**

Aya Mikami

This thesis is devoted to a case study of a convective system with the meso-γ-scale which appeared over the Okinawa Island, Japan on 23 and 25 July 2007. We used virtual temperature (*Tv*) and three components of wind velocities profiles observed by the 443 MHz wind profiler (443 MHz-WPR) with RASS (Radio Acoustic Sounding System), which has been continuously operated at the Ogimi Wind Pro_ler Facility (hereafter referred as the Ogimi observatory) of the National institute of Information and Communications Technology (NICT). We also employ the results from the NHM numerical model to study the detailed behavior of the convective system.

On 21-26 July, including the period of convective activities, Okinawa was covered with Pacific high pressure, but the height range below the middle layer (about 5 km) was convectively unstable, which is clari_ed through analysis of 12-hourly routine balloon observations at the Naha weather station of Japan Meteorological Agency (JMA). Before a rain started on 23 and 25 July, CAPE was as large as about 1200-1250 J/kg, and CIN was small (about 2-3 J/kg), so convections tend to be generated easily under such background condition.

Strong convective clouds were recognized with a typical horizontal and temporal scale of 10 km and 40 - 60 minutes, respectively. Many convective systems were generated during 1100-1800 JST all over the Okinawa island, and one of them passed over the Ogimi radar site. We analyzed Brunt-Väisälä frequency square, N^2 as an index of the atmospheric static stability.

Just before the rain occurred on 23 and 25 July, the time-height structure of N^2 showed that a small N^2 region extended toward higher altitude up to 2.0 km. This peculiar structure was commonly seen at the place where the convective clouds are generated in the NHM forecast. By investigating the cloud water content from the NHM result, the cloud top height is found to correlate with the characteristic structure of low N^2 region. Before the convective system was generated on 23 and 25 July, the static stability became low below about 1 km altitude, which seemed to occur by inflow of the air with low *Tv* at the 1-3 km altitude as well as the increase of temperature by the solar radiation in the surface layer. When the convective system passed over the Ogimi radar observatory, the see-breeze from both east and west coasts of Okinawa Island collided to enforce the convergence below 1 km. We found that the synergetic effect of low static stability and the convergence triggered the generation of convective systems, which eventually grew up to 11 km over the radar site.

Retrieval of High Vertical Resolution Atmospheric Profiles from GPS Radio Occultation Measurements

**(Graduate School of Informatics,
Laboratory of Atmospheric Sensing and Diagnosis, RISH, Kyoto University)**

Lin Xinan

GPS RO is a novel satellite remote-sensing technique which uses the occulted GPS electromagnetic wave to observe the Earth's atmosphere. Characterized by its advantages of high accuracy, superior vertical resolution and self-calibration, GPS RO is a promising technique in many applications such as atmospheric sciences, meteorology, climate changes, weather prediction, and so on.

Geometric Optics (GO) and Radio Holography (RH) are two kinds of the retrieval methods for GPS-RO. Due to the limitation of Fresnel radius, the vertical resolution of GO is about 1.5 km around the tropopause, while RH methods do not have such limitation. In order to study atmospheric structures with small vertical scale we employ Full Spectrum Inversion (FSI) method, one of the RH methods, to retrieve the GPS-RO profiles from ground to 30 km.

We validate the FSI based results, by comparing them with the radiosonde profiles in Malaysia and North America that are collected nearby the GPS RO events within ±30 minutes time difference. The average discrepancy at 10-30 km altitude is less than 0.5 K. We further analyzed the vertical wave number spectrum of the temperature fluctuation at 20-30 km, which exhibits a good consistency with the model spectra of saturated gravity wave. By investigating the spectral density for the wave number range where the noise floor appears, the substantial vertical resolution of the FSI method is estimated as about 100-200 m at 20-30 km altitude. We have also considered a criterion for the upper limit of the FSI profiles, from the normalized perturbations of the bending angle.

The horizontal resolution of GPS RO for the atmospheric fluctuation is discussed. The horizontal resolution along-ray-track is not improved even though the vertical resolution is improved with FSI. Because of superior height resolution and measurement accuracy, GPS RO is expected to become one of the most important observation techniques of the atmosphere.

Zonally asymmetric temperature structure around the tropical tropopause and its relationship to deep convection in monsoon regions

(Graduate School of Science, Laboratory of Atmospheric Environment Information Analysis, RISH, Kyoto University)

Eriko Nishimoto

Tropical tropopause temperature is one of the most important factors which control the dehydration mechanism of air entering the lower stratosphere from the upper troposphere. Around the tropical tropopause during Northern Hemisphere (NH) summer and Southern Hemisphere (SH) summer, it is known that there exists zonally asymmetric temperature structure with 'horseshoe' shape, and it is theoretically interpreted as the Matsuno-Gill pattern, which is induced by near equatorial diabatic heating such as due to convection (*Highwood and Hoskins* [1998]). During NH summer, such a structure is coupled with deep convection within the Asian summer monsoon region, and is also associated with the distribution of minor constituents in the upper troposphere and the lower stratosphere (*Park et al.* [2007]). During SH summer, deep convection in the Australia summer monsoon region may also result in such a characteristic atmospheric structure. In this study, we investigate the climatological temperature structure around the tropical tropopause, and its variability associated with deep convection in monsoon regions. We use the reanalysis temperature data at 100hPa and the outgoing longwave radiation (OLR) data for the proxy of deep convection for about 23 years from January 1979 to August 2002. The southern oscillation index data are also examined because of the possible influence of the El Niño/Southern Oscillation (ENSO) on the interannual variation of deep convection.

Figure 1 shows the monthly-mean temperature climatology at 100hPa in August (NH summer) and February (SH summer) averaged over 23 years. In both months we find horseshoe-shaped zonal asymmetries; cold anomaly on the equator extends to north-west and south-west, surrounding warm anomaly in the west of it. Paying attention to this structure, we define the HorseShoe Index (HSI) as the difference between the mean temperature at 15N (T(15N)) and 15S (T(15S)) and that at the equator (T(0)): HSI=(T(15N)+T(15S))/2-T(0). Negative HSI values suggest that the horizontal distribution of cold anomalies represents a horseshoe shape. A longitude-time section for HSI shows two prominent HSI minima in NH summer (Jun-Oct) at 40E-120E and in SH summer (Dec-May) at 100E-120E. The NH summer minimum is extended more widely at longitude and has a larger absolute value than the SH summer one. We calculated correlation coefficients between HSI and OLR for each of the NH and SH summers. HSI at 40E-120E and that at 100E-120E are related to OLR within the Asia monsoon region (70E-140E, 5N-20N) in NH summer and the Australia monsoon region (110E-140E, 15S-5N) in SH summer, respectively. The interannual variation of HSI and OLR in the SH summer region is dominant, and it is found to be related to ENSO. We can conclude that deep convection within the Asian summer monsoon and the Australia summer monsoon regions could produce the characteristic temperature structure around the tropopause as a response of deep convective activity.

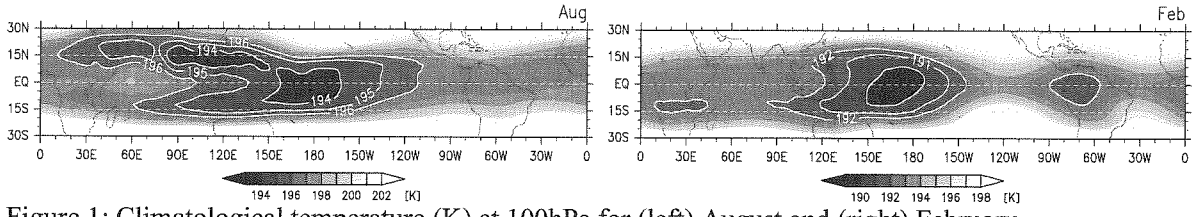

Figure 1: Climatological temperature (K) at 100hPa for (left) August and (right) February.

References

[1] Highwood, E. J., and B. J. Hoskins (1998), *Q. J. R. Meteorol. Soc., 124,* 1579-1604.

[2] Park, M., et al. (2007), *J. Geophys. Res., 112,* D16309, doi:10.1029/2006JD008294.

Study of three-dimensional structure of ionosphere based on 630-nm airglow observation with FORMOSAT-2/ISUAL

(Graduate School of Informatics, Laboratory of Radar Atmospheric Science, RISH, Kyoto University)

Masashi Yamaoka

There is 630-nm airglow by atomic oxygen in the ionospheric F-region. The emission occurs when oxygen molecules ionized by the daytime ultraviolet rays recombine with electrons in the nighttime. It is known that the airglow and the total electron content of the ionosphere well correlated by comparison of observations of all-sky cameras and GPS-receiver network in Japan. The observation of the 630-nm airglow is useful to clarify spatial structures of the ionosphere. Since observations have primarily been carried out by imagers on the ground, the three-dimensional structures are not fully understood. In order to investigate the three-dimensional structures, we carried out 630-nm airglow observation with the ISUAL instrument on board of the FORMOSAT-2 satellite. ISUAL observations of 630-nm airglow were conducted for a total 14 days in December 2006, May—June 2007, and April—May 2008 in the region from Australia to Japan. We estimated altitude profile of the airglow layer. The estimated peak altitude was 220 km—280 km. There were bright emissions near the equator and around 30 S. Simultaneous observations between ISUAL and a ground-based imager were successful over Darwin at 15 UT on May 16, 2007. Figure 1 shows an example of the limb-scan image from ISUAL (top panel), and the horizontal image of airglow over Darwin, Australia (bottom panel). We studied structures of the MSTID (Medium-Scale Traveling Ionospheric Disturbance). By using height information from ISUAL and horizontal distribution of airglow from the imager, we modeled three-dimensional structure of the airglow. Reconstructed ISUAL image from the model agreed well with the real data. We further tried to estimate three-dimensional structures of the ionosphere based on the ISUAL data only. From much clearer images of airglow on December 21, 2006 and May 16, 2007, we successfully estimated reasonable structures of the MSTID and equatorial anomaly, respectively. From these studies we showed that the limb imaging of 630-nm airglow from space is a useful tool to study the ionosphere structures.

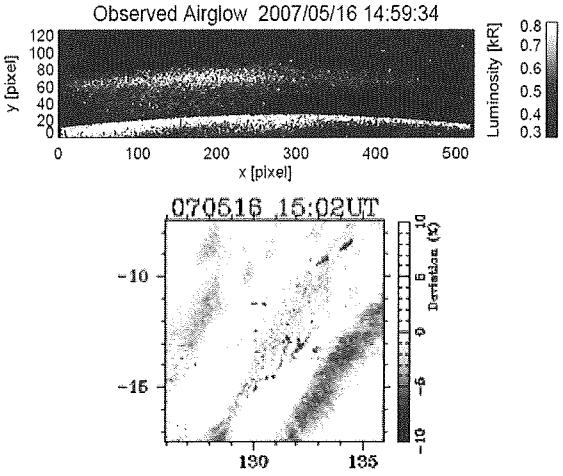

Figure 1. (top) Limb image of 630 nm airglow from ISUAL, and (bottom) corresponding horizontal image from the OMTI of Nagoya University at Darwin, Australia. Observations were conducted at around 15 UT on May 16, 2007.

References

We thank NSPO (National Space Organization), Taiwan for giving us chances of FORMOSAT-2/ISUAL experiment of 630-nm airglow. We are grateful to Solar-Terrestrial Environmental Laboratory, Nagoya University for providing us with airglow imager data from Darwin, Australia.

Production of moldable cellulose nanofiber-reinforced phenolic resin composites

**(Graduate School of Agriculture,
Laboratory of Active Bio-based Materials, RISH, Kyoto University)**

Kosuke Sasakawa

Microfibrillated cellulose obtained by the mechanical fibrillation of pulp is expected to be an alternative nano filler to realize high-strength and low-thermal expansion composites. Although an increase in filler content increases the strength of composites, a strong aggregation of cellulose nanofibers generated by hydrogen bonds deteriorates the moldability of the composites at high fiber contents. Therefore, the optimum condition to attain high strength as well as good moldability was studied using phenolic resin as the matrix substance and microfibrillated chemi-thermomechanical pulp(CTMP) containing high amounts of lignin as the filler. The lignin is expected to suppress hydrogen bonding among cellulose nanofibers and act as a compatibilizer between cellulose and PF resin.

Materials and methods

A 1wt% water suspension of CTMP (Quesnel River Company, Q250 and B75) was processed with a grinder (Super Mascolloider, Masuko Industrial) at 1500 rpm. The water soluble low molecular weight phenol formaldehyde (PF) resin (DIC, IG-1002) was mixed to the CTMP slurry to obtain 10 to 70wt% fiber content at oven-dried condition. The mixtures were dried at 50 ℃ to remove water. The dried-mixtures were crushed and molded to disk-shaped samples, The samples were set between hot plates at 120℃ and compressed under 5MPa for one minute. The changes of the distance between the hot plates were used to evaluate the thickness changes of the samples, a measure of moldability. Then, the samples were heated at 150℃ for eight minutes to assure full curing of the PF resin.

Results and discussion

The table and figure show the effects of the fiber content on the mechanical property of the samples. The CTMP nanofibers reinforced PF resin composites exhibited good moldability up to a fiber content of 30%. The flexural strength of PF resin doubled by adding only 10wt% of CTMP nanofibers, although the increase of the Young's modulus was around 60%. The flexural strength reached values around 160MPa at a 20wt% fiber content.

On the basis of these results, transfer molding of the CTMP nanofibers mixed PF resin compounds was studied at a 20wt% fiber content. The transfer molding of the compound was successful, and the Young's modulus and flexural strength of the molded composite were 5.3 GPa and 115.3 MPa, respectively. Considering that the Young's modulus and flexural strength of the transfer molded composites reinforced by CTMP pulp were 4.5GPa and 69.5 MPa, respectively, it is concluded that the reinforcement by microfibrillated CTMP pulp can improve the strength of PF significantly, while enabling transfer molding.

Table 1. Mechanical properties of CTMP nanofibers reinforced PF resin

CTMP content (wt%)	Density(g/cm³)	Frexural strength (MPa)	Young's modulus (GPa)
0	1.24	77.4	4.1
10	1.33	147.1	6.6
20	1.35	156.2	7.1
30	1.36	134.5	6.4

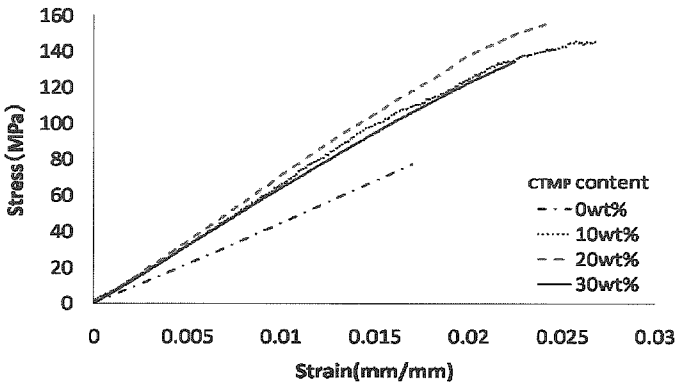

Figure 1. Stress-strain curves of CTMP nanofibers reinforced PF resin

Development of Ultra-Low Density Material made from Wood fiber and Konjac glucomannan

(Graduate School of Agriculture, Laboratory of Sustainable materials, RISH, Kyoto University)

Masashi Oriyama

【Introduction】 Recently, a concern about the global environment is rising and possible problems in the future are worried. One of these problems is exhaustion of fossil resources. A large amount of fossil resources are used in chemical products. Foam plastic materials which are used as an insulator are also mainly made from fossil resources. Therefore, development of the alternative materials made form non-fossil resources is required. In this study, the main aim was to develop an ultra-low density material being equal with plastic foam without using fossil resources. As a key material, konjac glucomannan (KGM) which is gel polymer was used, and ultra-low density material was made only from KGM and wood fiber.

【Materials and Methods】 Wood fiber made from *Shorea* spp. and purified KGM powder with the average molecular weight of 1,000,000~2,000,000 were used as raw materials. Wood fiber were mixed with KGM powder dissolved into hot water of 80°C to be 0.7wt% and stirred for 30 minute. After cooling down to 60°C in the room temperature, a little amount of calcium hydroxide solution was added as coagulant. The mixture was stirred quickly and poured to a molding case. It was heated at 60°C for 1h and boiled for 10minutes. The formed gel was freeze-dried. Wood fiber content was varied from 0.0 to 75.0%. [Mechanical property] Three-point bending test and compression test were performed according to JIS A 9511. [Thermal conductivity] Thermal conductivity was measured by transient heat probe method according to JIS A 1412-2. [Humidity control capacity] Temperature and relative humidity inside steel box within material were measured in the climatic chamber. The temperatures of the climatic chamber varied sinusoidally around 25°C, which had three wave periods of 3, 6, 24h. [Sound absorption coefficient] Normal incident sound absorption coefficient was measured based on the two-microphone transfer-function method according to JIS A 1405-2. Frequency ranged from 200 to 3,200 Hz.

【Results and Discussion】 The densities of the newly developed materials increased with increasing wood fiber content, being ranged from 0.010 to 0.035g/cm^3. The density of material was about 1/10 of insulation fiberboard and was almost same as foam plastic materials. The values of MOR in bending and compressive strength increased with increasing the density, and showed 60kPa and 20kPa, respectively, with the fiber content of 75.0%. Fig.1 shows the thermal conductivity in a relation to the material density. The values of the thermal conductivity ranged from 0.036 to 0.042W/mK with increasing the density. These values were much lower than conventional wood-based materials, and comparable with that (0.035W/mK) of polystyrene foam with density of 0.025g/cm^3. The humidity control capacity of the material increased with increasing wood fiber content. The material with the fiber content of 75.0% showed almost the same humidity control capacity as Sugi (flat-sawn), however, faster response to the humidity change. The sound absorption coefficient of the material with fiber content of 75.0% showed higher performance than that of insulation fiberboard and was similar to that of glass wool.

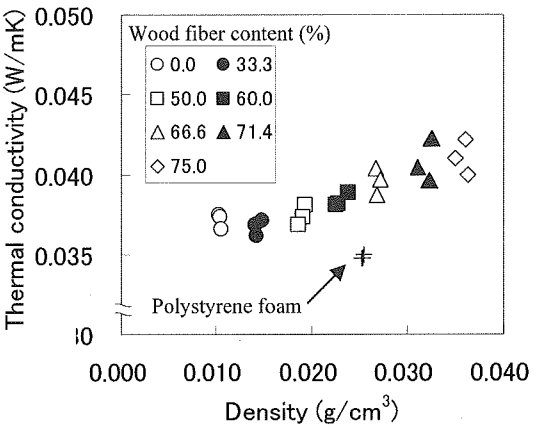

Fig.1. Thermal conductivity as a function of material density.

Study on the aging mechanism of wood and its application
- Analysis of color properties by comparing the accelerated aging wood with the natural aging wood from historical buildings –

**(Graduate School of Agriculture,
Laboratory of Sustainable Materials, RISH, Kyoto University)**

Miyuki Matsuo

Introduction

The deterioration of wood as a material is due to biodegradation, weathering, and aging. In appropriate conditions which can avoid biodegradation and weathering, the service life of wood can exceed a thousand years and aging becomes a main source of the wood deterioration. The elucidation of wood aging mechanism is important not only for the preservation and restoration of wooden historical buildings but also for basic wood research which provides the effective use of wood materials. Though some empirical data have suggested that wood aging is a mild thermal oxidation at room temperature, a few papers have reported on its theoretical evaluation and the detailed mechanisms. On the other hand, sculptors and carpenters have used the color of wood as a criterion of aging. This may be because the color properties conspicuously express the aging of wood. This study deals with the aging on wood color; the color changes of natural aging wood were compared with those of accelerated aging wood by using the kinetic analysis to discuss the mechanism of color change during aging. In addition, color changes of cellulose were also compared with those of wood to evaluate the contribution of cellulose to the color changes of wood.

Materials and Methods

Specimens for accelerated aging were cut out from 360-years-old Hinoki (*Chamaecyparis obtusa* Endl.) from Kiso, Japan. Oven dried specimens were heated in an air-circulating oven at 90, 120, 150, and 180 °C for a duration ranging from 0.5 hour to approximately 2 years. Natural aging wood samples were cut out from eight natural aging wood samples collected from historical buildings. The aging times of these samples, which were determined by dendrochronology and radiocarbon dating, ranged from 569 to 1573 years. Cellulose specimens (Whatman No.1 filter paper, made of cotton cellulose) were heated in an air-circulating oven at 180 °C. The color of the specimens was measured with a spectrophotometer (KONICA MINOLTA CM-2600d). The CIELAB color parameters (L^*, a^*, b^*) and the color differences (ΔE^*_{ab}) were used for the analysis. Three locations in each specimen were measured, and the average color values with the standard deviations were calculated.

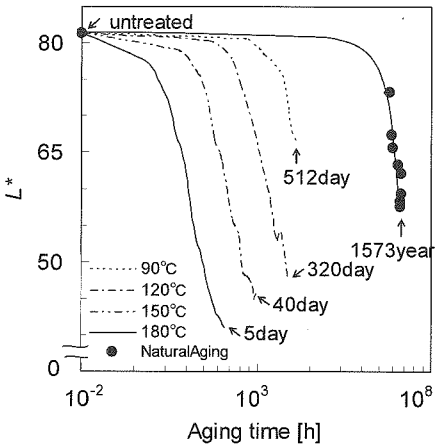

Figure 1. Changes of L^* during natural aging and accelerated aging as a function of aging time.

Results and Discussion

Figure 1 shows the changes of L^* during accelerated aging and natural aging wood samples as an example. Similar behaviors were observed irrespective of accelerated aging or natural aging, suggesting that the same processes might cause these color changes. The Arrhenius plots, which described the relationship between the changes of L^* during accelerated aging and heating temperature, were extrapolated to an ambient temperature to predict the changes during natural aging. By comparing the natural color changes with the prediction, it was concluded that color changes during natural aging were mainly explained as a thermal oxidation process. This conclusion was supported by the result that color changes of heat-treated natural aging wood exhibited the similar behavior with that of accelerated aging wood. However, the natural color changes were somewhat faster than the prediction. The color changes of cellulose heated at 180 °C showed the similar behavior with that of natural and accelerated aging wood. This result indicates that cellulose is one of major components that contribute to wood color change during aging.

Effect of Drying Methods on Durability and Strength Performance of Japanese Cedar for Post and Beam Timber Construction

**(Graduate School of Agriculture,
Laboratory of Structural Function, RISH, Kyoto University)**

Akihiro Kousoku

Introduction

To promote Japanese cedar usage, it is needed to increase reliability of timber as the construction material. To do so, drying techniques that can improve stability or strength and grading techniques that can be done in nondestructive way are important. Although lots of drying schedules of Japanese cedar has been developed, there is not enough information about how much drying atmosphere can affect the characteristics of timbers, especially in full scale. For example, the honeycombs or evaporations of extractives due to high temperature could cause the loss of strength or durability of timber. In this research, to intend to use Japanese cedar as the material for post and beam residential house, Japanese cedar were dried in 4 ways to examine and compare their strength, durability and performance of joint.

Methods

Two hundred forty logs of Japanese cedar in Kyoto were collected and divided into 2 groups according to the color of heartwood (red and black). According to MOE measured by nondestructive way, each 2 groups separated into 4 small groups respectively so that they could have the same average and standard deviation. Each small group was dried in 4 different methods; air drying, mild temperature drying (90 degree Celsius at highest), high temperature drying (110 degree), and high temperature set drying (120 degree). For the indicators of strength, MOE in nondestructive ways (longitudinal vibration method, torsional vibration method, and TGH method), full-scale compression, and full-scale shear test were examined. To evaluate the durability, forced and selective termite test and rotting test were conducted. Finally, to evaluate the joint characteristics, full-scale column and sill pullout test were carried out.

Result and Discussion

Nondestructive test result showed that, as the MOE examined in log was bigger than that in sawn timber, it was better to grade timber after sawing. And it also showed that there was not significant difference between MOE and shear stiffness calculated in different ways. But the shear stiffness of air and mild dried specimen calculated by torsional vibration method were highly decreased and this result indicated that the crack or back split should be taken into account to calculate the shear stiffness traversing the cracks. The strength or stiffness estimated by full-scale compression and shear test didn't show the significant difference. Since they showed good correlation with density and MOE despite of drying schedule, it was confirmed that grading by density or MOE is important to estimate the characteristics of strength. In the fungi and termite test, high temperature dried specimen had reduced its weight more than air dried one. Although it was hard to get the correlation between the reduction ratio of density and compression strength, it became clear that the less the density the specimen had, the less its compression strength or stiffness became. The joint strength didn't show significant difference in any types of joint and this was because there was no difference in compression or shear strength that were the main mechanism of these joint.

Above all, conclusions were as follows:

1. Drying schedule could effect on durability of Japanese cedar.
2. As far as these 4 drying schedule, however, didn't affect on strength or stiffness.
3. Grading is very important to ensure the strength or MOE of timber.

The effect of different foundation systems on the fungal flora in the crawl space of a new wooden Japanese house

(Laboratory of Innovative Humano-Habitability, RISH, Kyoto University)

Aya Toyoumi

In order to establish novel preventive measures against damage of wooden houses by decay fungi with less chemical, we periodically monitored the fungal flora in two different foundation systems in the crawl space of an experimental Japanese house.

Either a layer of concrete or just soil as the foundation system were employed, and moisture content of foundation timbers, temperature and humidity of the crawl space were measured. Fungi were sampled by the following methods: a) from the crawl space atmosphere with a PDA plate, b) from foundation timbers with a soft plastic tape, and c) from small wood blocks laid on a layer of concrete or on soil. Visually pre-identified basidiomycetes were served for further DNA analyses. A decay test was conducted with these fungi: 16 white rot fungi and a brown rot fungus.

Numbers of fungal colonies in the concrete section were significantly lower than those in the soil section. The soil section generally showed higher humidity and moisture content of foundation timbers than in the concrete section. These findings suggested that the soil strongly influenced the water condition of the crawl space, indicating the higher decay risk in the soil section.

To analyze the effect of air flow on the fungal flora, all ventilation slits were air-tightly closed with an aluminum tape. This resulted in higher numbers of fungal colonies, humidity and moisture content of foundation timbers in the soil section (Table1.). These results indicate that the ventilation is indispensable for a house with a soil foundation system to reduce the risk of fungal attack. On the other hand, for a house with a concrete floor the ventilation would best be closed in terms of fungal deterioration. Considering the risk of other deteriorating agents, it is strongly recommended to construct innovative inspection/monitoring options for the concrete foundation without ventilation.

Table 1. Temperature, humidity, the MC of foundation timbers, the CFUs/cm^2 of the fungal samples from foundation timbers in the crawl space, and the CFUs/plate of the fungal samples from the atmosphere of the crawl space when the test sections were air-tightly closed to the outside.

	Soil section		Concrete section	
	Before closing	After closing	Before closing	After closing
Temperature (°C)	13.3	8.9	13.6	8.9
RH (%)	83	98	67	62
Average MC of foundation timbers (%)	22	28	15	14
Fungi from the crawl space atmosphere (CFU/plate)	29.6	106.5	2.8	0

This study clearly indicated the importance of foundation system in wooden houses, and the higher decay risk in the soil floor than in the concrete floor.

Acknowledgements

The author wishes to thank to Prof. Shuichi Doi (Tsukuba University) and Dr. Sakae Horisawa (Kochi University of Technology) for their kind cooperation. This research was partially supported by the TOSTEM foundation and the Cooperative Study Program of Research Institute for Sustainable Humanosphere, Kyoto University (Wood Composite Hall).

Microwave Technology as a Non-Destructive Termite Control Method

(Laboratory of Innovative Humano-Habitability, RISH, Kyoto University)

Kazushi Nakai

Microwave treatment is superior to conventional heating in a few aspects. Conventional heat treatment generally takes relatively longer because the heating periods depend on the thermal conduction of materials, whereas microwave can quickly raise the temperature interior of materials by different heating mechanism. Therefore, feasibility of microwave technique was discussed with three economically important Japanese termite species, *Coptotermes formosanus* Shiraki, *Reticulitermes speratus* (Kolbe), and *Incisitermes minor* (Hagen) in the laboratory, since the technique is expected to be an environmentally friendly alternative to the chemical treatment

The main object of this research was to develop a non-destructive termite control method by using microwave energy. Maximum power density was 100 mW/cm^2 and two levels of frequencies, 2.45 GHz and 5.8 GHz, were selectively studied based on practical applicability in the field.

In direct irradiation test, microwave was irradiated onto 100 workers of termites of *C. formosanus* in a plastic petri dish. Surface temperatures of termites before and after irradiation were measured by a radiation thermometer to determine thermal difference. Mortality development after exposure was recorded for 3 weeks in a termite culturing room. In addition, to determine the effect of microwave energy repellent to termites, the shielded area was created in the same irradiation space. The activity of termites was recorded by a digital video camera.

In indirect irradiation test, a 52 mm-diameter plastic petri dish with *I. minor* in was sandwitched by two wood specimens. Microwave energy was emitted onto the surface of upper wood specimen. The thermal differences in temperatures interior and exterior of wood specimens were measured by using K-type thermocouples and the radiation thermometer. Number of dead termites during exposure was counted regularly.

Thermal difference before and after direct irradiation was recognized as variations in temperature based on surface temperature of termite body The results suggested that microwave energy used in this study could not raise the temperature high enough to kill termites. Table 1 shows the mortality of each termite species 3 weeks after the direct microwave irradiation at 5.8GHz, 100mW/cm^2 . There was no significant difference in the mortality between exposed and non-exposed (control) termites, regardless of test termite species. This finding clearly supported that microwave energy did not affect termite physiologically. The repellent behavior of termites may be attributed to the inhomogeneous response related to frequency or termite species as indicated by statistical analysis of shot images. Thus, the effect of microwave was reflected only as heating of termites, and related to termite repellency, although the termites were less sensitive in the electromagnetic field.

On the other hand, in the indirect irradiation test, the temperature inside the wood specimens increased with exposure time. Both levels of microwave irradiation caused in higher mortality than the direct irradiation. At 2.45 GHz, the thin wood specimens were not heated high enough to induce 100% mortality, whereas all termites were killed in thicker specimens. The frequency level 5.8 GHz irradiation could raise the temperature within specimens, although 5.8 GHz irradiation was not attributed to uniformity of heating in whole irradiation area. These results demonstrated that the effect of microwave irradiation varied with thickness of wood, and that selection of microwave frequency suitable for wood dimension was extremely important to terminate the infestation of termites. Eradication of termites inside the wood by using microwave seems applicable at an adequate frequency, considering penetration depth in accordance with wood dimension.

Table 1. Mortality of termite (%) (mean±SD) at 3 weeks after irradiation at 5.8GHz, 100mW/cm^2

Termite species	Exposure time (min)			
	Control	15	30	60
C. formosanus	15.5 ± 10.2	17.8 ± 20.1	17.8 ± 5.1	22.7 ± 6.0
R. speratus	23.5 ± 13.3	15.3 ± 8.1	15.4 ± 4.2	20 ± 8.1
I. minor	8.6 ± 9.2	6.7 ± 11.5	17.8 ± 20.4	13.3 ± 11.5

Three-dimensional electromagnetic particle simulations of a magnetron based on the real model

(Graduate School of Electrical and Electronic Engineering, Laboratory of Computer Simulation for Humanosperic Sciences, RISH, Kyoto University)

Yosuke Uranishi

Magnetron is a cylindrical diode which converts input DC to microwave at high efficiency and large capacity. It has a cathode in the center and an anode which covers the cathode with some internal resonance cavities. Each of the internal resonators opens out into the anode-cathode space. Electrons continuously emitted from the cathode interact with electromagnetic field(EM) in the anode-cathode space. The electron kinetic energy transferred to the microwave energy through the resonance.

It is very hard to analyze theoretically the electron resonance with the electromagnetic field in the internal space bounded by complex shaped conductors of magnetrons. In order to get higher efficiency and lower noise of magnetron, we first have to quantitatively understand the internal phenomena in magnetrons.

We have developed a three dimensional magnetron simulator using Particle In Cell(PIC) method. To simulate the electrons-EM field resonance in a real magnetron, we used the cartesian coordinate system so that we could model precisely the commercial magnetron named as 2M210M1F1 designed by Panasonic for microwave ovens. In the simulation, we obtained 2.64GHz self-oscillation microwave with efficiency of 73% ,which almost agrees with the real efficiency. This agreement assures that the developed simulator can quantitatively simulate the real magnetron behavior.

Next, to obtain the information of relationships between the internal structures of magnetorons and characteristics of output microwaves, we tested different shapes of cathodes and antennas. As a result, characteristics of output power and efficiency changed on some level.

Finally, we simulate the injection locking method that enables us to control the output phase and frequency of microwaves by injecting a reference microwave signal. As a result, We could successfully controll the output phase and frequency and observe the transient state of synchronisation.

Acknowledgements

Computation in the present study was performed with the KDK system of Research Institute for Sustainable Humanosphere (RISH) and Academic Center for Computing and Media Studies at Kyoto University as a collaborative research project.

Competing Process between Mirror Instability and L-mode Electromagnetic Ion Cyclotron Instability in the Earth's Magnetosheath

(Graduate School of Electrical and Electronic Engineering, Laboratory of Computer Simulation for Humanosperic Sciences, RISH, Kyoto University)

Masafumi Shoji

Spacecraft observations show that the mirror instability dominates over the L-mode electromagnetic ion cyclotron (EMIC) instability in the magnetosheath (see Figure 1), although the theoretical linear growth rate of the L-mode EMIC wave is higher than that of the mirror mode waves [1]. This has been a long-standing puzzle. To analyze the competing processes between the L-mode EMIC and mirror instabilities, we performed one-, two- and three-dimensional (1D, 2D and 3D) hybrid simulations, assuming anisotropic energetic ions[2].

In the 2D model, the energy of the L-mode waves is higher in the initial stages because their linear growth rate is larger than that of the mirror mode. In the 3D model, however, the energy of the mirror mode waves is larger than that of the L-mode waves for all times. This is because there are more directions of the wavenumber vectors of the mirror mode waves (degrees of freedom) in the perpendicular direction to the ambient magnetic field.

After the saturation of these instabilities, inverse cascading of L-mode EMIC waves and coalescence of the mirror mode waves take place in both models. We also developed a new 2D model to analyze the coalescence of monochromatic mirror mode structure. At this stage, the coalescence is slower process than the inverse cascading, and thus the temperature anisotropy of the protons is controlled by the inverse cascading process. Through the coalescence, the scale size of the mirror mode structure in the transient coalescence process of the 3D model (~ 40 ion inertial lengths) becomes in good agreement with planetary magnetosheath observations.

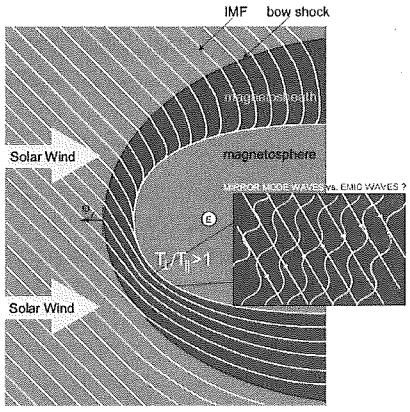

Figure 1. The logo of Kyoto University. The figure caption should be under the figure.

Furthermore, we analyzed the relation between the mirror instability and the magnetic peaks/dips which are observed in the magnetosheath. The 3D simulation result indicates that the mirror instability contributes only to the magnetic peaks actually observed in the magnetosheath.

Acknowledgements

Computation in the present study was performed with the KDK system of Research Institute for Sustainable Humanosphere (RISH) and Academic Center for Computing and Media Studies at Kyoto University as a collaborative research project.

References

[1] Tsurutani, B. T., E. J. Smith, R. R. Anderson, K. W. Ogilvie, J. D. Scudder, D. N. Baker, and S. J. Bame, "Lion roars and nonoscillatory drift mirror waves in the magnetosheath," *J. Geophys. Res.*, vol. 87, no. A8, pp. 6060-6072, 1982.

[2] Shoji, M, Y. Omura, B. T. Tsurutani, O. P. Verkhoglyadova, and B. Lembege, "Mirror instability and L-mode Electromagnetic Ion Cyclotron Instability: Competition in the Earth's Magnetosheath, *submitted to J. Geophys. Res.*

Research and Development of Microwave Irradiation Systems for Pretreatment of Woody Biomass

(Graduate School of Engineering, Laboratory of Applied Radio Engineering for Sustainable Humanosphere, RISH, Kyoto University)

Hiroaki Suzuki

Toward ethanol production from woody biomass, there are two main processes: saccharization and alcohol fermentation. Microwave irradiation pretreatment to the woody biomass before the enzyme saccharification process induces dissociation of cell wall components and increases enzyme reactive area. These effects improve efficiency of the enzyme saccharification. The objective of the present study is development of highly-efficient microwave irradiation systems for the pretreatment of the woody biomass. Two types of microwave irradiation cavities were studied: a batch-process type, shown in Fig.1, and a continuous-process type.

Internal electric fields and Specific Absorption Rate (SAR) values distribution were simulated with 3D electromagnetic simulator. New cavity models were developed for 2.45GHz irradiation and for 5.8GHz irradiation that showed more even SAR values distribution than that of the previous batch-type cavity model. Then, the simulation results were compared to heating efficiency of practical experiments. It is found that there was temperature distribution in the mixture from the practical experiments of the batch-type cavity.

A continuous-type cavity was also developed for the sake of continuous pretreatment of woody biomass. After developing the continuous-type cavity, total electric energy balance per a practical treatment was measured. From measurement results, we evaluated heat efficiency and effects of heat loss and power absorption at a glass plate, which was inserted into microwave irradiation port in order to heat woods and solvents under a high pressure. To improve these losses, various shapes of dielectric materials were put in front of the glass plate. Some shapes of teflons were very effective to lower a reflection ratio.

References

[1] Suzuki H., T. Mitani, N. Shinohara, M. Oyadomari, T. Watanabe, T. Tsumiya and H. Sego, "Study on a Microwave Irradiation Cavity for Pretreatment of Ethanol Production from Woody Biomass", 2008 Global Congress on Microwave Energy Applications, pp.411-414, 2009.

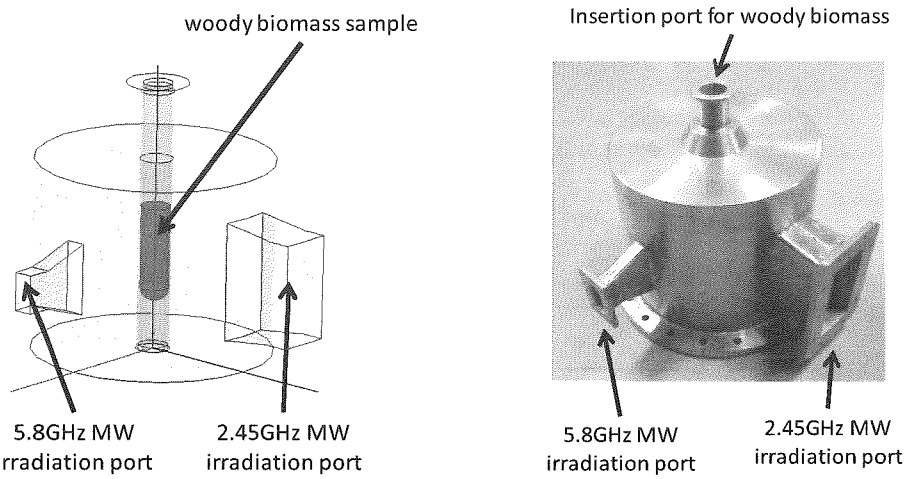

(a) A structure of 3D electromagnetic simulation (b) A test cavity designed by the simulation

Figure 1. Development of a batch-type microwave irradiation cavity.

Development and a field experiment of a retrodirective system for microwave power transmission

(Graduate School of Engineering, Laboratory of Applied Radio Engineering for Sustainable Humanosphere, RISH, Kyoto University)

Fumito Takahashi

Although we have studied so far microwave power transmission with mainly indoor experiment using an anechoic chamber, the microwave power transmission will be used outdoor such as SPS (Solar Power Satellite). Because our present experimental systems are too large and heavy, we need to develop a field experiment system which is light, small, and low cost. Outdoor noises make the accuracy of DOA (Direction Of Arrival) estimation worse and we have to study DOA estimation methods robust against noise.

We have developed a field experiment system of a microwave power transmission system composed of a beam transmitting system and a pilot signal transmitting system. There are two ideas for field experiments, one is an airship experiment, and the other is a software retrodirective system experiment.

In the airship experiment, we estimate DOA with the developed field experiment system. We performed indoor and field experiments. In the indoor experiment we could totally estimate the DOA accurately.

As we changed the distance between the two reception antenna elements longer to evaluate the estimation accuracy, the accuracy became better. In the field experiment the result was worse than that of the indoor experiment. But we considered that there were no problems for the airship experiment.

In the software retrodirective system experiment, we used phased array antennas composed of eight elements for the microwave power transmission and array antennas composed of four elements for the DOA estimation. In the indoor experiment we could estimate DOA accurately and the DOA estimation program could follow with the direction of the pilot signal as it moved continuously. We could also transmit the microwave power accurately to the DOA. In the field experiment we could also accurately estimate DOA and the accuracy of the field experiment was almost equal to that of the indoor experiment.

We also studied the "TF (Time Frequency)-MUSIC" method, a DOA estimation method robust against noise compared with the MUSIC method. This method estimates DOA on the time-frequency domain. We compared these methods and found the superiority of the TF-MUSIC method to the MUSIC method under low SNR.

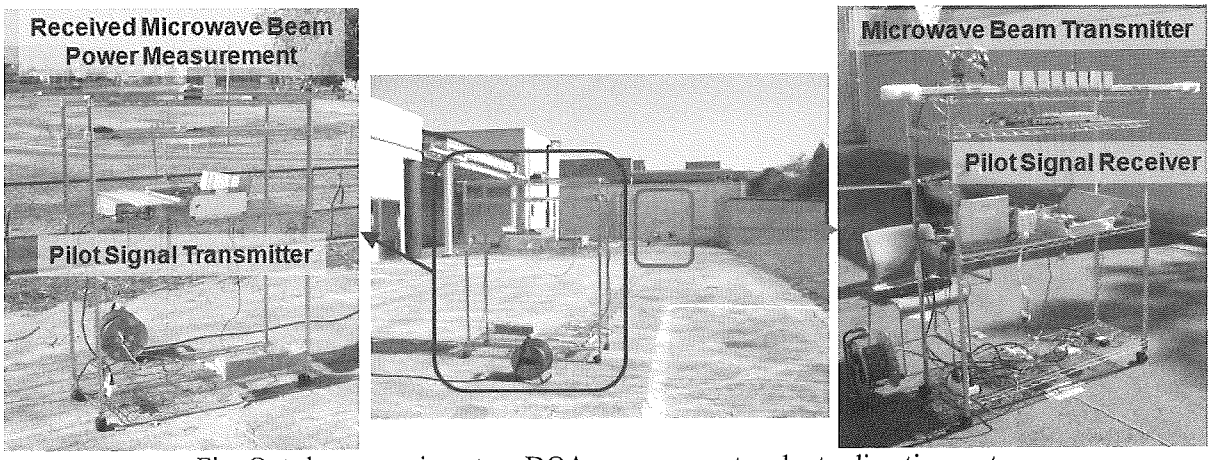

Fig. Out-door experiment on DOA measurement and retrodirective system.

Development of high-power rectennas with GaN schottky diode

(Graduate School of Engineering, Laboratory of Applied Radio Engineering for Sustainable Humanosphere, RISH, Kyoto University)

Yushi Miyata

As a new application of wireless power transmission technology, a wireless power distribution system for buildings is proposed. This system supplies electric power wirelessly by transmitting microwave through building materials or deck plates which are used as microwave transmission waveguides.

First, the necessity of a rectifier circuit that converts microwave power into DC power is described. The size of the rectifier circuit is necessary to be smaller than 10cm3. Then, development of the rectifier circuit with GaN schottky diode is required for high-power rectification, because its breakdown voltage is much higher than that of Si schottky diode.

Next, rectifier circuits were designed with computer simulation. GaN diodes were connected in parallel, and the number of diodes was changed from 1 to 8. From simulation results, the efficiency was increased, when the number of diodes was increased. This is because the impedance was decreased, and power loss of diodes was reduced as the diodes was connected in parallel. Then, rectifier circuits with GaN schottky diode whose breakdown voltage is 40V were designed and experimentally produced. However, all of the developed rectifier circuits were low efficiency. This is because the influence of gold wire was wrong, or SPICE parameter was different from real value.

Next, we characteristics of GaN schottky diode whose breakdown voltage is 100V were examined by developing half-wave rectifier circuits. It is found that most diodes were normal behavior. Then, three patterns of rectifier circuits were newly developed. First, the rectifier circuit and a heat sink were glued with silver paste. However, the efficiency of this developed circuit was not increased. Second, a condenser was inserted between a diode and a ground. It is found that the efficiency was improved to be about 14.6%. The efficiency was increased about 5 points. Third, a stub was inserted between a diode and a ground. The efficiency was dependent on the stub length. When the stub length was 8mm, the efficiency was about 36.0%. As results, the third rectifier circuit provided the highest efficiency.

References

[1] Shinohara, N., Y. Miyata, T. Mitani, N. Niwa, K. Takagi, K. Hamamoto, S. Ujigawa, J. Ao and Y. Ohno, "New Application of Microwave Power Transmission for Wireless Power Distribution System in Buildings", Asia Pacific Microwave Conference 2008, H2-08, Hong Kong, Dec. 16-20, 2008.

Magnetohydrodynamic Analysis for Magneto-Plasma Sail Spacecraft

**(Graduate School of Engineering,
Laboratory of Space Systems and Astronautics, RISH, Kyoto University)**

Daisuke Sasaki

Exploration of the solar system can be accelerated using an advanced space propulsion system. One of the new propulsion systems suitable for deep space exploration is a magnetic sail propulsion system. Magnetic Sail(MS)is a sail propulsion system using an interaction between the solar wind and the artificial magnetic field around the spacecraft, and Magneto-Plasma Sail(MPS)is an advanced concept of the MS with plasma jet from the spacecraft in order to expand the magnetosphere. The solar wind energy is converted to the thrust of the MS and MPS. It generates a continuous, high thrust in the outward direction from the sun (see Figure on the right).

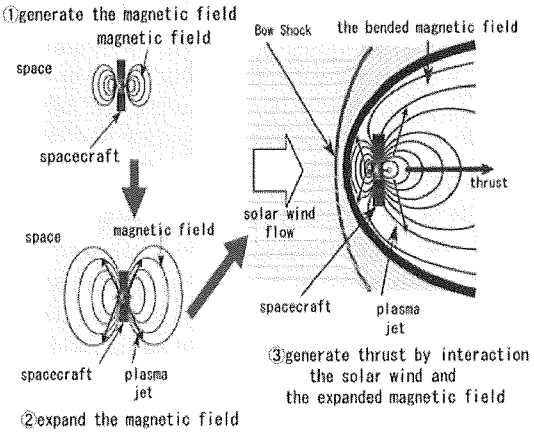

In this thesis, we investigate the thrust characteristics of the MPS [1-4]. First, we simulate the formation of a magnetosphere when the solar wind interacts with the magnetic field in axisymmetric two-dimensional MHD analysis. The magnetospheric size is found to be inflated by a plasma jet emitted from the spacecraft. The simulation results show that the magnetospheric size is unchanged as long as β value (plasma dynamic pressure divided by magnetic pressure at spacecraft position)is constant. Second, we study the thrust magnitude of the MPS. In the MPS, the thrust increases compared with the MS, whose magnitude depends on β of the plasma jet. The maximum strength of thrust is obtained in low β condition rather than in high β condition. The thrust is generated by the induced magnetic field produced by the magnetospheric current. In a case of high β ,a termination shock is produced inside the magnetosphere, where the current flows in the opposite direction to that on the magnetosphere. Therefore, in high β case, although the magnetosphere is more expanded than that of the MS, the thrust is decreased by the current on the termination shock compared to that with low β condition. Finally, we compare the specific impulse (Isp) and thrust/power ratio of the MPS with those of the conventional electric propulsion system (EP).We found that both Isp and the thrust/power ratio of MPS with low β case are higher than those of the EP.

Acknowledgements

The authors would like to acknowledge the support of Ass. Prof. I. Funaki of ISAS, Japan Aerospace Exploration Agency, Ass. Prof. T. Nakamura of Graduate School of Engineering, Kyoto University, and Ass. Prof. H. Usui, RISH. This research is supported by the JST/CREST program..

References

[1] Sasaki, D., Funaki, I., Yamakawa, H., Usui, H., and Kojima, H., "Thrust Production Mechanism of Magnetic Sail Spacecraft with Superconducting Coils," The 59th International Astronautical Congress, Glasgow, UK, September 29-October 3, 2008.

[2] Sasaki, D., Funaki, I., Yamakawa, H., Usui, H., Kojima, H., "Numerical Simulation of Magnetic Sail Spacecraft with Superconducting Coils," AIP Conference Proceedings, Vol. 1084, pp. 784-792, 2009.

[3] Minami, M., Funaki, I., Nakamura, T., Yamakawa, H., Nishida, N., Sasaki, D., Kojima, H., Ueda, Y., "Thrust Characteristics of Magnetic Sail Spacecraft Using Superconducting Coils," AIP Conference Proceedings, Vol. 1084, pp. 721-727, 2009.

Study on One-chip Analog Integration Circuit System for Miniaturized Plasma Wave Receivers

**(Graduate School of Engineering,
Laboratory of Space Systems and Astronautics, RISH, Kyoto University)**

Yuta Mizuochi

In the magnetosphere of the earth a multitude of physical phenomena are arising. Plasma waves, ones of them, have several modes and different exciting mechanisms. It has been needed for the space development to explain their characters.

Therefore, a plasma wave receiver (PWR) was developed to observe plasma waves arising in the magnetosphere of the earth and the interplanetary space. Analog circuits of PWR consist of amplifiers and analog filters. Six channels of analog circuits are needed to observe electric and magnetic fields. It makes analog components of PWR bigger than other circuits. Since miniaturizing onboard instruments for scientific observation is demanded, we have studied on the integration of the analog components by application specific integrated circuit technology. Some of analog circuits consisting of PWR has been designed and manufactured. Their operations have also been checked in the past study.

In this study [1-4], we designed an anti-aliasing filter for eliminating waves with frequency higher than 100kHz to reduce aliasing effect by digitize. We also designed a circuit system combined a 20dB amplifier and the anti-aliasing filter. We examined their properties, temperature dependence, noise properties and so on. From these results, we confirmed the designed anti-aliasing filter operated as planned and the system had gain of about 20.3dB, input noise level of 400nV=pHz at 10kHz and dynamic range of 90dB. We considered the designed circuits could be used for components of PWR from the results. Furthermore, we realized six channels of antialiasing filters in one chip which size is within 3mm $\times$ 3mm. This indicates PWR will be made much smaller than the past one.

For the next design, we have designed the one-chip analog integration circuits system including a differential amplifier, a low-pass filter, the 20dB amplifier and the anti-aliasing filter. From circuit simulation results for this system, we have obtained good results satisfying the specification of PWR. This system will change the style of observation in space.

References

[1] Mizuochi. Saito, Y., Y., Kojima, H., Ueda, Y., "Miniaturization of Plasma Wave Receiver for Small Scientific Satellite Missions," The 59th International Astronautical Congress, Glasgow, UK, September 29-October 3, 2008.

[2] Kojima, H., Mizuochi, Y., Fukuhara, H., Yagitani, S., Ikeda, H., Iwai, H., Takizawa, Y., Yamakawa, H., Ueda, Y., and Usui, H., "Miniatuarization of Plasma Wave Receivers onboard Scientific Satellites and its Application to the Sensor Network System for Monitoring the Electromagnetic Environment in Space," The 27th International Symposium on Space Technology and Science, Tsukuba, Japan, July 5 - 12, 2009.

[3] Kojima, H., Saito, Y., Mizuochi, Y., Takizawa, Y., Iwai, H., Yagitani, S., Yamakawa, H., and Ueda, Y.,"Monitor System for Space Electromagnetic Environments,"Paper 2008-r-2-08, The 26th International Symposium on Space Technology and Science, Hamamatsu, Japan, June 1-8, 2008.

[4] H. Kojima, Y. Mizuochi, H. Fukuhara, S. Yagitani, H. Ikeda, H. Iwai, Y. Takizawa, H. Yamakawa, Y. Ueda and H. Usui, "Miniaturization of Plasma Wave Receivers onboard Scientific Satellites and its Application to the Sensor Network System for Monitoring the Electromagnetic Environment in Space," European Geophysical Union General Assembly, Austria, 2009.

Publications in FY 2008
(Articles published in refereed journals)

Horikawa Y, Clair B, Sugiyama J, "Varietal difference in cellulose microfibril dimensions observed by infrared spectroscopy," Cellulose, vol.16, no.1, pp.1-8, 2009.

Kanzaki T, Horikawa Y, Makino A, Sugiyama J, Kimura S, "Nanotube and three-way nanotube formation with nonionic amphiphilic block peptides," Macromolecular Bioscience, vol.8, no.11, pp.1026-1033, 2008.

Hartati S, Sudarmonowati E., Park YW. Kaku T, Kaida R, Baba K, Hayashi T, "Overexpression of poplar cellulase accelerates growth and disturbs the closing movements of leaves in sengon," Plant Physiology, vol.147, no.2, pp.552-561, 2008.

Hayashi T, Kaku T, Kaida R, Baba K, "Overexpression of cellulases in plant," Cellulose Communications, vol.15, no.4, pp.148-152, 2008, (in Japanese).

Ikegaya H, Hayashi T, Kaku T, Iwata K, Sonobe S, Shimmen T, "Presence of xyloglucan-like polysaccharide in Spirogyra and possible involvement in cell-cell attachment," Phycological Research, vol.56, no.3, pp.216-222, 2008.

Kojiro K, Furuta Y, Ohkoshi M, Ishimaru Y, Yokoyama M, Sugiyama J, Kawai S, Mitsutani T, Ozaki H , Sakamoto M , Imamura M, "Changes in micropores in dry wood with elapsed time in the environment," Journal of Wood Science, vol.54, no.6, pp.515-519, 2008.

Nakamura I, Makino A, Sugiyama J, Ohmae M, Kimura S, "Enzymatic activities of novel mutant endoglucanases carrying sequential active sites," International Journal of Biological Macromolecules, vol.43, no.3, pp.226-231, 2008.

Horikawa Y, Sugiyama J, "Accessibility and size of Valonia cellulose microfibril studied by combined deuteration/rehydrogenation and FTIR technique," Cellulose, vol.15, no.3, pp.419-424, 2008.

Taniguchi T, Ohmiya Y, Kurita M, Tsubomura M, Kondo T, Park YW, Baba K, Hayashi T, "Biosafety assessment of transgenic poplars overexpressing xyloglucanase (AaXEG2) prior to field trials," J. Wood Sci., vol.54, no.5, pp.408-413, 2008.

Tsukihara, T., Y. Honda, R. Sakai, T. Watanabe, T. Watanabe, "Mechanism for oxidation of high-molecular-weight substrates by a fungal versatile peroxidase, MnP2," Appl. Environ. Microbiol, vol.74, pp.2873-2881, 2008.

Nishimura, H., S. Tsuda, H. Shimizu, Y. Ohashi, T. Watanabe, Y. Honda, T. Watanabe, "*De novo* synthesis of (Z)- and (E)-7-hexadecenylitaconic acids by a selective lignin-degrading fungus, *Ceriporiopsis subvermispora*," Phytochemistry, vol.69, pp.2593-2602, 2008.

Nishimura, H., K. Murayama, T. Watanabe, Y. Honda, T. Watanabe, "Absolute configuration of ceriporic acids, the iron redox-silencing metabolites produced by a selective lignin-degrading fungus, *Ceriporiopsis subvermispora*," Chem. Phys. Lipids, vol.159, pp.77-80, 2009.

Nakatsubo, T., Y. Kitamura, N. Sakakibara, M. Mizutani, T. Hattori, N. Sakurai, D. Shibata, S. Suzuki, T. Umezawa, "At5g54160 gene encodes Arabidopsis thaliana 5-hydroxyconiferaldehyde O-methyltransferase," J. Wood Sci., vol.54, pp.312-317, 2008.

Nakatsubo, T., L. Li, T. Hattori, S. Lu, N. Sakakibara, V.L. Chiang, M. Shimada, S. Suzuki, T. Umezawa, "Roles of 5-hydroxyconiferaldehyde and caffeoyl-CoA O-methyltransferases in monolignol biosynthesis in *Carthamus tinctorius*," Cellulose Chemistry and Technology , vol.51, pp.511-520, 2007, (printed in 2008).

Nakatsubo, T., M. Mizutani, S. Suzuki, T. Hattori, T. Umezawa, "Characterization of *Arabidopsis thaliana* Pinoresinol Reductase that is a new type enzyme related in lignan biosynthesis," Journal of the Biological Chemistry, vol.283, pp.15550-15557, 2008.

PUBLICATIONS

Hattori, T., K. Okawa, M. Fujimura, M. Mizoguchi, T. Watanabe, T. Tokimatsu, H. Inui, K. Baba, S. Suzuki, T. Umezawa, M. Shimada, "Subcellular localization of the oxalic acid-producing enzyme, cytochrome c dependent glyoxylate dehydrogenase, in brown-rot fungus *Fomitopsis palustris*," Cellulose Chemistry and Technology , vol.51, pp.545-553, 2007, (printed in 2008).

Noguchi, A., Y. Fukui, A. Iuchi-Okada, S. Kakutani, H. Satake, T. Iwashita, M. Nakao, T. Umezawa, E. Ono, "Sequential glucosylation of a furofuran lignan, (+)-sesaminol, by *Sesamum indicum* UGT71A9 and UGT94D1 glucosyltransferases," Plant J., vol.54, pp.415-427, 2008.

Hattori, T, "Mechanisms for carbon metabolism of copper-tolerant mushrooms," Seizonken Kenkyu, vol.4, pp.1-9, 2008, (in Japanese).

Verrier, P. J., Bird, D., Burla, B., Dassa, E., Forestier, C., Geisler, M., Klein, M., Kolukisaoglu, Ü., Lee, Y-S/. Martinoia, E., Murphy, A., Rea, P. A.., Samuels, L., Schulz, B., Spalding, E. J., Yazaki, K., Theodoulou, F. L., "Plant ABC proteins- unified nomenclature and updated inventory," Trends in Plant Sci., vol.13, no.4, pp.151-159, 2008.

Sasaki, K., Mito, K., Ohara, K.,Yamamoto, H., Yazaki, K., "Cloning and characterization of naringenin 8-prenyltransferase, a flavonoid-specific prenyltransferase of Sophora flavescens," Plant Physiol., vol.146, no.3, pp.1075-1084, 2008.

Yazaki, K., Sugiyama, A., Morita, M., Shitan, N., "Secondary transport as an efficient membrane transport mechanism for plant secondary metabolites.," Phytochem. Rev., vol.7, pp.513-524, 2008.

Sugiyama, A., Shitan, N., Tomohisa Kuzuyama, Yazaki, K., "Development of transgenic plants producing prenylated poyphenols," Bio Industry, vol.26, no.1, pp.41-48 , 2008, (in Japanese).

Sasaki, K., Yazaki, K., "Discovery of plant prenyltransferase gene modulating functions of flavonoids," Bio Industry, vol.25, no.10, pp.58-65, 2008, (in Japanese).

Sasaki, K., Tsurumaru, Y., Yazaki, K., "Prenyltransferase responsible for the increase in biological activities of polyphenols," Biosci & Ind., vol.66, no.9, pp.509-513, 2008, (in Japanese).

Tsubasa Shoji, T., Inai, K., Yazaki, Y., Sato, Y., Takase, H., Shitan, N., Yazaki, K., Goto, Y., Toyooka, K., Matsuoka, K., Hashimoto, T., "MATE-type transporters Implicated in vacuolar sequestration of nicotine in tobacco roots," Plant Physiol., vol.149, no.2, pp.708-718, 2009.

Akashi, T., Sasaki, K., Aoki, T., Ayabe, S., Yazaki, K., "Molecular cloning and characterization of a cDNA for pterocarpan 4-dimethylallyltransferase catalyzing the key prenylation step in the biosynthesis of glyceollin, a soybean phytoalexin," Plant Physiol., vol.149, no.2, pp.683-693, 2009.

Kamimoto, Y., Hamamoto, M., Shitan, N., Yazaki, K., "Unusual expression of an Arabidopsis ATP-binding cassette transporter ABCC11," Plant Biotechnol., vol.26, no.2, pp.261-265, 2009.

Morita, M., Shitan, N., Sawada, K., Van Montagu, M., Inzé, D., Rischer, H., Goossens, A., Oksman-Caldentey, K-M., Moriyama, Y., Yazaki, K., "Vacuolar transport of nicotine is mediated by a novel multidrug and toxic compound extrusion (MATE) transporter in Nicotiana tabacum.," Proc. Natl. Acad. Sci. USA, vol.106, no.7, pp.2447-2452, 2009.

Sasaki, K., Tsurumaru, Y., Yazaki, K., "Prenylation of flavonoids by the biotransformation of yeast expressing plant membrane-bound prenyltransferase SfN8DT-1.," Biosci. Biotech. Biochem., vol.73, no.3, pp.759-761, 2009.

Satomi Y., Ohara K., Yazaki K., Ito M., Honda G., Nishino H., "Production of the monoterpene limonene and modulation of apoptosis-related proteins in NIH3T3 cells by introduction of the limonene synthase gene isolated from the plant Schizonepeta tenuifolia.," Biotechnol Appl. Biochem., vol.52, no.3, pp.185-190, 2009.

T. Hayashi, Y.W. Park, A Isogai, T. Nomura, "Cross-linking of plant cell walls with dehydrated fructose by smoke-heat treatment," J. Wood Sci., vol.54, pp.90-93, 2008.

T. Taniguchi, Y. Ohmiya, M. Kurita, M. Tsubomura, T. Kondo, Y.W. Park, K. Baba, T. Hayashi,

"Biosafety assessment of transgenic poplars overexpressing xyloglucanase (AaXEG2) prior to field trials," J. Wood Sci., vol.54, pp.408-413, 2008.

R. Kaida, T. Hayashi, T.S. Kaneko, "Purple acid phosphatase in the walls of tobacco cells," Phytochem, vol.69, pp.2546-2551, 2008.

Takabe, T., A. Uchida, F. Shinagawa, Y. Terada, H. Kajita, Y. Tanaka, T. Takabe, T. Hayashi, T. Kawai, "Overexpression of DnaK from a halotolerant cyanobacterium Aphanothece halophytica enhances growth rate as well as abiotic stress tolerance of poplar plants," Plant Growth Reg., vol.56, pp.265-273, 2008.

S. Hartati, E. Sudarmonowati, Y.W. Park, T. Kaku, R. Kaida, K. Baba, T. Hayashi, "Overexpression of poplar cellulase accelerates growth and disturbs the closing movements of leaves in sengon," Plant Physiol, vol.147, pp.552-561, 2008.

H. Ikegaya, T. Hayashi, T. Kaku, K. Twata, S. Sonobe, T. Shimmen, "Presence of xyloglucan-like polysaccharide in Spirogyra and possible involvement in cell-cell attachment," Phycological Res., vol.56, pp.216-222, 2008.

E.J. Mellerowicz, P. Immerzeel, T. Hayashi, "Xyloglucan: The molecular muscle of trees," Annals Bot, vol.102, pp.659-665, 2008.

T. Hayashi, R. Kaida, T. Kaku, K. Baba, "Enhancement of saccharification by overexpression of various endoglycanase in poplar," J. Brasil Sci., vol.55, pp.145-149, 2008.

K. Ozaki, A. Uchida, T.Takabe, F. Shinagawa, Y. Tanaka, T. Takabe, T. Hayashi, T. Hattori, A.K. Raid, T. Takabe, "Enrichment of sugar content in melon fruits by hydrogen peroxide treatment," J. Plant Physiol, vol.166, pp.569-578, 2009.

Dutta G., T. Tsuda, P. V. Kumar, M. C. A. Kumar, S. P. Alexander, T. Kozu, "Seasonal variation of short-period (<2 hr) gravity wave activity over Gadanki, India (13.5N, 79.2E)," J. Geophys. Res., vol.113, doi:10.1029/2007JD009178, 2008.

Tsurutani, B.T., O.P. Verkhoglyadova, A. J. Mannucci, A. Saito, T. Araki, K. Yumoto, T. Tsuda, M.A. Abdu, J.H.A. Sobral, W.D. Gonzalez, H. McCreadie, G.S. Lakhina, V.M. Vasyliūnas, "Prompt Penetration Electric Fields (PPEFs) and Their Ionospheric Effects During The Great Magnetic Storm of October 30-31, 2003," J. Geophys. Res., vol.113, doi:10.1029/2007JA012879, 2008.

Alexander, S. P., T. Tsuda, Y. Kawatani, "COSMIC GPS Observations of Northern Hemisphere Winter Stratospheric Gravity Waves and Comparisons with an Atmospheric General Circulation Model," Geophys. Res. Lett., vol.35, doi:10.1029/2008GL033174, 2008.

Alexander, S.P, T. Tsuda, "High-Resolution Radio Acoustic Sounding System (RASS) Observations and Analysis up to 20km," J. Atmos. and Ocean Tech., vol.25, no.8, pp.1383-1396, 2008.

Sarma, T.V.C, D. Narayana Rao, J. Furumoto, T. Tsuda, "Development of radio acoustic sounding system (RASS) with Gadanki MST radar – first results," Annales Geophysicae, vol.26, no.9, pp.2531-2542, 2008.

Alexander, S., P., T. Tsuda, Y. Kawatani, M. Takahashi, "Global distribution of atmospheric waves in the equatorial upper troposphere and lower stratosphere: COSMIC observations of wave mean flow interactions," J. Geophys. Res., vol.113, doi:10.1029/2008JD010039, 2008.

Shepherd, M., G. T. Tsuda, "Large-scale planetary disturbances in stratospheric temperature at high-latitudes in the southern summer hemisphere," Atmos. Chem. Phys., vol.8, pp.7557-7570, 2008.

Suzuki. H., K. Shiokawa, M. Tsutsumi, T. Nakamura, M Taguch, "Atmospheric gravity waves identified by ground-based observations of the intensity and rotational temperature of OH airglow," Polar Sci., vol.2, pp.1-8, 2008.

Fujiwara. Y., Y. Hamaguchi, T. Nakamura, M. Tsutsumi, M. Abo, "Meteor orbit determinations with a Multistatic Receivers Using the Radar," Earth Moon Planet, vol.102, pp.309-314, 2008.

PUBLICATIONS

Horinouchi, T., "A numerical study of upward-propagating gravity waves in two different MJO," Geophys. Res. Lett., vol.35, no.17, L17802 , 2008.

Kawatani, Y., M. Takahashi, K. Sato, S. P. Alexander, T. Tsuda, "Global distribution of atmospheric waves in the equatorial upper troposphere and lower stratosphere: AGCM simulation of sources and propagation," J. Geophys. Res., vol.114, doi:10.1029/2008JD010374, 2009.

Rao, D. N., M. V. Ratnam, S. Mehta, D. Nath, S. G. Basha, V. V. M. J. Rao, B. V. K. Murthy, T. Tsuda, K. Nakamura, "Variation of the COSMIC Radio Occultation Data over Gadanki(13.48°N, 79.2°E): A Tropical Region," Terr. Atmos. Ocean. Sci., vol.20, no.1, doi:10.3319/TAO.2008.01.23.01(F3C), 2009.

Hayashi, H., J. Furumoto, X. Lin, T. Tsuda, Y. Shoji, Y. Aoyama, Y. Murayama, "FORMOSAT-3/COSMIC Radio Occultation Soundings: Preliminary Results of Statistical Comparisons Utillzing Balloon-borne Observations," Terr. Atmos. Ocean. Sci., vol.20, no.1, pp.51-58, 2009.

Suzuki, S., K. Shiokawa, A. Z. Liu, Y. Otsuka, T. Ogawa, T. Nakamura, "Characteristics of equatorial gravity waves derived from mesospheric airglow imaging observations," Ann. Geophys., vol.27, pp.1625-1629, 2009.

Yue, J., S. L. Vadas, C.Y. She, T. Nakamura, S. Reising, D. Krueger, H. Liu, P. Stamus, D. Thorsen, W. Lyons, T. Li , "Concentric gravity waves in the mesosphere generated by deep convective plumes in the lower atmosphere near Fort Collins, Colorado ," J. Geophys. Res., vol.114, doi:10.1029/2008JD011244, 2009.

Li, T. C.-Y. She, H.-L. Liu, J. Yue, T. Nakamura, D.A. Krueger, Q. Wu, X. Dou, S. Wang, "Observation of local tidal variability and instability, along with dissipation of diurnal tidal harmonics in the mesopause region over Fort Collins, Colorado (41_N, 105_W)," Geophys. Res. Lett., vol.114, doi:10.1029/2008JD011089, 2009.

Tsuda, T., M. V. Ratnam, S. P. Alexander, T. Kozu, Y. Takayabu, "Horizontal Distribution of Atmospheric Wave Energy in the Tropics Revealed by GPS Radio Occultation Temperature Data during 2001-2006," Earth Planets Space, in press, 2009.

Ejiri, M.K., M. J. Taylor, T. Nakamura, S. Franke, "Mesospheric Gravity Waves and Diurnal Tidal Interactions at a Critical Level," J. Geophys. Res, vol.114, in press, 2009.

Takashima, H., M. Shiotani, M. Fujiwara, N. Nishi, F. Hasebe, "Ozonesonde observations at Christmas Island (2°N, 157°W) in the equatorial central Pacific," J. Geophys. Res., vol.113, no.D10112, doi:10.1029/2007JD009374, 2008.

Suzuki, J., M. Shiotani, "Space-time variability of equatorial Kelvin waves and intraseasonal oscillations around the tropical tropopause," J. Geophys. Res., vol.113, no.D16110, doi:10.1029/2007JD009456, 2008.

Yokoyama, T., Y. Otsuka, T. Ogawa, M. Yamamoto, D. L. Hysell, "First three-dimensional simulation of the Perkins instability in the nighttime midlatitude ionosphere," Geophys. Res. Lett., vol.35, no.L03101, doi:10.1029/2007GL032496, 2008.

A. K. Patra, T. Yokoyama, Y. Otsuka, M. Yamamoto, "Daytime 150-km echoes observed with the Equatorial Atmosphere Radar in Indonesia: First results," Gephys. Res. Lett., vol.35, no.L06101, doi:10.1029/2007GL033130, 2008.

Hassenpflug, G., M. Yamamoto, H. Luce, S. Fukao, "Description and demonstration of the new Middle and Upper atmosphere Radar imaging system: 1-D, 2-D, and 3-D imaging of troposphere and stratosphere," Radio Sci, vol.43, no.RS2013, doi:10.1029/2006RS003603, 2008.

Saito, S., M. Yamamoto, H. Hashiguchi, "Imaging observations of nighttime mid-latitude F-region field-aligned irregularities by the MU radar ultra-multi channel system," Ann. Geophys., vol.26, no.8, pp.2345-2352, 2008.

M. K. Yamamoto, Y. Ohno, H. Horie, N. Nishi, H. Okamoto, K. Sato, H. Kumagai, M. Yamamoto, H. Hashiguchi, S. Mori, N. O. Hashiguchi, H. Nagata, S. Fukao, "Observation of particle fall velocity in

cirriform cloud by VHF and millimeter-wave Doppler radars," J. Geophys. Res., vol.113, no.D12210, doi:10.1029/2007JD009125, 2008.

J.-S. Chen, G. Hassenpflug, M. Yamamoto, "Tilted refractive-index layers possibly caused by Kelvin Helmholtz instability and their effects on the mean vertical wind observed with multiple-receiver and multiple-frequency imaging techniques," Radio Sci., vol.43, no.RS4020, doi:10.1029/2007RS003816, 2008.

Yamamoto, M, "Digital beacon receiver for ionospheric TEC measurement developed with GNU Radio," Earth Planets Space, vol.60, pp.e21-e24, 2008.

M.D. Yamanaka, H. Hashiguchi, S. Mori, P. Wu, F. Syamsudin, T. Manik, Hamada J.-I., M.K. Yamamoto, M. Kawashima, Y. Fujiyoshi, N. Sakurai, M. Ohi, R. Shirooka, M. Katsumata, Y. Shibagaki, T. Shimomai, Erlansyah, W. Setiawan, B. Tejasukmana, Y.S. Djajadihardja, J.T. Anggadiredja, "HARIMAU Radar-Profiler Network over the Indonesian Maritime Continent: A GEOSS Early Achievement for Hydrological Cycle and Disaster Prevention," J. Disaster Res., vol.3, no.1, pp.78-88, 2008.

Saito S., S. Fukao, M. Yamamoto, Y. Otsuka, T. Maruyama, "Decay of 3-m-scale ionospheric irregularities associated with a plasma bubble observed with the Equatorial Atmosphere Radar," J. Geophys. Res., vol.113, no.A11318, doi:10.1029/2008JA013118, 2009.

Yokoyama, T., D. L. Hysell, Y. Otsuka, M. Yamamoto, "Three-dimensional simulation of the coupled Perkins and Es-layer instabilities in the nighttime midlatitude ionosphere," J. Geophys. Res., vol.114, no.A03308, .doi:10.1029/2008JA013789, 2009.

Seto, T.H., Y. Tabata, M.K. Yamamoto, H. Hashiguchi, T. Mega, M. Kudsy, M.D. Yamanaka, S. Fukao, "Comparison Study of Lower-tropospheric Horizontal Wind over Sumatra, Indonesia Using NCEP/NCAR Reanalysis, Operational Radiosonde, and the Equatorial Atmosphere Radar," SOLA, vol.5, pp.21-24, 2009.

Sakurai, N., M. Kawashima, Y. Fujiyoshi, H. Hashiguchi, T. Shimomai, S. Mori, J-I. Hamada, M.D.Yamanaka, Y.I.Tauhid, T. Sribimawati, B. Suhardi, "Internal structures of migratory cloud systems with diurnal cycle over Sumatera Island during CPEA-I campaign," J. Meteor. Soc. Japan, vol.87, no.1, pp.57-170, 2009.

Nakagaito, A. N., H. Yano, "Toughness enhancement of cellulose nanocomposites by alkali treatment of the reinforcing cellulose nanofibers," Cellulose, vol.5, no.2, pp.323-331, 2008.

Nogi, M., H. Yano, "Transparent nanocomposites based on cellulose produced by bacteria offer potential innovation in electronics device industry," Advanced Materials, vol.20, pp.1849-1852, 2008.

Iwamoto, S., K. Abe, H. Yano, "The effect of hemicelluloses on wood pulp nano-fibrillation and nanofiber network characteristics," Biomacromolecules, vol.9, pp.1022-1026, 2008.

Hsieh, Y.-C., H. Yano, M. Nogi, S.J. Eichhorn, "An estimation of the Young's Modulus of bacterial cellulose filaments," Cellulose, vol.15, no.4, pp.507-513, 2008.

Nakagaito, A. N., H. Yano, "The effect of fiber content on the mechanical and thermal properties of biocomposites based on microfibrillated cellulose," Cellulose, vol.15, no.4, pp.555-559, 2008.

Iwatake, A., M. Nogi, H. Yano, "Cellulose nanofiber-reinforced polylactic acid," Composites Science and Technology, vol.68, no.9, pp.2103-2106, 2009.

Md. Iftekhar Shams, H. Yano, "Development of selectively densified surface laminated wood based composites," Eur. J. Wood Prod., vol.67, pp.169-172, 2009.

Md. Iftekhar Shams, H. Yano, "A new method for obtaining high strength phenol formaldehyde (PF) resin impregnated wood composites at low pressing pressure," Journal of Tropical Forest Science, vol.21, no.2, pp.175-180, 2009.

Nogi, M., S. Iwamoto, A.N. Nakagaito, H. Yano, "Optically transparent nanofiber paper," Advanced

Materials, vol.21, no.16, pp.1595-1598, 2009.

Okahisa, Y., A. Yoshida, S .Miyaguch, H. Yano, "Optically transparent wood-cellulose nanocomposite as a base substrate for flexible Organic Light-Emitting Diode displays," Composites Science and Technology, in press, 2009.

Suryanegara, L., A. N. Nakagaito, H. Yano, "The effect of crystallization of PLA on the thermal and mechanical properties of microfibrillated cellulose-reinforced PLA composites," Composites Science and Technology, vol.69, pp.1187–1192, 2009.

Nakagaito, A. N., Fujimoto, Hama, H. Yano, "Production of microfibrillated cellulose (MFC)-reinforced polylactic acid (PLA) nanocomposites from sheets obtained by a papermaking-like process," Composites Science and Technology, vol.69, no.7-8, pp.1293-1297, 2009.

Ifuku, S., M. Nogi, K. Abe, M. Yoshioka, M. Morimoto, H. Saimoto, H. Yano, "Preparation of chitin nanofibers with a uniform width as r-chitin from crab shells," Biomacromolecules, vol.10, no.6, pp.1584-1588, 2009.

S.S. Munawar, K. Umemura, S. Kawai, "Effect of alkali, mild steam and chitosan treatments on the properties of pineapple, ramie and sansevieria fiber bundles.," J. Wood Science, vol.54, no.1, pp.28-35, 2008.

T. Mori, K. Umemura, M. Sasada, M. Norimoto, "Development of drift pins and plates made from bamboo fiber for timber structures," J. the Society of Materials Scinece, Jpn., vol.57, no.4, pp.328-332, 2008, (in Japanese).

K. Umemura, S. Kawai, "Preparation and characterization of maillard reacted chitosan films with hemicellulose model compounds.," J. Appl. Polym. Sci., vol.108, no.4, pp.2481-2487, 2008.

K. Umemura, H. Yamauchi, T. Ito, M. Shibata, S. Kawai, "Durability of isocyanate resin adhesives for wood V. Changes of color and chemical structure in photo degradation.," J. Wood Science, vol.54, no.4, pp.289-293, 2008.

S.S. Munawar, K. Umemura, S. Kawai, "Manufacture of oriented board using the mild steam treated some plant fiber bundles.," J. Wood Science, vol.54, no.5, pp.369-376, 2008.

Z.W. Guan, A. Kitamori, K. Komatsu, "Experimental study and finite element modelling of Japanese "Nuki" joints Part one: Initial stress states subjected to different wedge configurations," Engineering Structures, vol.30, pp.2032-2040, 2008.

Z.W. Guan, A. Kitamori, K. Komatsu, "Experimental study and finite element modelling of Japanese "Nuki" joints Part two: Racking resistance subjected to different wedge configurations," Engineering Structures , vol.30, pp.2041–2049, 2008.

K. Komasu, Y. Kataoka, T. Mori, S. Takino, K. Jung, A. Kitamori, T. Shiratori, M. Minami, "Concept of Proposed House and Outline for Structural Performance. – Development of Wooden Post & Beam Construction by Utilizing Natural Construction Materials (Part 1) –," AIJ J. Technol. Des., vol.14, no.28, pp.447-452, 2008, (in Japanese).

I. Hassel, P. Berard, K. Komatsu, "Development of wooden blocks' shear wall -Improvement of stiffness by utilizing elements of densified wood - ," Holzforschung, vol.62, no.5, pp.584-590, 2008.

K. Hwang, E. Wong, K. Komatsu, "Flexural, in-plane shear and nail shear properties of falcataria-rubberwood laminated veneer board for flooring," Holzforschung, vol.62, pp.731-736, 2008.

J. Shanks, W.S. Chang, K. Komatsu , "Experimental study on mechanical performance of all-softwood pegged mortice and tenon connections," Biosystems Engineering, doi:10.1016/j.biosystemseng. 2008.03.012, 2008.

K. Komatsu, S. Takino, T. Mori, Y. Ito, R. Kataoka, "Lateral Shear Performance of Nailed Plywood Sheathed Shear Wall with Opening and Portal Frame with Nailed Plywood Sheathed hanging Wall," J. Structural Engineering, vol.54B, pp.119-128, 2008, (in Japanese).

PUBLICATIONS

K. Jung, A. Kitamori, K. Komatsu, "Evaluation on structural performance of compressed wood as shear dowel," Holzforschung, vol.62, pp.461-467, 2008.

M. Nakatani, T. Mori, K. Komatsu, "Study on the Beam-Column Joint of Timber Frame Structures using Lagscrewbolts and Special Connectors," J. Structural and Construction Engineering, Transactions of AIJ, vol.73, no.626, pp.599-606, 2008, (in Japanese).

T. Shiratori, K. Komatsu, A. Leijten , "Modified traditional Japanese timber joint system with retrofitting abilities," Structural Control and Health Monitoring, doi: 10.1002/stc.240, 2008.

W.S. Chang, J. Shanks, A. Kitamori, K. Komatsu, "The structural behaviour of timber joints subjected to bi-axial bending," Earthquake Engineering and Structural Dynamics, vol.38, pp.739–757, 2009.

H. Shimizu, T. Mori, S. Murase, K. Tachibana, H. Isoda, K. Komatsu, S. Yoshikawa, Y. Fukuda, "Weight Appraisal of Newly Built Wood House -Weight measurement of full scale wood house-," AIJ J. Technol. Des., vol.15, no.29, pp.115-120, 2009, (in Japanese).

T. Mori, M. Nakatani, K. Komatsu, "Development on the Structural Performance of One Directional Timber Frame using Lagscrewbolts having an External Thread," J. Structural Engineering, vol.55B, pp.213-218, 2009, (in Japanese).

A. Kitamori, K. Jung, M. Minami, K. Komatsu, "Evaluation on Stiffness of Lattice Sehar Wall -Influence of gap and its verification by long term test-," J. Structural Engineering, vol.55B, pp.109-116, 2009, (in Japanese).

K. Nakata, K. Komatsu, "Development of Timber Portal Frames Composed of Compressed LVL Plates and Pins II Strength properties of compressed LVL joints as moment resisting joints," Mokuzai Gakkaishi, vol.55, no.3, pp.155-162, 2009, (in Japanese).

K. Jung, A. Kitamori, K. Komatsu , "Development of Joint System using Compressed Wooden Fastener Part1, Evaluation of pull-out and rotation performance for column and sill joint," J. Wood Sci., doi: 10.1007/s10086-009-1027-3, 2009.

Kubota, S., Y. Shono, N. Mito, K. Tsunoda, ""Termiticidal efficacies of fenobucarb and permethrin against Japanese subterranean termites *Coptotermes formosanus and Reticulitermes speratus* (Isoptera: Rhinotermitidae)," Jpn. Environ. Entomol. Zool., vol.19, no.1, pp.31-37, 2008.

Kubota, S., Y. Shono, N. Mito, K. Tsunoda, "Lethal dose and horizontal transfer of bistrifluron, a benzoylphenylurea, in workers of the Formosan subterranean termite (Isoptera: Rhinotermitidae)," J. Pestic. Sci., vol.33, no.3, pp.243-248, 2008.

Katsumata, N., K. Tsunoda, A. Toyoumi, T. Yoshimura, Y. Imamura, "Feeding preference of *Coptotermes formosanus* (Isoptera: Rhinotermitidae) for gamma-irradiated wood impregnated with benzoylphenylurea compounds under laboratory conditions," J. Econ. Entomol, vol.101, no.3, pp.881-884, 2008.

Kakitani, T., T. Hata, T. Kajimoto, H. Koyanaka, Y. Imamura, "Characteristics of a bioxalate chelating extraction process for removal of chromium, copper and arsenic from treated wood," Journal of Environmental Management, vol.90, no.5, pp.1918-1923, 2009.

Kajimoto, T., Y. Tachibana, Y. Maeda, S. Kubota, T. Hata, Y. Imamura, "Characterization of the Pulp-Like Fibers Seperated from Sugi with L-Lactic Acid," Mokuzai Gakkaishi, vol.54, no.6, pp.319-326, 2008, (in Japanese).

Sulistyo, J. T. Hata, M. Fujisawa, K. Hashimoto, Y. Imamura, T. Kawasaki, "Anisotropic thermal conductivity of three-layer laminated carbon-graphitic composites from carbonized wood,"" J. Mater. Sci., vol.44, pp.734-744, 2009.

Fujisawa, M., T. Hata, H. Kitagawa, P. Bronsveld, Y. Suzuki, K. Hasezaki, Y. Noda, Y. Imamura, "Thermoelectric properties of porous SiC/C composites," Renewable Energy, vol.33, pp.309-313, 2008.

Kartal, S. N., W. J. Hwang, Y. Imamura, "Combined effect of boron compounds and heat treatments on

wood properties - Chemical and strength properties of wood," J. Mat. Process. Technol., vol.198, pp.234-240, 2008.

Indrayani, Y., T. Yoshimura, Y. Imamura, "A novel control strategy for dry-wood termite *Incisitermes minor* infestation using a bait system," J. Wood Sci., vol.54, pp.220-224, 2008.

Miyauchi, T., M. Mori, Y. Imamura, "Leaching characteristics of homologues of benzalkonium chloride from wood treated with ammoniacal copper quaternary wood preservative," J. Wood Sci., vol.54, pp.225-232, 2008.

Erwin, S. Takemoto, W. J. Hwang, M. Takeuchi, T. Itoh, Y. Imamura, "Anatomical characterization of decayed wood in standing light red meranti and identification of the fungi isolated from the decayed area," J. Wood Sci., vol.54, pp.233-241, 2008.

Erwin, W. J. Hwang, Y. Imamura, "Micromorphology of abnormal and decayed xylem in rubberwood canker," J. Wood Sci., vol.54, pp.414-419, 2008.

Kartal, S. N., C. Kosel, B. Tarakanadha, Y. Imamura, "Adsorption of copper, chromium, and arsenic from chromated copper arsenate (CCA) treated wood onto various adsorbents," The Open Waste Manage. J., vol.1, pp.11-17, 2008.

Kartal, S. N., T. Yoshimura, Y. Imamurae, "Modification of wood with Si compounds to limit boron leaching from treated wood and to increase termite and decay resistance," Int. Biodeter. & Biodeg., vol.63, pp.187-190, 2009.

Indrayani, Y., T. Yoshimura, Y. Imamura, "A novel control strategy for dry-wood termite *Incisitermes minor* infestation using a bait system," J. Wood Sci., vol.54, no.4, pp.220-224, 2008.

Y. Omura,Y. Katoh, D. Summers, "Theory and simulation of the generation of whistler-mode chorus," J. Geophys. Res, vol.113, no.A04223, 2008.

N. Furuya, Y. Omura, D. Summers, "Relativistic turning acceleration of radiation belt electrons by whistler-mode chorus," Journal of Geophysical Research, vol.113, no.A04224, 2008.

Miyake, Y., H. Usui, H. Kojima, Y. Omura, H. Matsumoto, "Electromagnetic Particle-In-Cell simulation on the impedance of a dipole antenna surrounded by an ion sheath," Radio Sci, vol.43, no.RS3004, 2008.

M. Okada, H. Usui, Y. Omura, H. O. Ueda, T. Murata T. Sugiyama, "Spacecraft Plasma Environment Analysis via Large Scale 3D Plasma Particle Simulation, High-Performance Computing," Lecture Notes in Computer Science (LNCS), Springer-Verlag, vol.4759, no.2008, pp.383-392, 2008.

T. Oyama, H. Yamakawa, Y. Omura, "Orbital Dynamics of Solar Sails for Geomagnetic Tail Exploration," Journal of Spacecraft and Rockets, vol.45, no.2, 2008.

Y. Katoh, Y. Omura, D. Summers, "Rapid energization of radiation belt electrons by nonlinear wave trapping," Ann. Geophys, vol.26, no.3451-3456, 2008.

Y. Kasaba, J.-L. Bougeret, L.G. Blomberg, H. Kojima, S. Yagitani, M. Moncuquet, J.-G. Trotignon, G. Chanteur, A. Kumamoto, Y. Kasahara, J. Lichtenberger, Y. Omura, K. Ishisaka, H. Matsumoto, "The Plasma Wave Investigation (PWI) onboard the BepiColombo/MMO: First measurement of electric fields, electromagnetic waves, and radio waves around Mercury," Planetary and Space Science, in press, 2008.

A. Milillo, M. Fujimoto, E. Kallio, S. Kameda, F. Leblanc, Y. Narita, G. Cremonese, H. Laakso, M. Laurenza, S. Massetti, S. McKenna-Lawlor, A. Mura, R. Nakamura, Y. Omura, D.A. Rothery, K Seki, M. Storini, P. Wurz, W. Baumjohann, E.J. Bunce, Y. Kasaba, J. Helbert, A. Spraguer, and the other Hermean Environment WG members, "The BepiColombo mission: An outstanding tool for investigating the Hermean environment," Planetary and Space Science, in press, 2008.

Y. Miyake H. Usui, "Analysis of Photoelectron Effect on the Antenna Impedance via Particle-In-Cell Simulation," Radio Science, vol.43, no.RS4006, 2008.

Sonobe, T., J. Jitputti, K. Hachiya, T. Mitani, N. Shinohara, S. Yoshikawa, "Optical Properties of the Carbon-Modified TiO2 Prepared by Microwave Carbonization Process," Japanese Journal of Applied

Physics (JJAP), vol.47, no.11, pp.8456-8460, 2008.

Kasahara, Y., Y. Goto, K. Hashimoto, T. Imachi, A. Kumamoto, T. Ono, H. Matsumoto, "Plasma wave observation using waveform capture in the Lunar Radar Sounder on board the SELENE spacecraft," Earth Planets Space, vol.60, no.4, pp.341–351, 2008.

Nakamiya, M., Scheeres, D., Yamakawa, H., M, Yoshikawa, "Analysis of Capture Trajectories to Libration Points," Journal of Guidance, Control, and Dynamics, vol.31, No.5, pp.1344-1351, 2008.

Ueno, K., Funaki, I., Kimura, T., Horisawa, H., Yamakawa, H., "Thrust Measurement of Pure Magnetic Sail Using Parallelogram-pendulum Method," Journal of Propulsion and Power, vol.25, No.2, pp.536-539, 2009.

Yamaguchi, T, Kogiso, N., Yamakawa, H., "Optimal Interplanetary Trajectories for Impulsive Deflection of Potentially Hazardous Asteroids under Velocity Increment Uncertainties," Transactions of Japan Society for Aeronautical and Space Sciences, vol.51, No.173, pp.176-183, 2008.

H. Yamakawa, H. Ogawa, Y. Sone, H. Hayakawa, Y. Kasaba, T. Takashima, T. Mukai, T. Tanaka, M. Adachi, "BepiColombo Mercury Magnetospheric Orbiter Design," Acta Astronautica, vol.62, pp.699-706, 2008.

S. Y. Li, X. H. Deng, M. Zhou, R. X. Tang, K. Liu, H. Kojima, H. Matsumoto, "Statistical study of electrostatic solitary waves associated with reconnection: Geotail observations", Adv. in Space Res., vol.43, pp.394-400, 2008.

K. Shin, H. Kojima, H. Matsumoto, "Characteristics of electrostatic solitary waves in the Earth's foreshock region: Geotail observations", J. Geophys. Res., vol.113, doi:10.1029/2007JA012344, 2008.

Y. Kasaba, Y., J.-L. Bougeret, L. G. Blomberg, H. Kojima, S. Yagitani, M. Moncuquet, J.-G. Trotignon, G. Chanteur, A. Kumamoto, Y. Kasahara, J. Lichtenberger, Y. Omura, K. Ishisaka, H. Matsumoto, "The Plasma Wave Investigation (PWI) onboard the BepiColombo / MMO: First measurement of electric fields, electromagnetic waves, and radio waves around Mercury", Planetary Space Science, in print, 2008.

Y. Miyake, H. Usui, H. Kojima, Y. Omura, H. Matsumoto, "Electromagnetic Particle-In-Cell simulation on the impedance of a dipole antenna surrounded by an ion sheath", Radio Science, vol.43, doi:10.1029/2007RS003707, 2008.

Y. Ueda, M. Tsujimoto, K. Takeuchi, H. Koyanaka, M. Takano, Hydrogen gas sensor using nano-sized R-MnO2 powder, 214th Meeting of ECS(The Electrochemical Society), ECS Trans. vol.16, no.11, pp.287-292, 2008

M. Bando A. Ichikawa,"Adaptive Regulation of Nonlinear Systems by Output Feedback," Journal of Robotics and Mechatronics, vol.20, No.5, pp.719-725, 2008.

Sustainable Humanosphere 第5号

発　行　日　　平成21年9月10日
編集兼発行者　　京都大学 生存圏研究所
京都府宇治市五ヶ庄
印　刷　所　　ユニバース印刷
京都府長岡京市友岡 2-10-2